IN THE UNITED STATES PATENT AND TRADEMARK OFFICE

APPLICANT:	Robert J. Sicurelli Jr. and Samuel Masyr
SERIAL NO.:	09/990,932
TITLE:	Flexible Post In A Dental Post and Core System
FILED:	November 21, 2001
EXAMINER:	John J. Wilson
MAILING DATE OF ACTION:	August 1, 2007
GROUP ART UNIT	3732

SECTION 132 DECLARATION

I,Lawrence E. Brecht, DDS, hereby declare:

I am a specialist in the dental restorative field.

My education and experience is as follows:

Doctor of Dental Surgery-New York University College of Dentistry, New York, NY – June 1985

Resident in General Practice-Brigham & Women's Hospital Boston, MA – July 1985 – June 1986

Postdoctoral Fellow in Operative Dentistry-Harvard School of Dental Medicine, Boston, MA July 1985 – June 1986

Resident in Prosthodontics – Veterans Administration Medical Center, New York, NY July 1986 – June 1988

Resident in Maxillofacial Prosthetics - Veterans Administration Medical Center, New York, NY July 1988 – June 1989

Currently Clinical Associate Professor of Prosthodontics, New York University College of Dentistry, New York, NY

Design Realization lecture 13

John Canny/Dan Reznik

10/7/03

Last Time

- Fantastic plastics!

This time

- S-t-r-e-t-c-h-i-n-g material properties: composites and cellular materials
- Chemistry takes us pretty far. But we can also customize material properties with geometry:
  - Composites: distinct materials tightly bound together.
  - Cellular materials: customized fine structure for desired stiffness/strength.

Composites: Fiber-based

- Fiberglass is the classic composite:
  - Glass fibers (often woven)
  - Two-part polyester or epoxy resin
- Epoxy strength = 60MPa
- Glass fiber *tensile* strength = 500 MPa

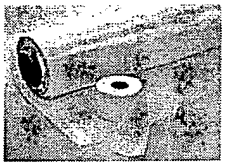

- The composite can achieve a significant percentage of the fiber strength (300MPa typical), *along the fiber direction*.

Composites: Fiber-based

- Laminates: to get strength in several directions, the fibers are either:
  - Laminated in sheets in different directions, or
  - Made from a woven fabric with threads in several directions.
- Glasses are chosen for different attributes:
  - Tensile strength
  - Stiffness
  - Electrical insulation...
- Glass and polymer do not react, but the polymer must adhere very well to the fiber for strength.

Composites: Carbon & Kevlar

- Recall (lecture 10) that carbon fiber and kevlar fibers both have diamond-like tensile strength (~ 4 GPa), or about 70x epoxy.
- Modulus also increases by about 50x.
- Surprisingly, carbon fiber has the same structure as (soft) graphite: But these sheets are long and thin in CF, whereas they are flat (and slippery) in graphite.

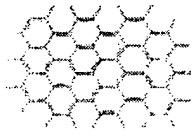

Workability

- Glass, carbon, kevlar sheets and two-part resins are easy to work with, and used for:
  - Boat making and repair.
  - Custom surfboards, snowboards…
  - Motorcyle and auto racing.
  - Furniture (e.g. chairs)…
- Construction by mold-making, fiber laying, resin application.
- See http://www.fibreglast.com/

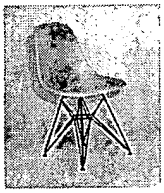

Natural fiber composites

- Wood is a natural composite of cellulose fiber and a polymer called lignin.
- Bone is a hierarchical fiber composite:
- Bone
  - Osteons
    - Lamella
      - Collagen fibers
        - » Collagen fibrils

Particle composites

- Fiber composites are ideal for improving tensile strength. Particle composites can:
  - Improve compressive stiffness.
  - Decrease weight without sacrificing strength (hollow glass sphere + polymer composite).
  - Make the material magnetic (refrigerator magnets).
  - Improve electrical or thermal characteristics (polymer metal composites).
- Traditional fiber and particle composites have fibers/particles of around micron size.

Nano-particle composites

- Exciting area, has seen dramatic results lately.
- Much less exotic than it sounds.
  - Many nano-particulate materials are commercially available at moderate cost.
- Advantages of nano-particles
  - Allows small features (< 1 micron) of composite, important for electronics or complex machines.
  - Composite is more homogeneous, consistent physical behavior.
  - Some material properties depend on dimension, and are tunable by particle size.

Nano-particle Solar Cells

- Developed by Paul Alivisatos at Berkeley.
- Nanometer (7x60) sized inorganic rods are oriented vertically and held in a polymer matrix.
- Very simple (room temperature) process.
- Potential for very low-cost, large area solar cells. 2 local companies work on this.

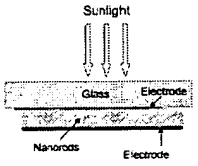

Hierarchical materials

- Often we want large volume materials with low density – e.g. for ships, packing and aircraft.
- How do you maximize strength?
- The classical triangular truss is a good design.
  - Really 1-dimensional, so very low density.
- But its not the best possible…

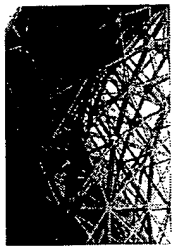

Hierarchical materials

- Long, straight members will buckle under high load.
- Strength can be increased using hierarchical structure (trusses made from trusses)
- The Eiffel tower used this structure (because of limited beam length!), and was by far the strongest structure for weight at the time.

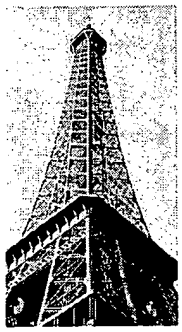

Hierarchical material fabrication

- Its impossible to build small hierarchical trusses by conventional methods.
- But 3D printers are limited neither by complexity or by geometry (the many cavities which cant be created by casting or milling).
- Hierarchical structures are the natural way to build low-density, high-strength volumes with 3D printing.

Cellular materials

- Honeycomb: two flat sheets sandwiching a layer of honeycomb.
- Very strong resistance to bending.
- Used for aircraft floors.
- Good vibration resistance.

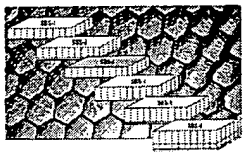

- Soft honeycombs used for shock absorption. Sometimes visible in athletic shoes.

Honeycomb strength

- Honeycomb is a very efficient structure for bending stiffness.
- In a normal Beam, the bending stiffness is EI, where E is Young's modulus, I is the "moment of inertia" of the beam cross-section.

- $I = b\,a^3/12$, (b is depth into the page).

Honeycomb strength

- In a honeycomb structure, the mass is concentrated in the top and bottom sheet.

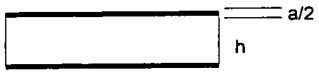

- The moment of inertia is

$$I = b\,a\,h^2/4 \quad (b \text{ is depth})$$

- Much higher bending stiffness for a given weight ($h >> a$)

Cellular hierarchies

- Honeycomb has some weakness. The cell faces can collapse under pressure.
- By adding small cells to reinforce the large ones, we eliminate the weakness.
- This structure is used in animal bone, and a number of plant materials.

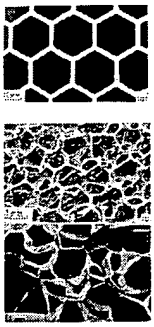

Plastic foams

- Plastic foams are usually thermoplastics.
- Traditional methods use volatile hydrocarbons mixed with the polymer.
- On heating, they create bubbles in the polymer.
- The voids are rather irregular, and the foam has lower strength than theoretically possible.

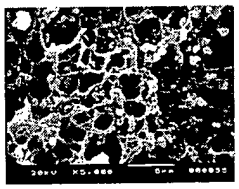

Plastic foams

- Lately microcell foams have been developed.
- The foams use a gas (CO_2 or Nitrogen) dissolved under pressure to create voids.
- Under sudden change in pressure/temperature, small voids form, and do not have time to join into larger voids.
- Result is more uniform cells and better strength.

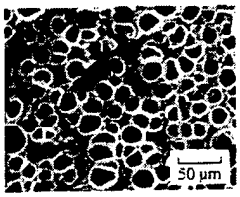

Plastic foams

- But the uniform cell foams are like single-scale trusses, and susceptible to failure across large faces. Greater strength would result from multi-scale cells.
- Still an open problem how to do this...

Director of Maxillofacial Prosthetics-Jonathan and Maxine Ferencz
Advanced Education Program in Prosthodontics at New York University
College of Dentistry, New York, NY
Clinical Assistant Professor of Surgery (Maxillofacial Prosthetics)
Director of Craniofacial Prosthetics-The Institute of Recontructive Plastic
Surgery at Langone-New York University Medical Center, New York, NY
(See attached curriculum vitae)

With respect to measurement of the Modulus of Elasticity on dental posts by an Instron machine, the measurements are done as follows:
The standard for testing dental materials to determine the mechanical properties (such as Young's Modulus) of a material, is performed using a vertical pull device such as the one made by INSTRON Inc. Fiber reinforced composites have a mechanical property called "anisotropy". This means that if pulled vertically (as is the case with an with Instron" machine) the fibers engage more vs. transversely where more resin and less fibers engage the forces. Therefore the transverse values by definition will be lower due to innate material properties. In order to report consistent values for materials the vertical methods afforded through the use of an Instron machine are generally employed in dental materials testing For reinforced composites (such as those made of resin and fiber) applying the testing force at transverse angles other than a vertical orientation would incorporate more resin and less fiber into the results and should not be considered the standard because in any transverse calculation the resin is the weakest link and will skew the results. The vertical test is the standard because all traditional materials have been tested that way such as gold and other alloys.

I further declare that all statements made herein of my own knowledge are true and that all statements made on information and belief are believed to be true; and further that these statements were made with knowledge that willful false statements and the like so made are punishable by fine or imprisonment, or

both, under Section 1001 of Title 18 of the United States Code, and that such willful false statements may jeopardize the validity of the application or any patent issuing thereon.

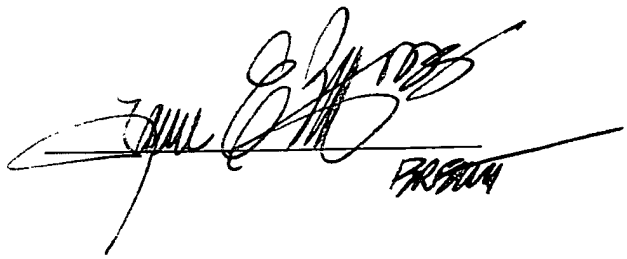

Dated: April 29, 2008

Lawrence E. Brecht, B.A., D.D.S.
275 Madison Avenue
Suite 2900
New York, N.Y. 10016-1101
(212) 557-1300
FAX (212) 557-1675
lebrecht@nycpros.com

Personal Information:

Date of Birth:	September 20, 1958, New York, NY
Married:	June 22, 1985 – Bernadette Joyce
Children:	Katharine – Born September 30, 1987
	Olivia – Born October 11, 1990
	Sarah – Born March 23, 1994
Home Address:	115 Van Rensselaer Avenue
	Shippan Point
	Stamford, CT 06902 - 8019
Telephone:	(203) 964-0885
E-mail (other):	lawrence.brecht@med.nyu.edu
Citizenship:	United States of America

Education:

Archbishop Molloy High School
Briarwood, NY
NYS Regents Diploma, June, 1976

Columbia College in the City of New York
New York, NY
B.A. Biology/Psychology, October, 1980

New York University College of Dentistry
New York, NY
Doctor of Dental Surgery, June, 1985
Class Salutarian

Residency/ Fellowship:

7/1/85 - 6/30/86

Brigham & Women's Hospital/Harvard Medical School
Boston, MA
Department of Dentistry
Resident in General Practice Dentistry

7/1/85 - 6/30/86

Harvard School of Dental Medicine
Boston, MA
Department of Operative Dentistry
Postdoctoral Clinical Fellow

7/1/86 - 6/30/88	**Veterans Administration Medical Center** New York, NY Department of Dentistry Resident in Combined Prosthodontics
7/1/88 - 6/30/89	**Veterans Administration Medical Center** New York, NY Department of Dentistry Resident in Maxillofacial Prosthetics
7/1/88 - 6/30/89	**Veterans Administration Medical Center** New York, NY Department of Dentistry Chief Resident - Department of Dentistry
7/1/88 - 6/30/89	**New York University Medical Center** New York, NY Institute of Reconstructive Plastic Surgery Visiting Surgeon (Maxillofacial Prosthetics)
7/1/86 - 6/30/89	**New York University College of Dentistry** New York, NY Department of Prosthodontics & Occlusion Clinical Fellow in Prosthodontics

Academic Appointments:

9/1/95 - Present	**New York University College of Dentistry** New York, NY Division of Restorative & Prosthodontic Sciences Clinical Associate Professor of Prosthodontic & Occlusion
9/1/89 - 8/31/95	Assistant Professor of Prosthodontics & Occlusion
9/1/87 - 8/30/89	**New York University College of Dentistry** New York, NY Department of Prosthodontics & Occlusion Postgraduate Teaching Fellow in Prosthodontics
10/1/92 - Present	**New York University School of Medicine** New York, NY Department of Surgery Assistant Professor of Clinical Surgery - Plastic Surgery

	Liaison to Advanced Education Program in Prosthodontics at New York University College of Dentistry
9/1/89 - 9/30/92	**New York University Medical Center** New York, NY Institute of Reconstructive Plastic Surgery Visiting Surgeon (Maxillofacial Prosthetics)/ Liaison to Advanced Education Program in Prosthodontics at New York University College of Dentistry
9/1/89 - 12/31/95	**Montefiore Medical Center-Albert Einstein College of Medicine** Department of Dentistry Clinical Instructor - Postgraduate Residency Program in Prosthodontics
2/1/92 - 7/1/00	**Harvard School of Dental Medicine** Boston, MA Department of Prosthetic Dentistry (Postgraduate Division) Lecturer in Prosthodontics (Maxillofacial)
Hospital Appointments:	
9/1/89 - 12/31/95	**Montefiore Medical Center** Bronx, NY Department of Dentistry Assistant Attending of Dentistry
7/1/92 - 12/31/92	**Brigham & Women's Hospital/Harvard Medical School** Boston, MA Department of Plastic Surgery Visiting Surgeon (Maxillofacial Prosthetics)
2/1/93 - Present	**New York University Medical Center-Tisch Hospital** New York, NY Institute for Reconstructive Plastic Surgery Assistant Attending in Plastic Surgery (Maxillofacial Prosthetics)
University Positions & Committees:	

New York University College of Dentistry
New York, NY
Division of Restorative & Prosthodontic Sciences
Department of Comprehensive Care & Applied

9/1/90 – Present	**Director - Maxillofacial Prosthetics** Advanced Education Program in Prosthodontics
9/1/89 – 8/30/90	**Co-director - Maxillofacial Prosthetics** Advanced Education Program in Prosthodontics
9/1/89 – 6/30/93	**Director of Prosthodontics for Advanced Standing Dentists Program & Clinic Chief**
9/1/90 – 7/30/93	**Senior Module Director,** Clinic 3A - Advanced Standing Dentists Program
9/1/89 – 8/30/90	**Assistant Director of Clinical Fixed Prosthodontics**
4/90, 5/94	Judge - Clinical Section - Student Table Clinic Committee
9/1/90 – 8/30/95	Student Table Clinic Planning Committee
6/1/91 – 10/31/95	**Prosthodontic Consultant** - Cleft Palate Team, New York University College of Dentistry Center for Dentofacial Deformities
12/91 – 10/31/95	Student - Faculty Planning Committee
12/93 – 10/31/96	Student - Faculty Grievance Committee
10/94 – 10/31/96	Ad-hoc Committee for Patient Care & Clinic Management
11/94 – 10/31/96	Faculty Grievance Committee
6/99	**Strategic Planning Committee** - Global Impact Group
3/1/99 – 6/30/2000	**Postgraduate Program in Prosthodontics** - Chair, Ad Hoc Committee on Clinical Productivity Standards
2/2003 - Present	Senior Honors Prosthodontics Selection Committee
11/2003	ADA Accreditation Panel - Postgraduate Program in Prosthodontics
2004	Head of development campaign to raise $150,000 in honor of Professor Francis V. Panno Postgraduate Prosthodontics Seminar Room

Lecture Responsibilities:

1989 - Current

Advanced Education Program in Prosthodontics:

- **Course Director** - Lecture Series in Maxillofacial Prosthetics (D40.8055001) (25 one hour sessions)
- **Course Director** - Literature Review in Maxillofacial Prosthetics (D40.8050001) (25 one hour sessions)
- **Course Director** - Hospital Experience in Maxillofacial Prosthetics (D40.9063001) (10 one hour sessions)

	Postgraduate Fellowship Program in Implant Dentistry
	Pre-doctoral Dental Program: Senior Prosthodontics Honors Program Faculty Removable Prosthodontics Lecture Series Fixed Prosthodontics Lecture Series Advanced Standing Dentists Lecture Series
9/1/93 - 8/31/95	• **Course Director** - Honors Program in Prosthodontics
	Prosthodontic Faculty In-service Training Lecture Series
	Continuing Dental Education Program
	NERB Remediation Program in Prosthodontics
Hospital Responsibilities & Committees:	
	New York University Medical Center **Institute for Reconstructive Plastic Surgery** Department of Surgery New York, NY
12/1/97 – Present	**Executive Committee – IRPS**
5/1/04 – Present	**Development Campaign Committee-** **50th Anniversary IRPS** (Planning and execution of $20 million to construct new physical facility for Institute of Reconstructive Plastic Surgery including identifying and procuring construction project manager and capital campaign firms)
11/1/05 – Present	**Future of the Institute Committee** (Charged to provide plan for future direction of Institute of Reconstructive Plastic Surgery and move to departmental status within the NYU Medical Center)
1/1/95 – Present	**Director of Dental Services**
12/1/93 – Present	**Prosthetic Director - Center for Craniofacial Prosthetics**
10/1/92 – Present	**Attending Prosthodontist:** Craniofacial Team Cleft Palate Team Ear Anomalies Team Craniofacial Prosthetics Team
7/1/97 - Present	**Department of Otolaryngology** Consultant-Swallowing Disorders Center

Montefiore Medical Center
Department of Dentistry
Bronx, NY

9/1/89 - 12/31/95 **Prosthodontic Consultant** - Cleft Palate Team / Center for Craniofacial Deformities

Professional Societies & Committees:

1985 - Current **Omicron Kappa Upsilon Dental Honor Society**

7/1/89 - 6/30/90	Chair - Auditing Committee
7/1/90 - 6/30/91	Auditing Committee, Publications Committee
7/1/91 - 6/30/92	Auditing Committee, Publications Committee
7/1/92 - 6/30/93	Publications Committee, Student Activities Committee
7/1/93 - 6/30/94	Auditing Committee Student Activities Committee
7/1/94 - 6/30/95	Chair-Auditing Committee Student Activities Committee
7/1/95 - 6/30/95	Chair-Auditing Committee
7/1/95 - 6/30/96	Chair-Auditing Committee
7/1/96 - 6/30/97	Chair-Auditing Committee

1985 - 1989 **American Association of Hospital Dentists**

1986 - Current **American College of Prosthodontists**

1/1/92 - 12/31/95	Committee on the Care of the Maxillofacial Patient
1/1/92 - 12/31/95	Computer Committee
1993, '94, '96, '97, '99	New York Section Delegate to Annual ACP Meeting House of Delegates Session
1999, 2003	Judge - Table Clinics Competition
2003 – 2005	Regional coordinator (NY, CT, VT)-Educational Foundation Annual Giving Campaign
2008 – Current	Board of Directors, Northeast Regional Representative

1991 - Current **American College of Prosthodontists - New York Section**
Liaison to Postgraduate Educational Programs
Program Chairman - 1992 Fall Meeting
5/1/93 - 4/30/97 Secretary

5/1/97 - 4/30/98 Vice-President
1/1/98 - 12/31/99 President
10/1/01 – 12/31/04 Nominating Committee

1987 - 1993 **Federation of Prosthodontic Organizations**

1990 - Current **American Cleft Palate-Craniofacial Association**

1991 - 1999 **Northeastern Gnathological Society**

1992 - 2002 **New York Head & Neck Society**

1992 - 1995 **American Association of Dental Schools**

1995 - 2000 **American Association of Dental Research**

1997 - Current **American Dental Association**

1997 - Current **New York State Dental Society**

1997 - Current **First District Dental Society**

1998 - Current **American Academy of Maxillofacial Prosthetics**

2002 – Current: **Fellow**
1998 – 2002: **Associate Fellow**
1999 – 2002: Insurance/Oral Health Committee
2002 – 2005: Education Committee, Insurance Committee, and Research Committee
2005 – Current: Fellowship Committee, Ectodermal Dysplasia Committee, ABP Examiner Committee (Chair), and Insurance/Oral Health Committee
2005 – Current: Board of Directors

1998 - Current **Greater New York Academy of Prosthodontics**

Fellow
1999 - Reception Committee
1999 - Spring Meeting Committee
2000 - Fall Arrangements Committee
2001 - Fall Arrangements Committee,
Spring Meeting Committee
2002 - Fall Arrangements Committee,
Dinner Meeting Committee
2003 - Fall Arrangements Committee, Vice-Chair Elect
2004 - Fall Arrangements Committee, Vice-Chairman
2005 - Fall Arrangements Committee, Chairman
Reception Committee, Chairman
Publication Committee, Vice-Chairman
Liaison to the ACP Forum

Site Selection Committee
2006 - Site Selection Committee, Chairman
Publications Committee, Chairman
Fall Arrangements Committee (Adviser)
Strategic Planning Committee
Program Committee, Finance Committee,
Membership Committee
2007 - Council Member, Site Selection Committee-Chairman, Publications Committee-Chairman
Program Committee, Membership Committee
2008 – Council Member, Secretary-elect, Site Selection Committee-Chairman, Publications Committee-Chairman, Editor, Membership Committee

1999 - Current <u>Academy of Prosthodontics</u>
Active Fellow
2001 – 2002: Associate Fellowship Committee (Co-Chair)
2003 – 2004: Audiovisual Committee
2004 – Discusser: Dr. Alan Hickey's presentation
2005 – Present: Program Committee, Communications Committee
2006 – Discusser: Dr. Kent Knoernschild & Dr. John Zarb presentation
2007 – Local Arrangements, Reception Committee
2007 – Discusser: Dr. Peter Stevenson-Moore presentation

2001 - Current <u>New York Academy of Dentistry</u>
Active Fellow
2002 – Current: Dinner Committee
2004 – Current: Membership Committee

Other Societies

1980 - Current **Columbia College Alumni Association**
1985 - Current **New York University College of Dentistry Alumni Association**

1993-1994	College & Undergraduate Affairs Committee
1993-1994	Program Committee
1995	Alumni Reunion Committee
2005	Class of 1985 20th Reunion Committee

1986 - Current **Harvard School of Dental Medicine Alumni Association**

1999	HSDM NY Region Alumni Reception Dinner Committee

Consultant Positions:

January, 2008 – Current	**NYUCD/NYUSoM Aesthetic and Reconstructive Research Consortium**
June, 2009	**Member-Scientific Advisory Board** 2nd International Symposium in Bone Conduction Hearing-Craniofacial Osseointegration Goteborg, SWEDEN
June, 2008	**Member-Scientific Advisory Committee** 3rd Advanced Digital Technology in Head and Neck Reconstruction Meeting, Cardiff, Wales, UK
April, 2007	**Member-Scientific Advisory Committee** 10th Biannual Conference on Pre-Prosthetic Surgery Charleston, SC
March, 2005	**Member-Scientific Advisory Committee** 2nd Advanced Digital Technology in Head and Neck Reconstruction Meeting, Banff, Alberta, CANADA
2008 – Current	**Reviewer** – *International Journal of Prosthodontics*
2005 – Current	**Reviewer** – *Special Care in Dentistry*
2004 – Current	**Reviewer** – *Cleft Palate-Craniofacial Journal*
2002 – Current	**Reviewer** – *Journal of Prosthetic Dentistry*

Board Certification Status:

Board-eligible in Prosthodontics
(Part I – Completed & Passed February 2003)

Invited Lectures/Presentations/Workshops/Visiting Professorships:

(May, 2009)	Academy of Prosthodontics Chicago, IL
(February, 2009)	American Prosthodontic Society Chicago, IL
July, 2008	**"The History of Nasoalveolar Molding and Columella Elongation "** Workshop in Nasoalveolar Molding Institute of Reconstructive Plastic Surgery Workshop in New York University Medical Center New York, NY

April, 2008	Flores, R, Obaid, S, Hshemi, T, Grayson, BH, Cutting, CB & **Brecht, LE:** **"Reduced Need for Alveolar Bone Grafting Following Presurgical Orthopedics and Primary Gingivoperiosteoplasty in Patients with Bilateral Clefts of the Lip, Alveolus and Palate"** American Cleft Palate-Craniofacial Association 65th Annual Scientific Session Philadelphia, PA
April, 2008	**"Nasoalveolar Molding and Pre-surgical Columella Elongation in Unilateral and Bilateral Clefts of the Lip, Alveolus and Palate"** Study Session Conference Workshop American Cleft Palate-Craniofacial Association 65th Annual Scientific Session Philadelphia, PA
March, 2008	**"Reconstructive and Esthetic Dental Treatment for the Cleft Palate Patient"** Comprehensive Management of the Cleft Lip/Palate Patient and Family Symposium Institute of Reconstructive Plastic Surgery New York University Medical Center New York, NY
January, 2008	**"The History of Nasoalveolar Molding and Columella Elongation "** Workshop in Nasoalveolar Molding Institute of Reconstructive Plastic Surgery Workshop in New York University Medical Center New York, NY
October, 2007	**"Dentofacial Aspects of Nasoalveolar Molding"** American Academy of Maxillofacial Prosthetics 55th Annual Scientific Session Scottsdale, AZ
October, 2007	**"Nasoalveolar Molding and Cleft Palate Care"** Japan Prosthodontic Society Tokyo, JAPAN
August, 2007	King, TW, Grayson, BH, **Brecht, LE**, & Cutting, CB: **"Anthropometric Evaluation of Nasal Morphology in Bilateral Cleft Lip and Palate Following Nasoalveolar Molding: 12 Year Follow-up"** International Society of Craniofacial Surgery XII Scientific Session-Salvador, Bahia, BRAZIL

July, 2007	**"The History of Nasoalveolar Molding and Columella Elongation "** Workshop in Nasoalveolar Molding Institute of Reconstructive Plastic Surgery Workshop in New York University Medical Center New York, NY
May, 2007	**"Nasoalveolar Molding"** Visiting Professor Maxillofacial Prosthetics and Hospital Dentistry UCLA School of Dentistry Los Angeles, CA
April, 2007	**"Nasoalveolar Molding and Pre-surgical Columella Elongation in Unilateral and Bilateral Clefts of the Lip, Alveolus and Palate"** Study Session Conference Workshop American Cleft Palate-Craniofacial Association 64th Annual Scientific Session Broomfield, CO
January, 2007	**"The History of Nasoalveolar Molding and Columella Elongation "** Workshop in Nasoalveolar Molding Institute of Reconstructive Plastic Surgery Workshop in New York University Medical Center New York, NY
December, 2006	**"Improving the Quality of Life for The Forgotten Patient-Advances in Cleft Palate Patient Management"** Greater New York Academy of Prosthodontics The Jazz at Lincoln Center 52nd Annual Scientific Program New York, NY
November, 2006	**"Nasoalveolar Molding-A Review of 15 Years Experience with an Evolving Technique"** Illinois Association of Craniofacial Teams Northwestern University Medical Center Chicago, IL
November, 2006	Navarro, B, **Brecht, L,** & Kitzis, D **"Prosthetic Rehabilitation of a Combined Maxillectomy and Mandibular Discontinuity Defect using Progressive Anterior Guidance in an Edentulous Patient"** American College of Prosthodontists Annual Session Miami, FL

November, 2006	Kapetanakos, MH, Brecht, LE, Vahidi, F & Jahangiri, L **"Nasoalveolar Molding and Simplification of Cleft Palate Care"** American College of Prosthodontists Annual Session Miami, FL
October, 2006	Navarro, B, **Brecht, L,** & Kitzis, D **"Prosthetic Rehabilitation of a Combined Maxillectomy and Mandibular Discontinuity Defect using Progressive Anterior Guidance in an Edentulous Patient"** American College of Prosthodontists-New York Section New York, NY
October, 2006	Kapetanakos, MH, Brecht, LE, Vahidi, F & Jahangiri, L **"Nasoalveolar Molding and Simplification of Cleft Palate Care"** American College of Prosthodontists-New York Section New York, NY
October, 2006	**"Nasoalveolar Molding and Columella Elongation" Continuing Education Workshop** International Congress on Maxillofacial Rehabilitation Combined AAMP/ICMP Meeting Maui, Hawaii
October, 2006	Navarro, B, **Brecht, L,** & Kitzis, D **"Prosthetic Rehabilitation of a Combined Maxillectomy and Mandibular Discontinuity Defect using Progressive Anterior Guidance in an Edentulous Patient"** International Congress on Maxillofacial Rehabilitation Combined AAMP/ICMP Meeting - *(Poster clinic)* Maui, Hawaii
September, 2006	**"The Role of the Maxillofacial Prosthodontist on Interdisciplinary Cleft Palate and Craniofacial Teams"** Institute of Reconstructive Plastic Surgery New York University Medical Center New York, NY
July, 2006	**"The History of Nasoalveolar Molding and Columella Elongation "** Workshop in Nasoalveolar Molding Institute of Reconstructive Plastic Surgery Workshop in New York University Medical Center New York, NY

April, 2006	**"Auricular Reconstruction-Prosthetic and Surgical Options"** National Foundation for Facial Reconstruction Workshop New York University Medical Center New York, NY
April, 2006	Garfinkle, J, Grayson, BH, **Brecht, LE** & Cutting CB **"Long-term Effects on Midface Growth of Gingivoperiosteoplasty with Presurgical Infant Orthopedics in Unilateral Cleft Lip and Palate"** American Cleft Palate-Craniofacial Association 63rd Annual Scientific Session Vancouver, British Columbia, CANADA
April, 2006	**"Nasoalveolar Molding and Pre-surgical Columella Elongation in Unilateral and Bilateral Clefts of the Lip, Alveolus and Palate"** Study Session Conference Workshop American Cleft Palate-Craniofacial Association 63rd Annual Scientific Session Vancouver, British Columbia, CANADA
April, 2006	**"Optimizing Esthetics with Procera® Restorations"** Nobel Biocare World Congress Baltimore, MD
February, 2006	**"Extreme Prosthetics: Maxillofacial Prosthodontics in the Patient Care Continuum"** Chicago Mid-Winter Dental Meeting American College of Prosthodontists Program Chicago, IL
February, 2006	**"The Role of the Maxillofacial Prosthodontist on Interdisciplinary Cleft Palate and Craniofacial Teams"** Institute of Reconstructive Plastic Surgery New York University Medical Center New York, NY
December, 2005	Venkatachalam, B & **Brecht, LE**: **"The Multidisciplinary Approach to Dental Treatment of a Patient with EEC Syndrome: A Case Report"** Greater New York Academy of Prosthodontics 51st Annual Scientific Session - *(poster clinic)* Jazz at Lincoln Center, New York, NY
October, 2005	**"The History of Nasoalveolar Molding and Columella Elongation "** Workshop in Nasoalveolar Molding Institute of Reconstructive Plastic Surgery Workshop in

New York University Medical Center
New York, NY

October, 2005

Venkatachalam, B & **Brecht, LE**:
"The Multidisciplinary Approach to Dental Treatment of a Patient with EEC Syndrome: A Case Report"
American College of Prosthodontics Annual Session
Annual Scientific Session *(poster clinic)*
Los Angeles, CA

October, 2005

Venkatachalam, B & **Brecht, LE**:
"The Multidisciplinary Approach to Dental Treatment of a Patient with EEC Syndrome: A Case Report"
American College of Prosthodontics –New York Section
Annual Scientific Session *(poster clinic)*
New York, NY

October, 2005

"An Update on the 21089 and Infant Cleft Palate Care: What We Now Know After 10 Years of NAM"
American Academy of Maxillofacial Prosthetics
53rd Annual Scientific Meeting
Los Angeles, CA

September, 2005

"Maxillofacial Prosthetic Care for Children with Cleft Lip, Alveolus and Palate, Hemifacial Microsomia and Other Anomalies of the Craniofacial Region"
Center for Disease Control & National Foundation for Facial Reconstruction Interdisciplinary Conference for Children Born with Craniofacial Malformations
New York University Medical Center, NY, NY

May, 2005

"Nasoalveolar Molding in Infants Born with Clefts of the Lip, Alveolus and Palate"
American Association of Orthodontics
105th Annual Session
San Francisco, CA
(Table clinic presentation-authors: Shetye, P, Grayson, BH, **Brecht, LE**, & Cutting, CB)
Awarded the Joseph E. Johnson Award for Clinical Excellence

April, 2005

"Nasoalveolar Molding and Presurgical Columella Elongation in Unilateral and Bilateral Clefts of the Lip, Alveolus and Palate"
Study Session Conference Workshop
American Cleft Palate-Craniofacial Association
62nd Annual Scientific Session
Myrtle Beach, SC

January, 2005	**"Maxillofacial and Craniofacial Prosthetics in Reconstructive Plastic Surgery"** Institute of Reconstructive Plastic Surgery Workshop in New York University Medical Center New York, NY
January, 2005	**'The History of Nasoalveolar Molding and Columella Elongation "** Workshop in Nasoalveolar Molding Institute of Reconstructive Plastic Surgery Workshop in New York University Medical Center New York, NY
October, 2004	**"The History of Nasoalveolar Molding and Columella Elongation "** Workshop in Nasoalveolar Molding Institute of Reconstructive Plastic Surgery Workshop in New York University Medical Center New York, NY
March, 2004	**"Cleft Palate Care from Infancy to Adulthood – The Prosthodontist's Role"** New York Academy of Dentistry New York, NY
March, 2004	**"The History of Nasoalveolar Molding and Columella Elongation "** Study Session Conference Workshop American Cleft Palate-Craniofacial Association 61st Annual Scientific Session Chicago, IL
February, 2004	**"Microvascular Reconstruction of the Pediatric Mandible"** Warren, SM, Borud, S, Brecht, LE, Longaker, MT & Siebert, JW Northwest Society of Plastic Surgeons 42nd Annual Meeting Lake Louise, Alberta, Canada
December, 2003	**"Maxillofacial and Craniofacial Prosthetics – Their Role in Interdisciplinary Team Care"** Institute of Reconstructive Plastic Surgery New York University Medical Center New York, NY
November, 2003	**"History and Evolution of Nasoalveolar Molding and Columella Elongation"** Workshop in Nasoalveolar Molding

Institute of Reconstructive Plastic Surgery
New York University Medical Center
New York, NY

October, 2003 — **"Nasoalveolar Modeling and Columella Elongation"**
Cutting, CB Grayson, BH, & Brecht, LE
American Society of Plastic Surgeons
Annual Scientific Session
San Diego, CA

June, 2003 — **"History and Evolution of Nasoalveolar Molding and Columella Elongation"**
Workshop in Nasoalveolar Molding
Institute of Reconstructive Plastic Surgery
New York University Medical Center
New York, NY

March, 2003 — **"Facial Prosthetics and Reconstructive Plastic Surgery'**
National Foundation for Facial Reconstruction
Board of Director's Meeting
New York, NY

March, 2003 — **"Maxillofacial & Craniofacial Prosthetics in Plastic Surgery"**
Institute of Reconstructive Plastic Surgery
New York University Medical Center
New York, NY

November, 2002 — **"Current Rehabilitation of the Cleft Palate Patient: The NYU/IRPS Experience"**
American Academy of Maxillofacial Prosthetics
50th Anniversary Annual Scientific Session
Orlando, FL

June, 2002 — **"Workshop in Nasoalveolar Molding & Columellar Elongation"**
Institute of Reconstructive Plastic Surgery
New York University Medical Center
New York, NY

May, 2002 — **"Nasoalveolar Molding and Columellar Elongation"**
Study Session Conference Workshop
American Cleft Palate-Craniofacial Association
59th Annual Scientific Session
Seattle, WA

December, 2001 — **"Maxillofacial & Craniofacial Prosthetics"**
Institute of Reconstructive Plastic Surgery
New York University Medical Center

New York, NY

November, 2001 — **"State of the Art in Craniofacial Rehabilitation"**
Dean's Development Program
New York University College of Dentistry
New York, NY

June, 2001 — **"The Long-term Effect of Presurgical Nasoalveolar Molding on Three-Dimensional Nasal Shape in Complete Unilateral Clefts"**
Grayson, BH, Cutting, CB, Maull, D, & Brecht, LE
9th International Congress on Cleft Palate and Related Craniofacial Anomalies
Goteborg, Sweden

June, 2001 — **"Treatment of the Infant with Cleft Lip, Alveolus and Palate"**
Grand Rounds-Department of Pediatrics
Stamford Hospital
Stamford, CT

May, 2001 — **"Reconstruction of the Pediatric Craniofacial Patient: Evolving Technologies and New Paradigms of Care"**
Academy of Prosthodontics
83rd Annual Scientific Session
Santa Fe, NM

April, 2001 — **"Presurgical Nasoalveolar Molding"**
American Cleft Palate-Craniofacial Association
58th Annual Scientific Session
Minneapolis, MN

April, 2001 — **"Interdisciplinary Management of the Craniofacial and Cleft Palate Patients"**
Visiting Professor
University of Pittsburgh
Cleft Palate-Craniofacial Team
Pittsburgh, PA

April, 2001 — **"Presurgical Nasoalveolar Molding in Early Cleft Palate Care"**
Visiting Professor
University of Pittsburgh
Department of Plastic Surgery
Pittsburgh, PA

February, 2001 — **"Interdisciplinary Management of the Craniofacial and Cleft Palate Patients"**

American Association of Orthodontists
Interdisciplinary Conference
Dallas Adams Mark Hotel
Dallas, TX

January, 2001 — **"Nasoalveolar Molding and Columellar Elongation in Early Cleft Palate Care"**
Grand Rounds-Combined Cleft Palate Teams: St. Charles Hospital, North Shore University Hospital, Long Island Jewish Medical Center, Stony Brook University Hospital
St. Charles Hospital
Port Jefferson, NY

December, 2000 — **"Maxillofacial & Craniofacial Prosthetics"**
Institute of Reconstructive Plastic Surgery
New York University Medical Center
New York, NY

November, 2000 — **"Modern Methods in the Early Management of Congenital Anomalies"**
3rd Joint Symposium-American Academy of Maxillofacial Prosthetics & International Congress of Maxillofacial Prosthetics
(Keynote Speaker/Panel Discussant)
Kauai, HI

November, 2000 — **"Prosthetic Management of Congenital Defects"**
The Italian Dental Society
Staten Island, NY

April, 2000 — **"Presurgical Nasoalveolar Molding & Columellar Lengthening"**
Study Session/Eye Opener
American Cleft Palate-Craniofacial Association
57th Annual Meeting
Atlanta, GA

April, 2000 — **"Associations Between Severity of Clefting and Maxillary Growth in ULCP Patients Treated with Infant Orthopedics"**
American Cleft Palate-Craniofacial Association
57th Annual Meeting
Atlanta, GA

April, 2000 — **"Cephalometric Analysis of Facial Morphology 5-Years Following Different Modes of Infant Orthopedics in UCLP Patients"**

American Cleft Palate-Craniofacial Association
57th Annual Meeting
Atlanta, GA

March, 2000

"Nasoalveolar Molding and Columellar Lengthening: State of the Art in Cleft Care"
Grand Rounds-Department of Dentistry
Overlook Hospital
Summit, NJ

February, 2000

"Nasoalveolar Molding and Columellar Lengthening: State of the Art in Cleft Care"
American Academy of Restorative Dentistry
70th Annual Scientific Meeting-Drake Hotel
Chicago, IL

December, 1999

"Maxillofacial & Craniofacial Prosthetics in Reconstructive Plastic Surgery"
Institute of Reconstructive Plastic Surgery
NYU Medical Center
New York, NY

October, 1999

"The Effect of Early Le Fort III Surgery on Permanent Molar Eruption in Patients with Craniosynostosis"
Grayson, BH, Santiago, PE, Brecht, LE, Degen, M & McCarthy, JG
International Society of Craniofacial Surgery
VIIIth International Congress
Taipei, Taiwan

October, 1999

"Cleft Palate Care: Interdisciplinary Advances"
American College of Prosthodontists
Annual Scientific Meeting
New York, NY

October, 1999

"Presurgical Infant Nasoalveolar Molding and Columellar Lengthening in the Cleft Palate Patient"
University of Glasgow-Canniesburn Hospital
Workshop
International Course in Advanced Cranio-Maxillofacial Surgery-Beardmore Conference Hotel
Glasgow, Scotland

October, 1999

"Prosthodontic Rehabilitation of the Cleft Patient"
University of Glasgow-Canniesburn Hospital
International Course in Advanced Cranio-Maxillofacial Surgery-Beardmore Conference Hotel
Glasgow, Scotland

July, 1999	**"Fabrication of a Nasoalveolar Presurgical Infant Orthopedic Molding Device for the Bilateral Cleft Palate Patient"** Faculty-Workshop on Treatment of Cleft Lip & Palate School of Dentistry-University of Western Ontario London, Ontario, Canada
June, 1999	**"Microvascular Reconstruction of the Pediatric Mandible"** Borud L, Siebert JW, & **Brecht LE** International Society of Reconstructive Microsurgery Annual Meeting Los Angeles, CA
June, 1999	**"Cleft Palate Care: Advances in the Interdisciplinary Approach"** Grand Rounds-Department of Dentistry Carolinas Medical Center Charlotte, NC
April, 1999	**"Craniofacial & Cleft Plate Prosthetics - The State of the Art"** Richmond County Dental Society Richmond Country Club, Staten Island, NY
April, 1999	**"Pre-surgical Naso-alveolar Molding (NAM) and Columella Elongation – An Intercenter Report of Technique and Outcomes"** (Study Session) American Cleft Palate-Craniofacial Association 56th Annual Meeting Scottsdale, AZ
April, 1999	**"Effect of Presurgical Nasal Molding on Unilateral Cleft Lip and Palate"** Lin, Grayson, Brecht, Lee & Cutting American Cleft Palate-Craniofacial Association 56th Annual Meeting Scottsdale, AZ
April, 1999	**"The Need for Surgical Columella Lengthening and Nasal Width Revision Before the Age of Bone Grafting in Patients with Bilateral Cleft Lip Following Presurgical Nasal Molding and Columella Lengthening"** Lee, Grayson, **Brecht**, Cutting, Lin American Cleft Palate-Craniofacial Association 56th Annual Meeting Scottsdale, AZ

April, 1999	**"Long-term Study of Midface Growth in Unilateral Cleft Lip and Palate Patients Following Gingivoperioplasty"** Lee, Grayson, Brecht, Cutting, Lin American Cleft Palate-Craniofacial Association 56th Annual Meeting Scottsdale, AZ
March, 1999	**"Current Concepts in Cleft Palate Care"** Columbia University School of Dental & Oral Surgery Graduate Prosthodontic Program New York, NY
December, 1998	**"Fabrication of a Nasoalveolar Presurgical Infant Orthopedic Molding Devices for Cleft Palate Patients"** "Simposio Actualization en Tratamiento Labio y Paladar Fisurado" Sociedad de Beneficiencia Hospital Aleman Santiago, Chile
December, 1998	**"Prosthodontic Considerations in the Care of the Cleft Palate Patient"** "Simposio Actualization en Tratamiento Labio y Paladar Fisurado" Sociedad de Beneficiencia Hospital Aleman Santiago, Chile
December, 1998	**"Prosthodontic Considerations in the Care of the Cleft Palate Patient"** Osseointegration Academy of Santiago Santiago, Chile
October, 1998	**"Cleft Palate Care: Interdisciplinary Advances"** American Academy of Maxillofacial Prosthetics 46th Annual Scientific Meeting Victoria, British Columbia, Canada
July, 1998	**"Fabrication of a Nasoalveolar Presurgical Infant Orthopedic Molding Device for the Bilateral Cleft Palate Patient"** Faculty-Workshop on Treatment of Cleft Lip & Palate School of Dentistry-University of Western Ontario London, Ontario, Canada
June, 1998	**"Cleft Palate Care: Interdisciplinary Advances"** Montefiore Medical Center/Jacobi Medical Center/Albert Einstein College of Medicine Grand Rounds-Dental Service/Cleft Palate Team Bronx, NY

June, 1998	**"Cleft Palate Care: Interdisciplinary Advances"** University of Connecticut School of Dental Medicine Farmington, CT
May, 1998	**"Cleft Palate Care: Advances in the Interdisciplinary Approach"** Academy of Prosthodontics 80th Annual Scientific Session Colorado Springs, CO
April, 1998	**"Cleft Palate Care: Interdisciplinary Advances"** Grand Rounds-Cleft Palate Team Eastman Dental Center-University of Rochester Rochester, NY
April, 1998	**"Esthetic Restoration of Craniofacial Defects–Osseointegrated Prostheses"** National Foundation for Facial Reconstruction Board of Directors New York, NY
March, 1998	**"Neonatal Auricular Cartilage Molding"** Brecht, LE, Grayson, BH & Thorne, CH Ear Reconstruction '98 - Choices for the Future Chateau Lake Louise Alberta, Canada
March, 1998	**"Indications for Autogenous vs. Prosthetic Auricular Reconstruction: The NYU Experience"** Thorne, CH, Brecht, LE, & Hammerschlag, PE Ear Reconstruction '98 - Choices for the Future Chateau Lake Louise Alberta, Canada
January, 1998	**"Aural Atresia: Surgical Outcome in a Multidiscipline Center"** Hammerschlag, PE, Brecht, LE, Thorne, CH, & Roland, TA. American Laryngological, Rhinological & Otological Society-Eastern Section Meeting New York, NY
December, 1997	**"Cleft Palate Care: Interdisciplinary Advances"** Greater New York Academy of Prosthodontics 43rd Annual Fall Scientific Meeting New York, NY

October, 1997	**"Engineering of Cartilaginous Human Shapes in Vitro Using Plasma Derived Polymer Substances and Chondrocytes"** Northeastern Society of Plastic Surgeons Bermuda
September, 1997	**"Esthetic Restoration of Orbital Defects–Osseointegrated Prostheses"** National Foundation for Facial Reconstruction Board of Directors New York, NY
September, 1997	**"Engineering of Cartilaginous Human Shapes in Vitro Using Plasma Derived Polymer Substances and Chondrocytes"** International Society of Craniofacial Surgery VIIth International Congress Santa Fe, NM
September, 1997	**"Osseointegrated Craniofacial Implants in Pediatric Auricular Reconstruction: Indications and Contraindications"** International Society of Craniofacial Surgery VIIth International Congress Santa Fe, NM
September, 1997	**"Reconstruction of Severe Periorbital Deformities Using Microsurgical Free Tissue Transfers"** International Society of Craniofacial Surgery VIIth International Congress Santa Fe, NM
July, 1997	**"Ear Reconstruction–The Prosthetic Options"** The Treacher Collins Symposium New York University Medical Center New York, NY
May, 1997	**"Craniofacial Applications of Osseointegration"** Harvard University Combined Residency Program/ Department of Dentistry Brigham & Women's Hospital Boston, MA
May, 1997	**"Twelve year Experience of Nasoalveolar Molding Therapy in Bilateral Cleft Palate Repair"** American Association of Plastic and Reconstructive Surgeons-Annual Meeting Portland, OR

May, 1997	**"Complications Associated with Antral Augmentation Procedures"** American Rhinologic Society Scottsdale, AZ
April, 1997	**"The Effect of Early LeFort III Surgery on Permanent Molar Eruption in Patients with Craniosynostosis"** American Cleft Palate–Craniofacial Association 54th Annual Scientific Session New Orleans, LA
April, 1997	**"Long Term Effects of Nasoalveolar Molding on Three-Dimensional Nasal Shape in Unilateral Clefts"** American Cleft Palate–Craniofacial Association 54th Annual Scientific Session New Orleans, LA
November, 1996	**"Current Concepts in Craniofacial Prosthetics"** Second District Dental Society Fort Hamilton, NY
September, 1996	**"Prosthodontic Management of Velopharyngeal Insufficiency"** Eighteenth Annual Symposium on Cleft Palate Surgery New York, NY
September, 1996	**"Cleft Palate Prosthodontics"** Eighteenth Annual Symposium on Cleft Palate Surgery New York, NY
June, 1996	**"Current Concepts in Craniofacial & Maxillofacial Prosthetics"** Department of Dentistry Carolinas Medical Center, Charlotte, NC
June, 1996	**"Nasal Orthopedic Molding Appliances in Unilateral and Bilateral Cleft Palate Patients"** Grand Rounds-Department of Dentistry Carolinas Medical Center, Charlotte, NC
May, 1996	**"Reconstruction of the Periorbital Soft Tissue with Microvascular Free Tissue"** American Association of Plastic and Reconstructive Surgeons-Annual Meeting Hilton Head, SC

May, 1996	**"The Interdisciplinary Approach to Management of the Craniofacial Patient"** Harvard University Combined Residency Program/ Department of Dentistry Brigham & Women's Hospital Boston, MA
April, 1996	**"Elimination of Alveolar Bone Grafting by Primary Gingivoperiosteoplasty"** American Cleft Palate Association 53rd Annual Meeting San Diego, CA
April, 1996	**"Cleft Palate Prosthetics"** Icarus Study Club New York, NY
March, 1996	**"The Long Term Effects of Mandibular Distraction: A Cephalometric Study"** American Association of Dental Research Annual Meeting San Francisco, CA
December, 1995	**"Maxillofacial Rehabilitation of the Head & Neck Cancer Patient"** Columbia University School of Oral and Dental Surgery New York, NY
November, 1995	**"Maxillofacial Prosthetics"** Institute of Reconstructive Plastic Surgery New York University Medical Center New York, NY
November, 1995	**"Reconstruction of the Periorbital Soft Tissue with Microvascular Free Tissue"** Northeast Society of Reconstructive Plastic Surgeons Boston, MA
October, 1995	**"Extraoral Applications of Osseointegration"** New York University Medical Center New York, NY
October, 1995	**"The Interdisciplinary Approach to Management of the Craniofacial Patient"** American College of Prosthodontists-Annual Meeting Washington, DC
July, 1995	**"Introduction to Dentistry"**

Institute of Reconstructive Plastic Surgery
New York University Medical Center, New York, NY

April, 1995 — **"Presurgical Columellar Elongation with One-stage Repair of the Bilateral Cleft Lip and Nose"**
American Cleft Palate Association-Annual Scientific Session
Tampa, FL

April, 1995 — **"Oronasal Molding Appliances for Infants with Unilateral or Bilateral Cleft Lip, Alveolus and Palate"**
Harvard University Combined Residency Program/
Department of Dentistry
Brigham & Women's Hospital
Boston, MA

April, 1995 — **"Brånemark Osseointegrated Implants in the Rehabilitation of Congenital Auricular Malformations"**
Forward Face - Annual Spring Meeting
New York University Medical Center
New York, NY

March, 1995 — **"Effect of Presurgical Nasal Molding on Cleft Lip and Nose Symmetry"**
American Association of Dental Research
Annual Session
San Antonio, Texas

March, 1995 — **"Columellar Elongation in the Bilateral Cleft Lip and Nose Patient"**
American Association of Dental Research
Annual Session
San Antonio, Texas

February, 1995 — **"Nasal Orthopedic Molding Appliances in Unilateral and Bilateral Cleft Palate Patients"**
American Prosthodontic Society-Scientific Session
Hyatt Regency Hotel
Chicago, IL

January, 1995 — **"Principles of Obturator Design"**
Harvard University Combined Residency Program/
Department of Dentistry
Brigham & Women's Hospital
Boston, MA

December, 1994 — **"Current Concepts in Maxillofacial Prosthetics"**
Harvard University Combined Residency Program/

Department of Dentistry
Brigham & Women's Hospital
Boston, MA

November, 1994 — **"Maxillofacial Prosthetics in the University-based Medical Center"**
Department of Dentistry
Montefiore Medical Center, Bronx, NY

November, 1994 — **"Nasal Orthopedic Molding Appliances in Unilateral and Bilateral Cleft Palate Patients"**
Greater New York Dental Meeting
New York, NY

November, 1994 — **"Current Concepts in Maxillofacial Prosthetics"**
Greater New York Dental Meeting
New York, NY

June, 1994 — **"Cleft Palate Prosthesis"**
Long Island Cleft Palate Parents Association
East Meadow, NY

June, 1994 — **"The Role of the Maxillofacial Prosthodontist in the University-Based Hospital"**
Postdoctoral Program in Prosthetic Dentistry
Harvard School of Dental Medicine, Boston, MA

June, 1994 — **"Prosthetic Rehabilitation of Maxillary Defects"**
Grand Rounds-Department of Dentistry
Brooklyn Hospital Center, Brooklyn, NY

May, 1994 — **"Current Concepts in Craniofacial & Maxillofacial Prosthetics"**
Postdoctoral Program in Prosthetic Dentistry
Harvard School of Dental Medicine, Boston, MA

February, 1994 — **"Nasal Orthopedic Molding Appliances in Unilateral and Bilateral Cleft Palate Patients"**
Institute of Reconstructive Plastic Surgery
New York University Medical Center
New York, NY

February, 1994 — **"Current Concepts in Craniofacial & Maxillofacial Prosthetics"**
Department of Dentistry
Carolinas Medical Center, Charlotte, NC

February, 1994 — **"The Role of the Maxillofacial Prosthodontist in a University Hospital"**

Grand Rounds-Department of Dentistry
Carolinas Medical Center, Charlotte, NC

January, 1994 — **"Implants in Maxillofacial Prosthetics"**
Harvard University Combined Residency Program/
Department of Dentistry
Brigham & Women's Hospital
Boston, MA

January, 1994 — **"Current Concepts in Craniofacial & Maxillofacial Prosthetics"**
Bay Ridge Dental Society
Brooklyn, NY

December, 1993 — **"Principles of Obturator Design"**
Harvard University Combined Residency Program/
Department of Dentistry
Brigham & Women's Hospital
Boston, MA

November, 1993 — **"Nasal Orthopedic Molding Appliances in Unilateral and Bilateral Cleft Palate Patients"**
Institute of Reconstructive Plastic Surgery
New York University Medical Center
New York, NY

November, 1993 — **"Current Concepts in Maxillofacial Prosthetics"**
Indian Dental Association (U.S.A.)
Rego Park, NY

November, 1993 — **"Current Concepts in Maxillofacial Prosthetics"**
Harvard University Combined Residency Program/
Department of Dentistry
Brigham & Women's Hospital
Boston, MA

October, 1993 — **"Nasal Orthopedic Molding Appliances in Unilateral and Bilateral Cleft Palate Patients"**
American College of Prosthodontists - 24th Annual Meeting - The Wyndham Hotel
Palms Springs, CA

October, 1993 — **"Implants in Maxillofacial Prosthetics"**
Department of Dentistry
Montefiore Medical Center, Bronx, NY

August, 1993 — **"Implants in Maxillofacial Prosthetics"**
Current Concepts in American Dentistry
International Continuing Dental Education Program

New York University College of Dentistry, NY, NY

March, 1993 — **"An Overview of Intraoral and Extraoral Implants in the Maxillofacial Patient "**
The Narrows Study Club
Brooklyn, NY

December, 1992 — **"The Application of Osseointegration in Maxillofacial Prosthetics"**
Current Concepts in American Dentistry
International Continuing Dental Education Program
New York University College of Dentistry, NY, NY

September, 1992 — **"Extraoral Applications of Brånemark Osseointegrated Implants"**
Current Concepts in American Dentistry
International Continuing Dental Education Program
New York University College of Dentistry, NY, NY

May, 1992 — **"A Review of the Current Literature in Maxillofacial Prosthetics"**
Department of Dentistry
Charlotte Memorial Hospital, Charlotte, NC

May, 1992 — **"The Role of the Maxillofacial Prosthodontist in a University Hospital"**
Grand Rounds-Department of Dentistry
Charlotte Memorial Hospital, Charlotte, NC

April, 1992 — **"Extraoral Applications of Brånemark Osseointegrated Implants"**
Postdoctoral Implant Fellowship Program
New York University College of Dentistry, NY, NY

February, 1992 — **"Current Concepts in Maxillofacial Prosthetics"**
Postdoctoral Program in Prosthetic Dentistry
Harvard School of Dental Medicine, Boston, MA

December, 1991 — **"Maxillofacial Prosthetics in the Treatment of the Head & Neck Cancer Patient"**
Grand Rounds - Department of Dentistry
Brigham & Women's Hospital, Boston, MA

November, 1991 — **"Brånemark Osseointegrated Implants in the Rehabilitation of Congenital Auricular Malformations"**
Institute of Reconstructive Plastic Surgery
New York University Medical Center, New York, NY

October, 1991	**"An Introduction to Maxillofacial Prosthetics and Dental Oncology"** Grand Rounds - Department of Oral & Maxillofacial Surgery The Brooklyn Hospital Center, Brooklyn, NY
August, 1991	**"An Introduction to Maxillofacial Prosthetics and Dental Oncology"** Department of Dentistry Montefiore Medical Center, Bronx, NY
January, 1991	**"Brånemark Osseointegrated Implants and the Restoration of the Edentulous Mandible"** Department of Dentistry Veterans Administration Medical Center, New York, NY
September, 1990	**"Maxillofacial Prosthetics in the Care of the Head & Neck Cancer Patient"** Grand Rounds - Department of Otolaryngology Montefiore Medical Center, Bronx, NY
August, 1990	**"An Introduction to Maxillofacial Prosthetics and Dental Oncology"** Dental Service - Montefiore Medical Center, Bronx, NY
September, 1989	**"Maxillofacial Prosthetics in the Care of the Head & Neck Cancer Patient"** Postgraduate Prosthodontic Program Montefiore Medical Center, Bronx, NY
July, 1989	**"Dental Considerations in the Patient Experiencing Cancer Chemotherapy"** Veterans Administration Medical Center New York, NY
July, 1989	**"Dental Considerations in the Patient Experiencing Radiation Therapy for Cancer of the Head & Neck Region"** Veterans Administration Medical Center New York, NY
May, 1989	**"Maxillofacial Prosthetics in the Care of the Head & Neck Cancer Patient"** Department of Dentistry Worcester City Hospital, Worcester, MA
March, 1989	**"A Student's Perspective of a Fixed Prosthodontic Honors Program"**

American Association of Dental Schools Meeting
San Francisco, CA

January, 1989 — **"Surgical and Prosthodontic Considerations in the Restoration of the Edentulous Mandible Utilizing Brånemark Implants"**
Veterans Administration Medical Center
New York, NY

May, 1988 — **"Biological Aspects of Osseointegration"**
Veterans Administration Medical Center
New York, NY

May, 1988 — **"A Comparative Analysis of Various Implant Systems - An Historical and Current Perspective"**
New York University College of Dentistry,
New York, NY

November, 1985 — **"Oral Manifestations of Lymphoma"**
Clinico-pathologic Conference
Harvard School of Dental Medicine, Boston, MA

Invited Discussor / Moderator:

April, 2007 — **Discusser** – Dr. Peter Stevenson-Moore
Academy of Prosthodontics 89th Annual Meeting
New York, NY

May, 2006 — **Discusser** – Dr. Kent Knoernschild & Dr. John Zarb
Academy of Prosthodontics 88th Annual Meeting
San Francisco, CA

December, 2004 — **Moderator – Greater New York Academy of Prosthodontics 50th Anniversary Meeting**
The Plaza Hotel, New York, NY

May, 2004 — **Discusser** – Dr. Alan Hickey
Academy of Prosthodontics 86th Anuual Meeting
Niagara Falls, Ontario, Canada

Publications:

Book Chapters Contributor:

Mazaheri, M & Brecht, L
Presurgical Infant Orthopedics
Chapter 45
In Losee, R & Kirschner, R (Eds.)

Comprehensive Cleft Care
New York – McGraw Hill & Co. *(submitted)*

Brecht, L & Mazaheri, M
Prosthetic Management of the Cleft Patient
Chapter 49
In Losee, R & Kirschner, R (Eds.)
Comprehensive Cleft Care
New York – McGraw Hill & Co. *(submitted)*

Brecht, L, Mazaheri, M & Cohen, S
Prosthetic Management of Velopharyngeal Deficiency
Chapter 43
In Losee, R & Kirschner, R (Eds.)
Comprehensive Cleft Care
New York – McGraw Hill & Co. *(submitted)*

Brecht, L:
Maxillofacial Prosthetics
Chapter 34
In Thorne, CH S, Beasley, R, & Aston, S (Eds.)
Grabb and Smith's Plastic Surgery
6th Edition, Boston - Brown, Little & Co.
January 2007

Brecht, L:
Craniofacial & Maxillofacial Prosthetics
Chapter 16
In, McCarthy, Galianos & Boutros (Eds.)
Current Therapies in Plastic Surgery
Philadelphia, Harcourt Health Sciences, *2005*.

Brecht, L:
Maxillofacial and Craniofacial Prosthetics
Chapter 43
In Benhaim, Longaker, Greer, Lorenz, Hedrick & Chang (Eds.)
The Handbook of Plastic Surgery
New York, NY - Thieme Medical Publishers, Inc., 2004.

Brecht, L:
Maxillofacial Prosthetics
In, Lockhart, P.B., *(Ed.)*
A Practical Guide to Hospital Dental Practice,
4th Edition. Boston, MASCO Publishers *2003*.

Brecht, L, Grayson, BH & Cutting, CB:
Current Concepts for Early Management of Cleft Lip and Palate
In Taylor, Thomas D. (Ed.)

Clinical Maxillofacial Prosthetics
Carol Stream, IL - Quintessence Publishing Co. Inc., 2000.

Santiago, PE, Degen, M, Brecht, LE, Grayson, BH & McCarthy, JG:
The Effect of Early LeFort III Surgery on Permanent Molar Eruption in Patients with Craniosynostosis
In Ray Chen l (Ed.)
Craniofacial Surgery 8 - The Proceedings of the VIIIth International Congress of the International Society of Craniofacial Surgery
Bologna, Italy - Monduzzi Editore, International Co., 2000.

Brecht, LE, Thorne, CH & McCarthy, JG:
Osseointegrated Craniofacial Implants in Pediatric Auricular Reconstruction: Indications and Contraindications
In Whitaker, l (Ed.)
Craniofacial Surgery 7 - The Proceedings of the VIIth International Congress of the International Society of Craniofacial Surgery
Bologna, Italy - Monduzzi Editore, International Co. 1998.

Brecht, L:
Craniofacial Prosthetics
In Aston, S, Beasley, R, & Thorne, CH (Eds.)
Grabb and Smith's Plastic Surgery
5th Edition, Boston - Brown, Little & Co., 1997.

Original Articles:

Lee, CTH, Garfinkle, JS, Warren, SM, **Brecht, LE**, Cutting, CB, & Grayson, BH:
Nasoalveolar Molding Improves Appearance of Children with Bilateral Cleft Lip/Palate
Plastic & Reconstructive Surgery – In Press

Warren, SM, Borud, S, Brecht, LE, Longaker, MT & Siebert, JW:
Microvascular Reconstruction of the Pediatric Mandible
Plastic & Reconstructive Surgery 119(2): 649-661, 2007.

Santiago, PE, Grayson, BH, Degen, M, Brecht, LE, Singh, DG & McCarthy, JG:
The Effect of an Early Le Fort III Surgery on Permanent Molar Eruption
Plastic & Reconstructive Surgery 115(2): 423-427, 2005.

Lee, CTH, Grayson, BH, Cutting, CB, Brecht, LE, Lin, WY:
Prepubertal Midface Growth in Unilateral Cleft Lip and Palate Following Alveolar Molding and Gingivoperiosteoplasty
Cleft Palate-Craniofacial Journal 41(4):375-380, 2004.

Thorne, CH, Brecht, LE, Bradley, JP, Levine, J & Longaker, MT:
Auricular Reconstruction: Indications for Autogenous and Prosthetic Techniques
Plastic & Reconstructive Surgery 107:1241-1252, 2001.

Peltomaki, T, Vendittelli, BL, Grayson, BH, Cutting, CB, Brecht, LE:
Associations Between Severity of Clefting and Maxillary Growth in UCLP Patients Treated with Infant Orthopedics
Cleft Palate-Craniofacial Journal 38(6):582-586, 2001.

Vendittelli, BL, Peltomaki, T, Grayson, BH, Cutting, CB, Brecht, LE:
Cephalometric Analysis of Facial Morphology 5 Years Following Different Modes of Infant Orthopedics in UCLP Patients
(Accepted for publication-Cleft Palate-Craniofacial Journal)

Grayson, BH, Santiago, PE, Brecht, LE, & Cutting, CB:
Presurgical Nasoalveolar Molding in Infants with Cleft Lip and Palate
Cleft Palate-Craniofacial Journal 36:486-498, 1999.

Maull, DJ, Grayson, BH, Cutting, CB, Brecht, LE, Bookstein, F, Khorrambadi, D, Webb, JA & Hurwitz, D:
Long Term Effects of Nasoalveolar Molding on Three-Dimensional Nasal Shape in Unilateral Clefts
Cleft Palate-Craniofacial Journal 36:391-397, 1999.

Zimbler, MS, Lebowitz, RA, Glickman, RS, Brecht, L, & Jacobs, JB:
Antral Augmentation, Osseointegration, and Sinusitis: The Otolaryngologist's Perspective
Am. J Rhinology 12:311-316, 1998.

Ting, V, Sims, CD, Brecht, LE, McCarthy, JG, Kasabian, AK, Connelly, PR, Elisseeff, J, Gittes, GK & Longaker, MT:

In Vitro **Prefabrication of Human Cartilage Shapes Using Fibrin Glue and Human Chondrocytes**
Ann. Plast. Surg. 40:413-421, 1998.

Cutting, CB, Grayson, BH, Brecht, LE, Santiago, P, Wood, R, & Kwon, SM:
Presurgical Columellar Elongation and Primary Retrograde Nasal Reconstruction in One-Stage Bilateral Cleft Lip and Nose Repair
Plast. Recconstruct. Surg. 101:630-639, 1998
(Awarded American Society of Maxillofacial Surgeons Best Paper Award for 1999- ASPRS/PSEF/ASMS Annual Meeting, October, 1999)

Cutting, CB, Grayson, BH & Brecht, LE:
Columellar Elongation in Bilateral Cleft Lip
Plast. Recconstruct. Surg. 102:1761, 1998

Hammerschlage, PE, Thorne, CH, Roland, TJ & Brecht, LE:
Aural Atresia: Surgical Outcome in a Multidiscipline Center
(Submitted for publication- Laryngoscope)

Santiago, PE, Grayson, BH, Gianoutsis, ME, Brecht, LE, Kwon, SM, & Cutting, CB
Reduced Need for Alveolar Bone Grafting by Presurgical Orthopedics and Primary Gingivoperiosteoplasty
Cleft Palate – Craniofacial Journal 35:77-80, 1998.

Ting, V, Sims, CD, McCarthy, JG, Brecht, LE, Kasabian, AK, Dublin, BK, Gittes, GK, & Longaker, MT:
Engineering of Cartilaginous Human Shapes *In Vitro* Using Plasma-derived Polymer Substances and Chondrocytes
Plast. Surg. Forum 20:63-65, 1997.

Cutting, CB, Grayson BH & Brecht, LE:
Presurgical Columellar Elongation with One Stage Repair of the Bilateral Cleft Lip and Nose.
Proc. Am, Cleft Palate Craniofac. Assoc. 52:58, 1995.

Letters:

Cutting, CB, Grayson, BH & Brecht, LE
Columellar Elongation in Bilateral Cleft Lip
Plast. Reconstruct. Surg. 102:1761-1762, 1998

Abstracts:

Obaid, S, Hashemi, T, Grayson, BH, Cutting CB, & **Brecht, LE**
Reduced Need for Alveolar Bone Grafting Following Presurgical Orthopedics and Primary Gingivoperiosteoplasty in Patients with Bilateral Clefts of the Lip, Alveolus and Palate
Proceedings of the 65th Annual Scientific Session American Cleft Palate-Craniofacial Association, p 66 April, 2008

Grayson, BH, Cutting CB, **Brecht, LE**, Maroutsis, MQ
Nasoalveolar Molding and Presurgical Columella Elongation in Patients with UCLP and BLCP
Proceedings of the 65th Annual Scientific Session American Cleft Palate-Craniofacial Association, p 61 April, 2008

Brecht, L
Dentofacial Aspects of Nasoalveolar Molding
Program of the 55th Annual Scientific Session American Academy of Maxillofacial Prosthetics, p 27-28 October, 2007

Brecht, L
Nasoalveolar Molding and Columella Elongation in Cleft Palate Care
Proceedings of the 2nd Joint Meeting of the Japan Prosthodontic Society and the Greater New York Academy of Prosthodontics, p 36. October 2007

King, TW, Grayson, BH, **Brecht, LE**, & Cutting, CB:
Anthropometric Evaluation of Nasal Morphology in Bilateral Cleft Lip and Palate Following Nasoalveolar Molding: 12 Year Follow-up
Proceedings of the XII Scientific Session-International Society of Craniofacial Surgery

Grayson, BH, Cutting CB, Brecht, LE, Maroutsis, MQ, & Garfinkle, JS
Nasoalveolar Molding and Presurgical Columella Elongation in Patients with UCLP and BLCP
Proceedings of the 64th Annual Scientific Session American Cleft Palate-Craniofacial Association, p 59 April, 2007

Garfinkle, JS, Grayson, BH, Brecht, LE & Cutting, CB
Anthropometric Evaluation of Nasal Morphology in Bilateral Cleft Lip and Palate Following Nasoalveolar Molding

Proceedings of the 64th Annual Scientific Session
American Cleft Palate-Craniofacial Association, p 58
April, 2007

Brecht, L
Improving the Quality of Life for The Forgotten Patient-Advances in Cleft Palate Patient Management
Program of Greater New York Academy of Prosthodontics, December, 2006

Brecht, L
Nasoalveolar Molding
Proceedings of the International Congress on Maxillofacial Reconstruction, p 20
October, 2006

Navarro, B, Brecht, L & Kitzis, D
Prosthetic Rehabilitation of a Combined Maxillectomy and Lateral Mandibular Discontinuity Defect using Progressive Anterior Guidance in an Edentulous Patient
Proceedings of the International Congress on Maxillofacial Reconstruction, p 108
October, 2006

Grayson, BH, Cutting, CB & Brecht, LE
Nasoalveolar Molding and Presurgical Columella Elongation in Unilateral and Bilateral Clefts of the Lip, Alveolus and Palate
Proceedings of the 63rd Annual Scientific Session
American Cleft Palate-Craniofacial Association, p 59
April, 2006

Garfinkle, J, Grayson, BH, Brecht, LE & Cutting, CB
Long-term Effects in Midface Growth of Gingivoperiosteoplasty with Pre-Surgical Infant Orthopedics in Unilateral Cleft Lip and Palate
Proceedings of the 63rd Annual Scientific Session
American Cleft Palate-Craniofacial Association, p 66
April, 2006

Brecht, LE
Maxillofacial Prosthetics in the Patient Care Continuum
Chicago Dental Society Review, p 67.
February, 2006

Venkatachalam, B & Brecht, LE:

The Multidisciplinary Approach to Dental Treatment of a Patient with EEC Syndrome: A Case Report
Greater New York Academy of Prosthodontics Program
December, 2005

Brecht, LE
An Update on the 21089 and Infant Cleft Palate Care: What We Now Know After 10 Years of NAM
Proceedings of the 53rd Annual Scientific Session, p 29.
October 2005
American Academy of Maxillofacial Prosthetics

Grayson, BH, Cutting, CB & Brecht, LE
Nasoalveolar Molding and Presurgical Columellar Elongation in Unilateral and Bilateral Clefts of the Lip, Alveolus and Palate
Proceedings of the 62nd Annual Scientific Session
American Cleft Palate-Craniofacial Association, p 74.
April, 2005

Grayson, BH, Cutting, CB & Brecht, LE
Nasoalveolar Molding and Presurgical Columellar Elongation in Unilateral and Bilateral Clefts of the Lip, Alveolus and Palate
Proceedings of the 61st Annual Scientific Session
American Cleft Palate-Craniofacial Association, p 62.
March, 2004

Warren, SM, Borud, LJ, Brecht, LE, Longaker, MT & Siebert, JW
Microvascular Reconstruction of the Pediatric Mandible
Northwest Society of Plastic Surgeons
Program-42nd Annual Meeting
February, 2004

Brecht, L
Cleft Palate Care from Infancy to Adulthood – The Prosthodontist's Role in the Team Approach
Program of the New York Academy of Dentistry
March, 2004

Brecht, L
Current Rehabilitation of the Cleft Palate Patient: The NYU/IRPS Experience
American Academy of Maxillofacial Prosthetics
Program of 50th Annual Scientific Session, p32.
November, 2002

Grayson, BH, Cutting, CB & Brecht, LE
Nasoalveolar Molding and Columellar Elongation
Proceedings of the 59th Annual Scientific Session
American Cleft Palate-Craniofacial Association, p60
May, 2002

Grayson, BH, Cutting, CB, Maull, D, & Brecht, LE
The Long-term Effect of Presurgical Nasoalveolar Molding on Three-Dimensional Nasal Shape in Complete Unilateral Clefts
Abstract #98 Program from the 9th International Congress on Cleft Palate and Related Craniofacial Anomalies
June, 2001

Brecht, LE, & Thorne, CH
Reconstruction of the Pediatric Craniofacial Patient: Evolving Technologies and New Paradigms of Care
Academy of Prosthodontics
p38 - 83rd Annual Scientific Session Program
May, 2001

INSERT 2 Abstracts from International Cleft Mtg June 2001, Goteborg, Sweden

Brecht, LE, Cutting, CB & Grayson, BH
Interdisciplinary Management of Craniofacial Anomalies and Cleft Palate Patients
American Association of Orthodontists
Interdisciplinary Care Conference Program, p 11.
February, 2001

Brecht, LE, Cutting, CB & Grayson, BH
Modern Methods in Restoration of Congenital Defects
American Academy of Maxillofacial Prosthetics &
International Congress of Maxillofacial Prosthetics
Joint Symposium Program, p 56.
November, 2000.

Santiago, PE, Grayson, BH, Degen, M, Brecht, LE, & McCarthy, JG:
The Effect of Early LeFort III Surgery on Permanent Molar Eruption in Patients with Craniosynostosis
International Society of Craniofacial Surgery
Program-VIIIth International Congress, p 175.
October, 1999

Brecht, LE
Prosthodontic Rehabilitation of the Cleft Patient

International Course in Advanced Cranio-Maxillofacial Surgery
University of Glasgow-Canniesburn Hospital
Conference Program & Abstracts,
October, 1999

Brecht, LE, Grayson BH, & Cutting, CB
Cleft Palate Care: Advances in the Interdisciplinary Approach
Academy of Prosthodontics
Program - 80th Annual Scientific Session
May, 1998

Brecht, LE, Grayson, BH, & Thorne, CH
Neonatal Auricular Cartilage Molding
Ear Reconstruction '98-Choices for the Future
Conference Program and Abstracts, p 82.
March, 1998

Thorne, CH, Brecht, LE, & Hammerschlag, PE
Indications for Autogenous vs. Prosthetic Auricular Reconstruction: The NYU Experience
Ear Reconstruction '98-Choices for the Future
Conference Program and Abstracts, p 72.
March, 1998

Hammerschlag, PE, Brecht, LE, Thorne, CH, & Roland, TA.
Aural Atresia: Surgical Outcome in a Multidiscipline Center
The Laryngoscope, Vol. 107 (11), p1574. November, 1997

Brecht, LE, Grayson, BH & Cutting, CB
Cleft Palate Care: Interdisciplinary Advances
Greater New York Academy of Prosthodontics
Program - 43rd Annual Fall Scientific Meeting
December, 1997

Brecht, LE, Thorne, CH & McCarthy, JG
Osseointegrated Craniofacial Implants in Pediatric Auricular Reconstruction: Indications and Contraindications
International Society of Craniofacial Surgery
Program-VIIth International Congress, p 155.
September, 1997

Siebert, JW, Jelks, GW, Brecht, LE & Longaker, MT
Reconstruction of Severe Periorbital Deformities Using Microsurgical Free Tissue Transfers

International Society of Craniofacial Surgery
Program-VIIth International Congress, p 147.
September, 1997

Ting, V, Sims, CD, McCarthy, JG, Brecht, LE, Kasabian, A, Dublin, BK, Gittes, G & Longaker, MT
Engineering of Cartilaginous Human Shapes in Vitro Using Plasma Derived Polymer Substances and Chondrocytes
International Society of Craniofacial Surgery
Program-VIIth International Congress, p 34.
September, 1997

Santiago, P, McCormick, S, Kwon, S, Gianoutsos, M, Levine, J, Brecht, L, McCarthy, JG, & Grayson, BH:
The Long Term Effects of Mandibular Distraction: A Cephalometric Study
Journal of Dental Research, Volume 75:144, 1996

Cutting, CB, Grayson, BH & Brecht, LE
Presurgical Columellar Elongation with One Stage Repair of the Bilateral Cleft Lip and Nose
American Cleft Palate Craniofacial Association
Proceedings-52nd Annual Meeting, Vol. 52:58, April, 1995

Brecht, LE, Turk, AE, Grayson, BH & Cutting, CB:
Effect of Presurgical Nasal Molding on Cleft Lip and Nose Symmetry
Journal of Dental Research, Volume 74:257, 1995

Brecht, LE, Grayson, BH, & Cutting, CB:
Columellar Elongation in the Bilateral Cleft Lip and Nose Patient
Journal of Dental Research, Volume 74:257, 1995

Brecht, LE, Grayson, BH & Cutting, CB:
Nasal Orthopedic Molding Appliances in Unilateral and Bilateral Cleft Palate Patients
Program of The 24th Annual Meeting of the American College of Prosthodontists, October, 1993

Miscellaneous Media:

Featured in television news segment on orbital rehabilitation of patient Louis Pepe wounded by Al

Qaeda terrorists on New York City's WPIX, August 30th, 2006

Featured in article by parents of twins with cleft palate deformities treated by team at NYU Medical Center through nasoalveolar molding.
New York Magazine January 5th, 2004 issue

Promotional video for **American College of Prosthodontists** April, 2004 (featured at October 2004 Annual Session of American College of Prosthodontists in Ottawa, Ontario, Canada)

Cutting, CB, Grayson, BH & Brecht, LE:
Instructional video **"Nasoalveolar Molding and Surgical Approaches to Bilateral Cleft Lip and Nose Repair"** for Plastic Surgery 2003 -The Premier Educational Experience, San

Grants & Financial Awards:

May, 2007
$50,000

Principal Investigator
Continuing-Grant from **National Foundation for Facial Reconstruction** in conjunction with the **Lebensfeld Foundation** for on-going clinical research on the application of percutaneous osseointegrated implant systems for pediatric patients with congenital and acquired facial defects. (Study site: **The Institute of Reconstructive Plastic Surgery at New York University Medical Center.**)

May, 2006
$50,000

Principal Investigator
Continuing-Grant from **National Foundation for Facial Reconstruction** in conjunction with the **Lebensfeld Foundation** for on-going clinical research on the application of percutaneous osseointegrated implant systems for pediatric patients with congenital and acquired facial defects. (Study site: **The Institute of Reconstructive Plastic Surgery at New York University Medical Center.**)

May, 2005
$50,000

Principal Investigator
Continuing-Grant from **National Foundation for Facial Reconstruction** in conjunction with the **Lebensfeld Foundation** for on-going clinical research on the application of percutaneous osseointegrated implant systems for pediatric patients with congenital and

acquired facial defects. (Study site: **The Institute of Reconstructive Plastic Surgery at New York University Medical Center.**)

May, 2004
$50,000

Principal Co-Investigator
Continuing-Grant from **National Foundation for Facial Reconstruction** in conjunction with the **Lebensfeld Foundation** for on-going clinical research on the application of percutaneous osseointegrated implant systems for pediatric patients with congenital and acquired facial defects. (Study site: **The Institute of Reconstructive Plastic Surgery at New York University Medical Center.**)

May, 2003
$50,000

Principal Co-Investigator
Continuing-Grant from **National Foundation for Facial Reconstruction** in conjunction with the **Lebensfeld Foundation** for on-going clinical research on the application of percutaneous osseointegrated implant systems for pediatric patients with congenital and acquired facial defects. (Study site: **The Institute of Reconstructive Plastic Surgery at New York University Medical Center.**)

May, 2002
$50,000

Principal Co-Investigator
Continuing-Grant from **National Foundation for Facial Reconstruction** in conjunction with the **Lebensfeld Foundation** for on-going clinical research on the application of percutaneous osseointegrated implant systems for pediatric patients with congenital and acquired facial defects. (Study site: **The Institute of Reconstructive Plastic Surgery at New York University Medical Center.**)

June, 1998
$20,000

Principal Co-Investigator
Continuing-Grant from **National Foundation for Facial Reconstruction** in conjunction with the **J. M. McDonald Foundation** for on-going clinical research on the application of percutaneous osseointegrated implant systems for pediatric patients with congenital and acquired facial defects. (Study site: **The Institute of Reconstructive Plastic Surgery at New York University Medical Center.**)

July, 1997
$ 104,500

Principal Co-Investigator
Grant from **Nobel Biocare** to study the long-term safety and efficacy of extraoral craniofacial implants in retaining auricular implants in the pediatric population.

(Study site: **The Institute of Reconstructive Plastic Surgery at New York University Medical Center.**)

June, 1995
$15,000

Principal Co-Investigator
Grant from **National Foundation for Facial Reconstruction** in conjunction with the **J. M. McDonald Foundation** for on-going clinical research on the application of percutaneous osseointegrated implant systems for pediatric patients with congenital and acquired facial defects. (Study site: **The Institute of Reconstructive Plastic Surgery at New York University Medical Center.**)

January, 1994

Heraeus Kulzer, Inc.
Principal Investigator
Kulzer "Dentacolor" curing unit and material support for the Advanced Education Program in Prosthodontics to carry out laboratory and clinical studies on Palavit® and Palaseal® resins.

October, 1993
$15,000

Principal Co-Investigator
Grant from **National Foundation for Facial Reconstruction** in conjunction with the **J. M. McDonald Foundation** for the purchase of equipment for development of percutaneous osseointegrated implant systems for patients with congenital and acquired facial defects. (Study site: **The Institute of Reconstructive Plastic Surgery at New York University Medical Center.**)

October, 1993
$13,250

Principal Co-Investigator
Grant from **National Foundation for Facial Reconstruction** in conjunction with the **Chatlos Foundation** for the purchase of equipment for development of percutaneous osseointegrated implant systems for patients with congenital and acquired facial defects. (Study site: **The Institute of Reconstructive Plastic Surgery at New York University Medical Center.**)

Honors & Professional Awards:

October 20, 2005 Co-author table clinic awarded **First Prize** in New York State Section of American College of Prosthodontics,**"The Multidisciplinary Approach to Dental Treatment of a Patient with EEC Syndrome: A Case Report"** - Venkatachalam, B & Brecht, LE.

May 20-25, 2005 Co-author of table clinic presentation that was awarded the **Joseph E. Johnson Award for Clinical Excellence** at the 105th Annual Session of the American Association of Orthodontics for the best table clinic (out of 64). **" Nasoalveolar Molding in Infants Born with Clefts of the Lip Alveolus and Palate"** Shetye, P, Grayson, BH, Brecht, LE & Cutting, CB.

December 8, 2004 – Recipient of **NYU Medical Center Team Achievement Award** as a member of the Cleft Lip/Cleft Palate Team.

Awarded Best Paper for 1999 by **The American Society of Maxillofacial Surgeons**, October, 1999: Cutting, CB, Grayson, BH, Brecht, LE, Santiago, P, Wood, R, & Kwon, SM:
"Presurgical Columellar Elongation and Primary Retrograde Nasal Reconstruction in One-Stage Bilateral Cleft Lip and Nose Repair"
Plast.& Recconstruct. Surg. 101:630-639, 1998.

Honoree of **Forward Face**, The Charity for Children with Craniofacial Conditions, March, 1999.

Omicron Kappa Upsilon (Omega Chapter), National Dental Honor Society (inducted as Alumni Member).

The Faneuil D. Weisse Medal, awarded for obtaining the second highest scholastic average for the four years of dental school.

The New York Graduate Chapter of Sigma Epsilon Delta Fraternity Award presented for excellence in Fixed Partial Prosthesis.

The Samuel Charles Miller Award presented to the Senior dental student attaining the highest degree of knowledge and skill in Periodontology.

The American Academy of Oral Pathology Award presented to the Senior dental student who has shown outstanding interest, accomplishment, and promise in the field of Oral Pathology.

The Dr. Arthur N. Caplin Scholarship Award presented to the Senior dental student who has demonstrated excellence in Removable Prosthodontics.

License Status: New York State License Certificate #041096
Northeast Regional Board Exam (Passed - May, 1985)

Private Practice:

1989-Present Practice Limited to Prosthodontics &
Maxillofacial Prosthetics
275 Madison Avenue - Suite 2900
New York, NY 10016

1989-1992 Practice Limited to Prosthodontics &
Maxillofacial Prosthetics (Faculty Practice)
Montefiore Medical Center
111 East 210th Street
Bronx, NY 10476

Community Service:

Member: Board of Directors *"Forward Face"*
Forward Face is a national organization committed to serving patients with craniofacial disorders and their families.
1995 - Present

Member: Advisory Board *"Cleft Advocate"*
Cleft Advocate is a national organization to promote knowledge about the cleft palate condition and provide support for patients and parents
2004 – Present

Member-Board of Trustees *"Broadsword and Shield Foundation"*
2008 – Present

Member: *Board of Education*
Greenwich Catholic School
Greenwich, CT
2000 – 2002: Strategic Planning Committee

Member: *St. Michael 's Men's Association*
Greenwich, CT
2000, 2001, 2002 - Director, Spring Retreat
2001 – 2002 Executive Committee-St. Michael's Parish

Member: *Our Lady Star of the Sea*
Shippan Point, Stamford, CT

14(1):13-29 (2003) Crit Rev Oral Biol Med

The Mechanical Properties of Human Dentin: a Critical Review and Re-evaluation of the Dental Literature

J.H. Kinney*
S.J. Marshall
G.W. Marshall

Division of Biomaterials and Bioengineering, Department of Preventive and Restorative Dental Sciences, Mail Stop 0758, University of California, San Francisco, San Francisco, CA 94143-0758;

***corresponding author, kinney3@llnl.gov**

Abstract

▲ Top
▼ Next

The past 50 years of research on the mechanical properties of human dentin are reviewed. Since the body of work in this field is highly inconsistent, it was often necessary to re-analyze prior studies, when possible, and to re-assess them within the framework of composite mechanics and dentin structure. A critical re-evaluation of the literature indicates that the magnitudes of the elastic constants of dentin must be revised considerably upward. The Young's and shear moduli lie between 20-25 GPa and 7-10 GPa, respectively. Viscoelastic behavior (time-dependent stress relaxation) measurably reduces these values at strain rates of physiological relevance; the reduced modulus (infinite relaxation time) is about 12 GPa. Furthermore, it appears as if the elastic properties are anisotropic (not the same in all directions); sonic methods detect hexagonal anisotropy, although its magnitude appears to be small. Strength data are re-interpreted within the framework of the Weibull distribution function. The large coefficients of variation cited in all strength studies can then be understood in terms of a distribution of flaws within the dentin specimens. The apparent size-effect in the tensile and shear strength data has its origins in this flaw distribution, and can be quantified by the Weibull analysis. Finally, the relatively few fracture mechanics and fatigue studies are discussed. Dentin has a fatigue limit. For stresses smaller than the normal stresses of mastication, ~ 30 MPa, a flaw-free

dentin specimen apparently will not fail. However, a more conservative approach based on fatigue crack growth rates indicates that if there is a pre-existing flaw of sufficient size (~ 0.3-1.0 mm), it can grow to catastrophic proportion with cyclic loading at stresses below 30 MPa.

Key words. Dentin, calcified tissues, mechanical properties, fatigue, fracture toughness

Introduction

▲ Top
▲ Previous
▼ Next

Dentin is the most abundant mineralized tissue in the human tooth. Therefore, knowledge of its mechanical properties is essential for predicting the effects of microstructural alterations due to caries, sclerosis, and aging on tooth strength. In clinical dentistry, knowledge of dentin properties is important for understanding the effects of the wide variety of restorative dental procedures that range from the design of preparations to choice of bonding methods.

In spite of this importance, over half a century of research has failed to provide consistent values of dentin's mechanical properties. The Young's modulus is unknown to within a factor of three; the shear modulus is uncertain by a factor of four; and the other elastic constants have not been measured. There is a six-fold uncertainty in the ultimate strength, and there have been few studies of fracture toughness or fatigue.

This is a review of the last 50+ years of research into the mechanical properties of dentin. It is a critical review, in the sense that the prior literature on the mechanical properties of dentin is often re-examined and re-interpreted within the context of dentin microstructure. For example, the widely varying

tensile strength data are re-examined in terms of the Weibull distribution function; the wide variations in previously reported tensile strengths can then be explained by a specimen size effect whose origin lies in the existence of a population of flaws in the dentin.

The bulk of this review focuses on the elastic properties of dentin. This emphasis is a necessary consequence of both the paucity of published data on other mechanical properties, and the fact that an understanding of elastic behavior is essential to the proper interpretation of physical measurements of failure. It was often necessary to re-evaluate the data on the elastic properties to reconcile the contradictions in the literature and reach consensus. Because the physical data were frequently not available in the more recent publications, indirect methods were used to test the meaningfulness of the results. This involved consideration of the entire elastic stiffness matrix to check the constraints forced upon all of the elastic constants from the measurement of a single property. In this way, it was possible to check for self-consistency with all of the elastic constants as well as the known microstructure.

After a brief discussion of the composition and microstructure of dentin, the review first considers its elastic and viscoelastic properties. Then, hardness, strength, fracture toughness, and fatigue are discussed in order. This organization loosely follows that of the last comprehensive review of dentin properties (Waters, 1980), with the exception that a more thorough treatment of fatigue and fracture toughness has been added. The review concludes by proposing reliable ranges for the magnitudes of mechanical properties. It is hoped that these recommendations, and the evidence on which they are based, spark additional discourse and research on the properties of dentin.

Dentin Microstructure

▲ Top
▲ Previous
▼ Next

The microstructure of dentin suggests a hierarchical approach to the understanding of its mechanical properties. At the smallest length scales are the constituent materials: a carbonated nanocrystalline apatite mineral phase (approximately 50% by volume) and a felt-work of type I collagen fibrils (see Fig. 1⊞). The collagen fibrils, approximately 30% by volume, are roughly 50-100 nm in diameter; they are randomly oriented in a plane perpendicular to the direction of dentin formation (Jones and Boyde, 1984). The mineral occupies two sites within this collagen scaffold: intrafibrillar (inside the periodically spaced gap zones in the collagen fibril) and extrafibrillar (in the interstices between the fibrils). The partitioning between these two sites is uncertain, although it is believed that between 70 and 75% of the mineral may be extrafibrillar (Bonar *et al.*, 1985; Pidaparti *et al.*, 1996). The mineral crystallites are needle-like near the pulp; the shape continuously progresses to plate-like with proximity to the enamel (Kinney *et al.*, 2001b). The crystallite thickness, ~ 5 nm, is invariant with location.

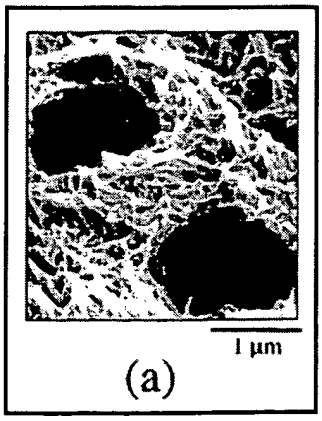

Figure 1. (a) SEM image of a fixed, demineralized dentin specimen showing the collagen fibrils that are randomly oriented in the plane perpendicular to the tubule lumens (after Marshall *et al.*, 1997). **(b)** A higher-resolution AFM image of an unfixed specimen obtained in water. The AFM image shows the periodic 67-nm hole and overlap zones characteristic of the Type I collagen fibrils found in dentin and bone (after Marshall *et al.*, 2001; Habelitz *et al.*, 2002b).

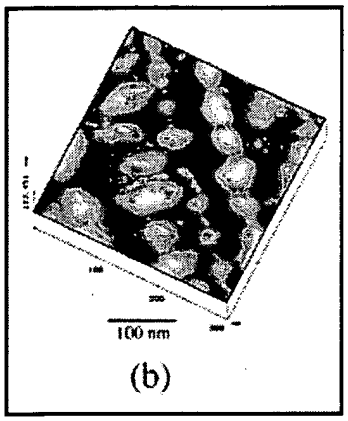

(b)

View larger version (183K):
[in this window]
[in a new window]

At a higher level of organization is an intermediate, or composite, length scale. At this length scale, dentin can be modeled as a continuous fiber-reinforced composite, with the intertubular dentin forming the matrix and the tubule lumens with their associated cuffs of peritubular dentin forming the cylindrical fiber reinforcement (see Fig. 2). The tubules run continuously from the dentin-enamel junction to the pulp in coronal dentin, and from the cementum-dentin junction to the pulp canal in the root. The regular, almost uni-axial, alignment of the tubules has led some to suggest that they play an important function in the orientation dependence of the mechanical properties (Waters, 1980).

Figure 2. (a) SEM and **(b)** AFM images of fully mineralized dentin specimens showing the tubule lumens with surrounding cuffs of peritubular dentin. The bar in the SEM photomicrograph is 10 μm. Labeling: L = tubule lumen, PT = peritubular dentin, IT = intertubular dentin

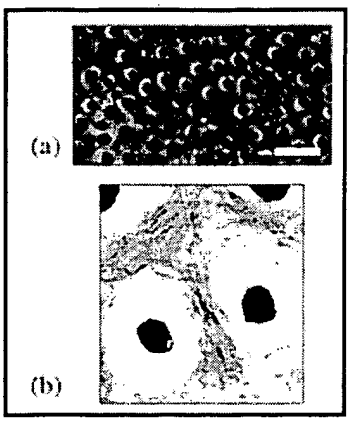

matrix. SEM image after Kinney *et al.* (2001a). AFM image after Kinney *et al.* (1993).

View larger version (99K):
[in this window]
[in a new window]

At the greatest length scale are the effective, or continuum, properties of dentin. The effective properties of dentin describe the response of the tooth to applied loads, and allow for predictions of tooth strength and fracture properties. Young's modulus, tensile and compressive strength, and fracture toughness are examples of these effective properties, and reflect the complex interactions of the constituent materials and the microstructure. At this largest length scale, we anticipate that the effective properties will depend on tubule density, orientation, and the local average density of the mineral phase. Ultimately, measurement of the effective properties, particularly the properties of altered forms of dentin (such as carious or transparent), will benefit from an understanding of the material behavior at all of these length scales.

The Elastic Properties of Dentin

▲ Top
▲ Previous
▼ Next

The elastic properties of dentin are of paramount importance in all discussions of tooth strength. The elastic constants, usually

defined in terms of a stiffness (C_{ij}) or compliance (S_{ij}) matrix, include the Young's modulus, shear modulus, and Poisson's ratio. Depending on the symmetry of the microstructure, the elastic constants have different degrees of independence. For example, an isotropic structure has only two independent elastic constants, while an orthotropic structure has nine independent elastic constants. Therefore, any study of the elastic properties of dentin must consider its symmetry.

THE YOUNG'S MODULUS

The slope of the proportional part of the stress-strain curve provides the Young's modulus, while the yield strength and the ultimate strength can be obtained from the nonlinear region of the stress-strain curve. Because uni-axial stress-strain behavior is among the most straightforward of measurements, it is surprising that there is so much uncertainty in the value of Young's modulus for dentin obtained by this method. This uncertainty in Young's modulus extends to all measurement techniques, including bending, indentation, and ultrasound. A graphed representation of the measurements of Young's modulus with the year in which they were reported is shown in Fig. 3 ⊞. The mean and standard deviation of these values are 13.2 GPa and 4.0 GPa, respectively. Unfortunately, over the past 50 years there has been an increase in the dispersion of the reported values; there is no evidence that this trend is abating. Therefore, it is appropriate to begin discussion of the Young's modulus of dentin by considering the constituent and composite-level organizational hierarchies in the hope that they may aid readers in discriminating between valid and invalid determinations of the effective modulus.

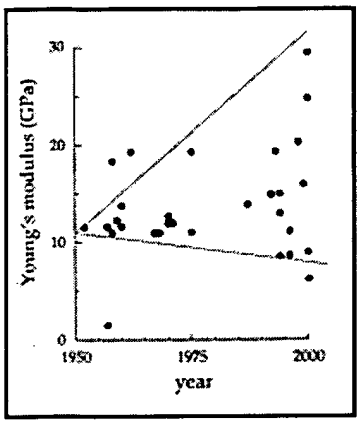

View larger version (14K): [in this window] [in a new window]

Figure 3. The Young's modulus as reported in the literature over the past 50 years. The data prior to 1999 appear in tabular form in the reference by Kinney *et al.* (1999). Data after 1999 are from Huo *et al.* (2000), Kinney *et al.* (2001a), Kishen *et al.* (2000), and Palamara *et al.* (2000). In the past few years, there has been a four-fold variation in the reported magnitude of the Young's modulus; the uncertainty in its value appears to be expanding with time. The uncertainty in the magnitude of the Young's modulus is probably not reflective of the actual variations in the mechanical properties of dentin. Rather, the uncertainty most likely arises from either a viscoelastic response (stress relaxation) or experimental artifact.

Constituent materials models

An early attempt to provide reasonable bounds for the continuum Young's modulus of dentin was proposed by Katz (1971). Dentin was considered to be a two-phase mixture of apatite mineral and collagen, with the volume fraction and Young's modulus of the mineral phase given by V_A and E_A, respectively, and the corresponding values for the collagen given by V_C and E_C. The effective Young's modulus of the mixture (E_e) was rigorously bounded from above and below by:

$$E_e \leq V_A E_A + V_C E_C \equiv V_A(E_A - E_C) + E_C \quad (1)$$

$$E_e \geq \frac{E_A E_C}{V_A E_C + V_C E_M} \quad (2)$$

The elastic properties of the constituent materials in their bulk form have been

measured with reasonable accuracy: $E_A \sim 110$ GPa and $E_C < 0.001$ GPa (Katz and Ukraincik, 1971; Balooch *et al.*, 1998). Substitution of these values into the above equations generates the upper and lower bounds for the Young's modulus that are shown in Fig. 4. Unfortunately, the large disparity between the moduli of the two phases leads to a wide separation between the upper and lower bounds in the vicinity of the known mineral concentration in dentin (40-50% by volume). The separation between the bounds is narrowed only slightly by the application of more restrictive, variational bounding methods (Hashin, 1983). Clearly, bounds based on the constituent materials properties are of no use for discriminating between experimental measurements, all of which lie well within the upper and lower bounds predicted in Eqs. 1 and 2.

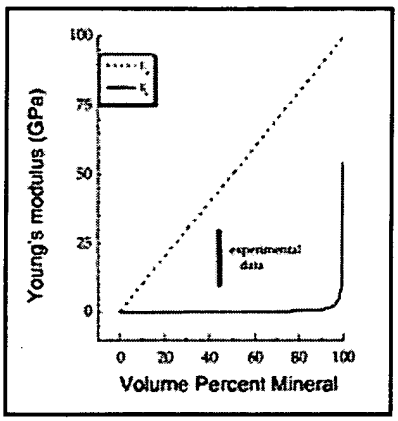

View larger version (18K): [in this window] [in a new window]

Figure 4. The upper (dashed line) and lower (solid line) theoretical bounds for the Young's modulus of a composite of hydroxyapatite mineral and type I collagen fibrils as calculated from Eqs. 1 and 2. The experimental data are shown as the solid bar at a volume percent mineral phase (45%) corresponding to the known composition of dentin. The graph emphasizes the difficulties of modeling mineralized tissues with bounds; The large difference in moduli between the two phases separates the upper and lower bounds by too great a magnitude to be useful.

Micromechanics models

Because of the large difference in modulus between the mineral and organic phases, we do not anticipate that improvement can be made by further refinements of bounds. Therefore, it is worthwhile considering a

micromechanics approach at the composite hierarchy of dentin microstructure. At this length scale, the dentinal tubules with their surrounding peritubular cuffs are like fibers, providing reinforcement to the intertubular matrix. Assuming that the moduli of the matrix (E_M) and the "fibers" (the lumens plus peritubular cuffs, E_F) are known, rough estimates of the bounds can be made by appropriate substitutions into Eqs. 1 and 2. However, direct substitution of E_M and E_F ignores the possibly complex interactions between the "fibers" and the matrix.

The interactions between fiber and matrix have been accounted for in self-consistent generalized micromechanics approaches to aligned fiber composites (Christensen, 1990). Analytical solutions have been derived for the case of aligned cylindrical fibers in an isotropic matrix. The fibers introduce a transverse anisotropy and require five equations for the independent elastic constants to be defined. These equations have been reformulated for dentin in terms of the Young's modulus of intertubular (E_l) and peritubular (E_{pt}) dentin (Kinney *et al.*, 1999). The expression for the effective longitudinal (in the direction of the tubules) Young's modulus, E_{el}, in terms of the tubule concentration, c, was derived:

$$E_{el} = cE_{pt}\left(1 - \frac{A_l}{A_{pt} + A_l}\right) + (1 - c)E_l + \gamma(c, v_l, v_{pt}) \quad (3)$$

In the above equation, γ is a "clamping" factor that accounts for mismatch in Poisson's ratio between the peritubular and intertubular dentins, and A_l and A_{pt} are the area fractions of the intertubular and peritubular dentin,

respectively. The area ratio in Eq. 3⊡ is apparently constant with position in the tooth, and is approximately equal to 0.25 (Pashley, 1989).

Only when the ratio of the peritubular and intertubular dentin moduli is greater than 3 is there a measurable effect of the tubules on stiffness for physiologically relevant tubule densities (5-15%). Thus, a theoretical framework now exists for estimating the effects of tubule orientation on the elastic properties: For physiologically relevant tubule densities, the anisotropy caused by the tubules is insignificant (Kinney *et al.*, 1999). This does not mean that dentin is elastically isotropic; rather, if dentin proves to be anisotropic, it is because the intertubular dentin matrix is anisotropic and not because of the tubules. Based on observations that the collagen fibrils in the intertubular matrix are aligned perpendicular to the tubule axis, we anticipate that dentin might have a transverse isotropic (hexagonal) symmetry (stiffer in the plane of the collagen fibrils).

The micromechanics model offers several advantages over bounding methods. Key is the ability of the model to make accurate estimates of the effective elastic constants based on a few simple measurements of the tubule concentration. The model has its drawbacks, however. Accurate values of the elastic constants of peritubular and intertubular dentin must be available, and this requires careful mechanical testing, which we will now review in greater detail.

Tensile and compressive measurements of Young's modulus

There have been numerous experimental attempts to measure the Young's modulus of dentin. The majority of these measurements have been performed in either tension or compression. The primary emphasis of the tensile studies

was to establish the ultimate tensile strength (UTS) of dentin; the determination of the Young's modulus appeared to be secondary to this effort.

The earliest "modern" measurement of Young's modulus in tension was published in 1962 (Bowen and Rodriguez, 1962). In that study, specimens of dentin, nominally 2 mm thick, were cut freehand with a rotary diamond disk under constant water irrigation. The specimens were narrowed in the middle, with a "radiused" shoulder (fillet) maintained so that stress concentration would be prevented. The knife-edges of an optical strain gauge (length, 6 mm) were attached directly to the specimens. The specimens were hydrated at least 1 hr in distilled water before being tested. The stress-strain curves were linear to failure, and the mean modulus of elasticity was 19.3 GPa (2.8×10^6 psi) with a coefficient of variation of 28%.

Five years later, Lehman (1967) measured the tensile properties of dentin with hollowed, cylindrical specimens from the root. As in the earlier study by Bowen and Rodriguez, the tensile stress-strain curves were linear to failure. However, the Young's modulus was 11.0 GPa, almost half that of the earlier study, and the coefficient of variation (53%) was almost double.

There were three important differences between the two studies. First, the latter study did not use strain gauges affixed to the specimen, thereby increasing the likelihood of grip effects like tow-in. Second, the specimens were hollowed along the root canal by means of a dental bur, increasing the probability of undetected flaws in the interior of the specimen. Third, the gauge sections were not "radiused", leaving a stress concentration that increased the chance of failure at grip ends, thereby invalidating the test.

Though it is difficult to reconstruct an experiment decades after the fact, we

are fortunate that Lehman reported all of his data. A close inspection shows that the modulus and ultimate tensile strength were strongly correlated ($p < 0.001$), with the higher values of elastic modulus associated with the specimens that had the highest tensile strength. Furthermore, 75% of the specimens failed in tension at or below 40 MPa, a low value suggesting that flaws introduced during specimen preparation may have affected the linear stress-strain behavior. When we restrict our focus to those specimens that failed above 40 MPa, we obtain a tensile modulus of 16.9 GPa with a coefficient of variation of 26%. This is more in line with the earlier work of Bowen and Rodriguez (1962).

Around the same time that the tensile measurements were being performed, other researchers were establishing the compressive properties of dentin. The earliest of these measurements was reported by Peyton *et al.* (1952). This study examined the compressive behavior of 1.8 mm in cross-section by 4.5-mm-long dentin specimens. Strain gauges were affixed to steel rods that were then used to apply load to the specimens. A Young's modulus of 11.6 GPa was reported.

Concerned that the low value of the Young's modulus obtained from their earlier study might have been caused by a combination of non-paralle! alignment of the load platens (tow-in) and possible stress relaxation effects, the same group repeated their earlier study with greater attention to experimental variables (Craig and Peyton, 1958). Placing the strain gauges directly on the specimen eliminated tow-in; stress relaxation effects were measured by careful cycling of the compressive load well below the proportional limit. These corrections raised the compressive Young's modulus to 18.5 GPa, in excellent agreement with the tensile measurements of the time.

Measurements of the modulus are sensitive to specimen preparation, experimental design, and stress relaxation; not accounting for these experimental variables leads to underestimation of the elastic constants. Therefore, the comments of Waters (1980) in his review article were surprising: "Craig and Peyton (1958) obtained values for the proportional limit and compressive strength in reasonable agreement with other workers, but their value of the modulus is, for some unaccountable reason, considerably higher." This comment reflects a bias toward favoring a low value for the Young's modulus of dentin—a bias perhaps enforced by the large number of low values reported in subsequent years (see Fig. 3⊞).

Testing of dentin in compression and tension was performed only infrequently in the years since Craig and Peyton. Two of these studies are particularly noteworthy. In the work reported by Stanford *et al.* (1960), dentin specimens were tested in compression. Even with corrections for platen deformation, the compressive modulus was 13.8 GPa, significantly less than reported in the earlier studies. Though it could be argued that the data were not adjusted for the affects of non-parallel alignment (tow-in), it is unlikely that this could account for all of the discrepancy. Furthermore, in tensile testing performed by Sano *et al.* (1994), similarly low values of Young's modulus were reported (13-15 GPa).

Both of the above studies were performed with great attention to detail, so instrumentation artifacts or flaws in specimen preparation cannot readily explain the lower values of elastic modulus. However, one detail worth mentioning is that, in both studies, the specimens were stored for an undisclosed amount of time in water. In the work reported by Sano *et al.* (1994), the tensile specimens were stored in 0.9% NaCl water at 4°C for about

24 hrs prior to being tested (Pashley, 2001, personal communication). Earlier studies have showed that short-term storage in saline solution degrades bond strengths (Goodis *et al.*, 1993), and that storage in water can reduce bend strength in bone (Gustafson *et al.*, 1996). Given the small size of dentin specimens, it is possible that even short-term storage in water or saline might reduce the elastic modulus by dissolution of the mineral phase. The effects of water storage will be considered in greater detail later.

In more recent work, Palamara *et al.* (2000) recorded the response of a grid pattern coated on the surfaces of dentin specimens during compressive loading. The results are of particular interest because, while the Young's moduli measured in orientations both parallel and orthogonal to the tubule axes (the principal structural directions) were identical, the modulus at 45° off-axis to the tubules was determined to be lower. The observation that the off-axis modulus was smaller than that measured in either principal axis requires that the intertubular dentin matrix be anisotropic. Since this is a significant finding, we must consider its veracity in greater detail.

Our analysis begins by a consideration of the simplest deviation from isotropic symmetry, cubic, which requires three independent elastic constants. The reciprocal Young's modulus in a cubic system along the direction of the unit vector l_i can be expressed in terms of the compliance matrix S_{ij} (Nye, 1972):

$$S'_{11} = S_{11} - 2(S_{11} - S_{12} - \frac{1}{2} S_{44})(l_1^2 l_2^2 + l_2^2 l_3^2 + l_3^2 l_1^2) \quad (4)$$

The variation of the Young's modulus with orientation depends only on the terms in l, and is zero for the principal orthogonal directions and a maximum

of 1/3 in the <111> directions. For the Young's modulus to be less in the off-axis directions, (S_{11}-S_{12}-S_{44}/2) must be less than zero. This requires the shear modulus, *G*, to be less than would be expected in an isotropic system:

$$G < \frac{E}{2(1 + v)} \tag{5}$$

With the values provided by Palamara *et al.* (2000), [E_{11} = 10.4 GPa and *E* (45°) = 7.7 GPa], we can calculate a rigorous upper bound for the shear modulus. For a cubic symmetry model, *G* < 2.9 GPa. This is less than would be required from isotropic symmetry for *v* = 0.25 (4.1 GPa).

One can argue that, from an analysis of the dentin microstructure, an orthotropic symmetry would be a more reasonable alternative to cubic. However, we find that the situation is only slightly altered from the analysis for cubic symmetry. For orthotropic symmetry, we begin with the general case of a lamina loaded in plane at an arbitrary angle *q* with respect to a principal axis, l_1, in this case parallel to the tubule axes. The Young's modulus as a function of *q* can be expressed as (Jones, 1975)

$$\frac{E_1}{E_q} = (1 + a - 4b)\cos^4(q) + (4b - 2a)\cos^2(q) + a \tag{6}$$

In Eq. 6, *a* and *b* are dimensionless variables given by

$$a = \frac{E_1}{E_2} \tag{7}$$

$$b = \frac{1}{4}\left(\frac{E_1}{G_{12}} - 2\nu_{12}\right)$$

Here, G_{12} is the shear modulus and ν_{12} is Poisson's ratio. For the data presented in Palamara *et al.* (2000), $a = 1$. The observation that E_q was less than both E_1 and E_2 places a rigorous restriction on the value of the shear modulus:

$$G_{12} < \frac{E_1}{2(a + \nu_{12})} = \frac{E_1}{2(1 + \nu)} \qquad (8)$$

The above restriction on the shear modulus is identical to the one derived for cubic symmetry. With the values reported in Palamara *et al.* (2000) for the off-axis Young's modulus, Eq. 6⊞ requires that the magnitude of the shear modulus be less than 2.5 GPa, very similar to the result obtained with a cubic symmetry model. This is an extremely low value for the shear modulus, and is not in agreement with results reported in those studies where the shear modulus has been measured independently. Sound velocity measurements in bovine dentin, to be discussed in a later section, provided a shear modulus of 8.0 GPa (Gilmore *et al.*, 1969), and a torsion pendulum measurement led to a value of 6.1 GPa (Renson and Braden, 1975). [NB: The value that we cite corrects the typographical error in the original paper by Renson and Braden (1975), where the decimal was placed in the wrong location.] These values were all significantly greater than what is required to explain the results of Palamara *et al.*

Though the largest source of error in measurements with grids lies in the accurate determination of displacement (strain), the absence of any

independent measure of displacement (*e.g.*, no strain gauges or cross-head displacements were reported) prevents us from assessing this as a possible source of error. However, the compression tests were conducted between 50 and 150 MPa, which is within the range of the proportional limit in compression (80-140 MPa) that has been established in earlier work (Craig and Peyton, 1958; Stanford *et al.*, 1960). It is therefore possible that Palamara *et al.* (2000) were operating beyond the yield stress when recording their grid displacements. This factor would explain the lower values of the Young's modulus, and could easily explain the off-axis anisotropy. Also, considerable relaxation (creep) could have occurred during the time intervals required to obtain the images of the grids. However, in the absence of additional data, the possibility that dentin is elastically anisotropic cannot be ignored. The question of elastic symmetry will be taken up again in a later section.

Indentation measurements of Young's modulus

Indentation, where a hardened stylus is brought into contact with a surface, has largely been used to measure hardness. The modern theory of indentation (Doerner and Nix, 1986; Oliver and Pharr, 1992), where force and stylus displacement are analyzed to measure Young's modulus, has been applied to mineralized tissues only in the last decade. The technique measures the indenter load as a function of depth of penetration, from which the contact stiffness, S_c (not to be confused with the compliance matrix), is obtained from the derivative of the unloading curve evaluated at the peak force (Fig. 5⊞). Care must be taken to remove any excess machine compliance, C_m, that is associated with the sample mounting (Kinney *et al.*, 1996):

Figure 5. A typical load-displacement curve

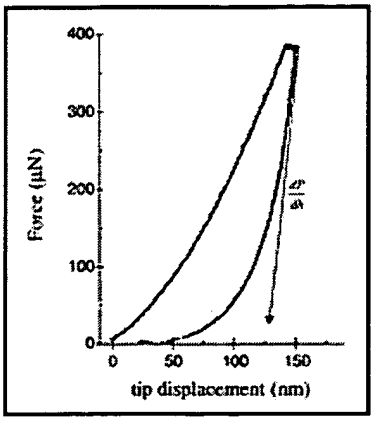

View larger version (17K): [in this window] [in a new window]

during AFM indentation of hydrated dentin. The slope of the initial unloading segment, dP/dh, is used to calculate the Young's modulus.

$$S_c = \frac{1}{[(1/S) - C_m]} \tag{9}$$

The indentation modulus E^*, sometimes referred to as the reduced modulus, is determined from the corrected contact stiffness, S_c, and the contact areas for each indentation, A, that are obtained from a tip shape calibration procedure (Doerner and Nix, 1986):

$$E* = \frac{\sqrt{\pi}}{2\sqrt{A}} S_C \tag{10}$$

From Eqs. 9 and 10, it is possible to obtain the Young's modulus of the probed specimen, E_s:

$$\frac{1}{E*} = \frac{(1 - v_s^2)}{E_S} + \frac{(1 - v_i^2)}{E_i} \tag{11}$$

$$E_S \cong E * (1 - v_s^2)$$

In Eq. 11⊞, v_s and v_i are the Poisson's ratios of the specimen and indenter stylus, and E_i is the Young's modulus of the indenter. The approximation in Eq. 11⊞ is valid because the modulus of the indenter is considerably larger than the modulus of the dentin.

Among the first to apply nanoindentation to the study of dentin and dental materials was van Meerbeek *et al.* (1993), who measured a Young's modulus of dentin of 19.3 GPa. This was followed by Kinney *et al.* (1996), who used nanoindentation to measure the Young's modulus of intertubular (18-21 GPa) and peritubular (29.8 GPa). Since then, nanoindentation has become a common technique for the determination of local mechanical properties of structural features in biological hard tissues (Rho *et al.*, 1999).

A significant drawback to the widespread use of nanoindentation in mineralized tissues is the inability to indent in water. To overcome this drawback, Balooch *et al.* (1998) applied the atomic force microscope (AFM) with a specially designed attachment called the Triboscope to perform indentations on fully hydrated specimens. In addition to allowing indentations to be made in water, the device also functioned as an AFM, allowing for precise positioning of the indenter and subsequent imaging of the indentation with microscopic spatial resolution. With this technique, Kinney *et al.* (1999) measured a pronounced decline in E with submersion in water. These investigators attributed this decrease to a combination of softening of the collagen phase and partial surface demineralization. Without knowing the effects of surface demineralization, they assumed that a plasticizing of the collagen fibrils and other noncollagenous proteins in the tissue caused the

majority of the decrease in modulus with time in water.

Although nanoindentation probes only a thin surface layer (< 1 μm), the mechanical properties obtained are assumed to be representative of the bulk material. Chemical changes in the surface layer of mineralized tissues resulting from storage solutions are, thus, important considerations for accurate determination of nanomechanical properties. This aspect of nanoindentation has been recently explored by Habelitz *et al.* (2002a), who studied changes in nanomechanical properties of dentin and enamel during storage in de-ionized water, calcium-chloride-buffered saline solution, and Hanks' Balanced Salt Solution (HBSS). The investigators were able to show that storing teeth in de-ionized water or $CaCl_2$ solution resulted in a large decrease in elastic modulus and hardness. After one day of storage, a decrease in the Young's modulus and hardness of up to 30% was observed. By one week of solution storage, mechanical properties dropped to below half of their initial values. In contrast, storing the specimens in HBSS did not significantly alter the mechanical properties for a time interval of two weeks. The behavior of the Young's modulus of specimens stored in water and HBSS is reproduced in Fig. 6⊞.

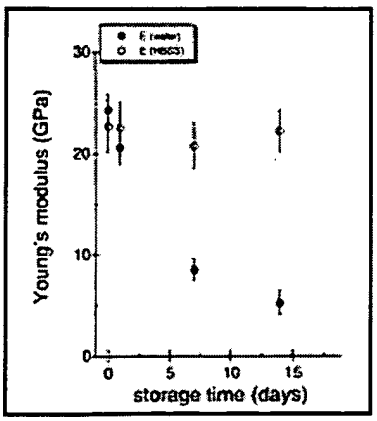

Figure 6. The Young's modulus of dentin as measured by AFM indentation. The solid circles represent repeated measurements obtained in water over the course of several days. The open circles show measurements obtained in Hanks' Balanced Salt Solution (HBSS). The water-stored specimens exhibited a rapid decline in modulus over 14 days. This decline was attributed to a loss of mineral from the near

View larger version (15K): [in this window] [in a new window]

surface layer. The specimens stored in HBSS, in contrast, maintained relatively constant modulus values over the same time period. The error bars are the standard deviations of the means of several specimens. Data from Habelitz *et al.* (2002a).

The decrease in modulus and hardness of dentin when stored in de-ionized water or $CaCl_2$ solution was attributed to partial demineralization of the near-surface layer. Because de-ionized water lacks calcium and phosphate ions, the chemical potential for dissolution of the mineral phase of dentin and enamel is high, and was assumed to be the major reason for the demineralization and softening of the tissues. Addition of calcium chloride to a saline solution also did not prevent demineralization. Since the pH of the $CaCl_2$ solution was slightly acidic (pH = 5.9), it was more likely to dissolve the calcium phosphate minerals. HBSS, on the other hand, was slightly basic (pH = 8.0) and was unable to dissolve the mineral phases by acidic attack. It is highly concentrated in Ca^{2+}, Mg^{2+}, Na^{+}, PO_4^{3-}, and Cl^{-} ions and has a composition comparable with that of the dental mineral phases. Therefore, the chemical potential of HBSS to dissolve the calcium phosphate phases in teeth is low, and surface demineralization was retarded.

By eliminating near-surface demineralization through proper specimen storage procedures, one can now obtain consistent values of the Young's modulus of hydrated peritubular and intertubular dentin. This is an important development, since it will allow for the study of the differences between wet and dry tissues, and provide elastic moduli more representative of *in vivo* conditions.

The nanoindentation method is limited in that it cannot be used to determine any of the other elastic constants, and it does not provide a direct measure of the continuum Young's modulus, since micromechanics arguments must be used to combine the separate measures of the inter- and peritubular dentin. Other techniques will now be described that have the potential to determine all of the second-order elastic constants of dentin completely.

Sonic measurements of the elastic constants

Measurement of sound speed is among the most accurate ways of determining the elastic constants of a material. For an isotropic material, the shear (G), bulk (K), and Young's (E) moduli are related to the longitudinal (V_l) and shear (V_s) wave velocities and the specimen density, ρ, by (Love, 1960):

$$G = \rho V_s^2 \tag{12}$$

$$K = \rho(V_l^2 - \frac{4}{3}V_s^2)$$

$$E = \rho V_s^2[\frac{3V_l^2 - 4V_s^2}{V_l^2 - V_s^2}]$$

Using the technique of ultrasonic interferometry, Gilmore *et al.* (1969) established the sound speeds in bovine dentin. With these data, and assuming isotropic elasticity, the investigators used Eqs. 12 to derive the second-order elastic constants. To facilitate comparisons with other measurements, we have reproduced the entire range in values of the elastic moduli from this work (Table 1⊞). The moduli, which are significantly higher than many more recent mechanical measurements, are in good agreement with nanoindentation (Habelitz *et al.*, 2002a).

View this table: [in this window] [in a new window] **TABLE 1 The Elastic Moduli of Dentin as Determined by Measurement of Sound Speed (Gilmore *et al.*, 1969) and by Resonant Ultrasound Spectroscopy (RUS) (Kinney*et al.*, 2002)**

The data from Gilmore *et al.* did not consider the possibility of anisotropy in the elastic constants. Lees and Rollins (1972) explored this possibility in a later study by measuring the longitudinal and shear wave velocities along orthogonal directions in the plane of the tubules. To facilitate these measurements, the investigators used the technique of critical angle reflection, where the angle of incidence of the sonic wave is scanned while the intensity of the reflected wave is monitored simultaneously. At certain critical angles, determined by the shear and longitudinal sound speeds in the specimen, the refraction vanishes, and there is a local maximum in the reflected signal. With Snell's law, it is possible to calculate the longitudinal and shear wave speeds from the values of these critical angles.

The main difficulty with this method lies in determining the principal symmetry directions in the tooth from only two orientations. Lees and Rollins assumed hexagonal (transverse isotropic) symmetry based on the microstructure of dentin. However, since the elastic properties were measured in only a single plane, the solution to the stiffness tensor for hexagonal symmetry was underdetermined. Therefore, the investigators assumed that the lower-sound speed values reported earlier by Gilmore *et al.* were obtained from measurements 45° with respect to the tubule axes. With this assumption, the complete elastic stiffness matrix was estimated (Table 2).

View this table: TABLE 2 The Second-order Elastic Constants as

[in this window] [in a new window] **Estimated from Critical Reflectance Ultrasound (Lees and Rollins, 1972) and by Resonant Ultrasound Spectroscopy (RUS) (Kinney *et al.*, 2002) for a Hexagonal Symmetry Model**

Lees and Rollins (1972) reported only the magnitudes of the elements in their derived stiffness tensor (C_{ij}). By matrix inversion, we can obtain the elements of the strain tensor, from which it is a simple task to calculate the Young's modulus. According to the hexagonal symmetry model and the stiffness tensor derived by Lees and Rollins, the Young's modulus in the tubule direction was 36 GPa, and 29 GPa in the perpendicular axis.

The Young's modulus, which can be derived from the stiffness matrix of Lees and Rollins (1972), is graphed in Fig. 7 as a function of tubule orientation. The transverse anisotropy in the critical reflectance data lies in contrast to what has been observed by either nanoindentation or compression testing along orthogonal axes. Also, the magnitude of the Young's modulus is significantly higher than that measured by Gilmore *et al.* Finally, the conclusion that the Young's modulus is higher in the direction of the tubules is at odds with both the micromechanics model, which dictates that the contribution to the elastic stiffness from the peritubular dentin should be negligible, and microstructural observations that the mineralized collagen fibrils lie perpendicular to the tubules.

Figure 7. The Young's modulus of dentin as a function of orientation of the tubules as calculated from the elastic constants of Lees and Rollins (1972). There was a pronounced hexagonal (transverse isotropic) anisotropy in

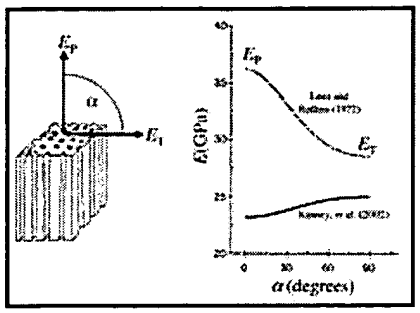

View larger version (21K):
[in this window]
[in a new window]

the Young's modulus, a result that was forced by *a priori* assumptions of the symmetry. The Young's modulus was greatest in the direction of the tubules (36 GPa) and much less in the orthogonal direction (29 GPa). The Young's modulus is compared with the values from the resonant ultrasound spectroscopy (RUS) measurements of Kinney *et al.* (2002). The RUS measurements, which were made without assumption as to material symmetry, also show hexagonal symmetry, but the stiffest orientation is now perpendicular to the axis of the tubules. This result is more consistent with what is known about the orientation of the collagen fibrils, which lie in a plane perpendicular to the tubule axis.

In spite of the practicality of critical angle reflection methods, we must be skeptical of the conclusions. The chief criticism, one that was acknowledged by the investigators, was that the assumption that prior measurement made in different laboratories and using different methods corresponded to the local minimums in the hexagonal symmetry model. This assumption forces an anisotropy that may not be representative of the actual symmetry of the specimen. In fact, from our knowledge of bone, the modulus should be greatest in the direction of the collagen fibrils (Pidaparti *et al.*, 1996). In dentin, this would mean that the elastic modulus should be greatest in the direction perpendicular to the tubules, the complete opposite of the critical angle results. Therefore, we must consider the possibility that Lees and Rollins (1972) made an incorrect assumption regarding the orientation of the specimens in the earlier work of Gilmore *et al.*

Clearly, what is needed is an ultrasonic method suited to small specimens, and

which allows for the determination of all of the elastic constants from a single orientation of the specimen and without assumptions as to the symmetry. Indeed, these requirements are met by a technique known as resonant ultrasound spectroscopy.

Resonant ultrasound spectroscopy (RUS) is a method for measuring single-crystal elastic constants with great precision (Migliori *et al.*, 1993). RUS makes use of Hooke's law and Newton's second law to predict the resonant modes of vibration of a specimen of known shape (Migliori *et al.*, 1993; Maynard, 1996). The entire stiffness tensor, C_{ij}, can be determined by comparison of the frequency spectrum produced by the resulting eigenvalue problem with the measured resonant frequencies (vibrational eigenmodes) of the specimen. It is important to note a significant difference between RUS and other sonic methods. In RUS, sound speed is not measured. Rather, the resonant frequencies of mechanical vibration are determined. This means that the stiffness tensor can be determined for small specimens from one measurement at a single orientation.

Since the development of RUS, the applications of this technique have been extended to include geological structures and complex particulate and fiber-reinforced composites (Jung *et al.*, 1999). Recently, this technique has been applied to small specimens of human coronal dentin, with interesting results (Kinney *et al.*, 2002). Cubes of dentin, approximately 2 mm on an edge, were mounted on opposing corners between two transducers in the RUS system. The resonant frequencies between 0.5 and 1.4 MHz were measured. The values of the resonant frequencies were calculated from an initial approximation of the stiffness tensor. The experimental and predicted

frequency distributions were then compared, and the residuals, F, were calculated. The elastic constants were adjusted from their initial values to minimize these residuals. Isotropic, cubic, and hexagonal material symmetry groups were modeled.

The elastic constants of hydrated and dry dentin, as measured by RUS, are listed in Table 1 for the isotropic, cubic, and hexagonal symmetry models. The best fit for the RUS data was with a hexagonal symmetry model, although deviations from isotropic symmetry were small. The angular deviation of the Young's modulus with respect to the axis of the dentinal tubules is graphed in Fig. 7. The Young's modulus was minimum in the direction of the tubules, and increased monotonically to maximum in the plane of the mineralized collagen fibrils. This should be compared with the critical angle results in the same Fig.

The measured anisotropy of the elastic constants of dentin can now be reconciled with its structural anisotropy. As in bone, the symmetry of the elastic constants is determined by the orientation of the collagen fibrils. However, the magnitude of the anisotropy (~10%) is not large. This may explain why previous studies have failed to detect anisotropic behavior in either the contact stiffness (Kinney *et al.*, 1999) or microhardness (Wang and Weiner, 1998a), since indentation techniques are known to be less sensitive to anisotropy (Vlassak and Nix, 1994). Furthermore, because the tubule orientation can vary widely across a specimen, a small anisotropy would most likely go undetected in a mechanical test of a larger specimen.

Viscoelastic behavior of dentin

Thus far, we have assumed that dentin is perfectly elastic at small strains, and

that the elastic constants do not depend on the strain rate. In other words, we have assumed that small deformations resulting from an imposed stress remain constant with time. In most biological tissues, this is not the case. At a constant stress, these materials continue to deform with time (creep). Therefore, if a constant strain is to be maintained, the applied stress must be continuously reduced (stress relaxation). Materials that exhibit a time-dependent response are called viscoelastic. If the time-dependence of the relaxation does not depend on the magnitude of the applied stress, the material exhibits linear viscoelasticity. On the other hand, if the time response changes with the applied stress, the material exhibits nonlinear viscoelasticity.

In a viscoelastic solid, the stress is out of phase with the strain. The amount of this phase shift is defined by a phase angle, δ, between the applied stress and the resulting strain. A detailed analysis defines the loss tangent of the phase angle in terms of a storage modulus, E', and a loss modulus, E'':

$$tan(\delta) = \frac{E''}{E'} \tag{13}$$

In a perfectly elastic solid, there would be no energy lost to creep deformation ($E'' = 0$), and the stress and strain would be in phase ($\delta = 0$). With increasing viscoelastic behavior, the phase angle would increase due to an increase in E'' and the corresponding decrease in E'. At extremely high strain rates (characteristic of ultrasound), or when stresses are too low to activate creep (typical of RUS), viscoelastic behavior should be less apparent. Therefore, the observation that the elastic constants determined by both RUS and sound velocity measurements are of similar magnitude, and that they are also higher than those determined by other methods, suggests that viscoelastic effects

might contribute to the lower modulus values measured with mechanical testing. Indeed, Craig and Peyton (1958) measured a significant contribution from "stress-relaxation" during their compression loading studies, and nanoindentation measurements display continuous creep during the static load segment prior to unloading (*e.g.*, Kinney *et al.*, 1996; and also Fig. 5⊞ in this review).

The classic analysis of viscoelasticity is based on the Maxwell element, a spring and dashpot arranged in series. The time-dependent relaxation modulus—for example, $E(t)$—can be written for a single element, i, as:

$$E(t) = E_i e^{-t/\tau_i} \tag{14}$$

where E_i represents the stiffness of the spring element i, and τ_i is the relaxation time of the element. A parallel arrangement of a group of Maxwell elements can be treated as a simple sum:

$$E(t) = \sum_{i=1}^{n} E_i e^{-t/\tau_i} \tag{15}$$

For an infinite number of Maxwell elements, the relaxation modulus can be written as a function of the continuous relaxation spectrum, $H(\tau)$, and the reduced modulus at infinite relaxation time, E_o (Ferry, 1970):

$$E(t) = E_o + \int_{-\infty}^{\infty} H(\tau) e^{-t/\tau} d \ln \tau \tag{16}$$

Similarly:

$$E'(\omega) = E_\infty + \int_{-\infty}^{\infty} \frac{H(\tau)\omega^2\tau^2}{(1 + \omega^2\tau^2)} d\ ln\ \tau \qquad (17)$$

$$E''(\omega) = \int_{-\infty}^{\infty} \frac{H(\tau)\omega\tau}{(1 + \omega^2\tau^2)} d\ ln\ \tau$$

A few studies have explored stress relaxation in dentin (Korostoff *et al.*, 1975; Tengrove *et al.*, 1995). Still, little is known about its time-dependent behavior. In what appears to have been the most detailed study of viscoelasticity in dentin, Korostoff *et al.* (1975) measured stress relaxation in specimens prepared from the roots of human incisors, cuspids, and premolars. The cylindrical specimens were machined to dimensions approximately 6.4 mm tall, and had a 3.8-mm outer and a 1.1-mm inner diameter. The specimens were loaded in compression at 37°C to a constant strain, ε_c, of 0.6%. The relaxation modulus, $E_r(t)$, was determined from the experimentally observed drop in applied load, $L(t)$, and the change in specimen height, Δh_c:

$$E_r(t) = \frac{\sigma(t)}{\varepsilon_c} = \frac{h_o\sigma(t)}{\Delta h_c} = \frac{4h_oL(t)}{\Delta h_c\pi(d_o^2 - d_i^2)} \qquad (18)$$

In Eq. 18, h_o was the original specimen height, and d_o and d_i were the outer and inner specimen diameters, respectively.

Korostoff *et al.* (1975) observed an exponential decline in the relaxation modulus with time from the shortest time measured ($t \sim 30$ sec) to a maximum relaxation time ($t \sim 10^4$ sec). Beyond 10^4 sec, no further stress relaxation was detected. They established the fully reduced modulus, E_o, to be 12.0 GPa. The

magnitude of the reduced modulus was as much as 40% lower than the instantaneous value at $t = 0$. This means that the Young's modulus measured by mechanical testing could range between 12 and 20 GPa, or greater, depending on the strain rate. Thus, it is probable that stress relaxation accounts for much of the discrepancy between mechanical testing and sonic measurements. This possibility can be explored more thoroughly by reconsideration of the AFM data.

It is well-known that the indenter stylus continues to displace inward during the constant load portion of an indentation measurement of dentin. This continued displacement is evidence that creep relaxation is occurring; the standard procedure for analyzing the indenter load/displacement data does not account for this relaxation. Recently, Feng and Ngan (2002) derived a correction formula for creep during indentation measurements. The correction is applied to the contact stiffness, S_m, measured at the beginning of unload:

$$\frac{1}{S_C} = \frac{1}{S_m} - \frac{\dot{h}_h}{|\dot{P}|} \tag{19}$$

In Eq. 19, S_c is the corrected contact stiffness to be used in Eq. 10, and the correction factor is the ratio of the time derivatives of the change in indenter displacement, h_h, during the constant hold cycle, and of the load, P, at the beginning of the unloading cycle.

This information has never been reported for indentation measurements on calcified tissues. However, approximate values for the correction factor can be obtained by estimation from the graphed representations of load and

displacement with time. A graphed representation of both the stylus displacement and the load as a function of time is shown in Fig. 8. These data were obtained from a typical AFM indentation measurement on wet intertubular dentin (*e.g.*, Kinney *et al.*, 1999). We approximated the creep relaxation rate by taking the slope of the displacement *vs.* time at the midpoint of the unloading cycle (1.7 nm/sec in this example); *dP/dt* was approximated at a point midway between the maximum load and the minimum load during the unloading cycle (131 μN/sec in this example). When the correction was applied to this specimen of wet dentin, the calculated Young's modulus increased from 20.6 GPa to 25.5 GPa, in excellent agreement with the RUS data (23.2-25.0 GPa; Table 1).

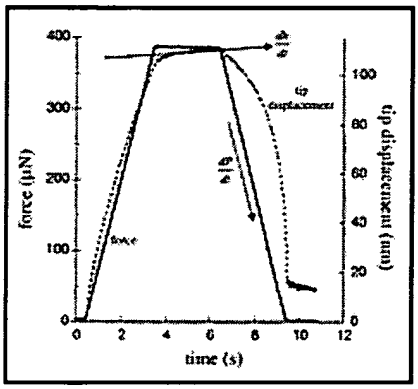

View larger version (23K): [in this window] [in a new window]

Figure 8. The applied force (solid line) and the tip displacement (dashed line) graphed as a function of time for a typical AFM indentation of hydrated intertubular dentin. In this example, the profile of the applied force was trapezoidal: a three-second loading phase, a three-second hold at maximum load, and a three-second unloading phase. At constant load, the indenter tip continues its inward displacement at a rate (*dh/dt*) that is approximated by the slope of the dashed line at the midpoint of the hold phase. The unloading rate is given by *dP/dt*. These factors are used to correct the AFM data for creep relaxation. In this example, the correction to the contact stiffness raises the Young's modulus by about 20%.

It now appears as if creep relaxation can explain the small differences between AFM indentation and RUS measurements of the modulus. However, the creep

mechanisms, and their possible dependence on the magnitude of the applied stress, remain unknown. An important question, given the absence of a well-defined time-dependent equation of state, is, what values of the elastic constants should be used to describe elastic deformation that occurs under physiological loading conditions? For example, what magnitudes of the elastic constants should be used in the frequency range of physiological interest (ν = 1 Hz ~ $1/t$)? This question can be answered only partially at this time.

A complete analysis of the time-dependent equation of state for dentin requires knowledge of the relaxation spectrum, $H(\tau)$, over all time scales. Then, the elastic constants can be formulated by expressions like Eq. 16. In principle, $H(\tau)$ can be obtained by analysis of the stress relaxation data. Prior to availability of computers and digitally instrumented load frames, this procedure was complicated; approximations were used to derive $H(\tau)$ from $E(t)$. For example, Korostoff *et al.* (1975) used an approximation method attributed to Alfrey and Doty (1945):

$$H(\tau) \cong [\frac{-dE(t)}{d\ \ln\ (t)}]_{t\ =\ \tau} \qquad (20)$$

With this approximation, Korostoff *et al.* (1975) evaluated the relaxation spectrum for root dentin for relaxation times from 30 sec to ~ 10^4 sec. The important result was the finding that the relaxation spectrum was constant over the three decades examined. Though the magnitude of H varied among specimens (H = 0.38 MPa; SD = 0.14), it was in all cases independent of the relaxation time. This was an important result; a constant value of H greatly simplifies the evaluation of the integral relationships in Eqs. 16 and 17.

There were admitted shortcomings with the study. Most critical, no

information was provided about stress relaxation at time scales shorter than 30 sec. Physiological time scales of greatest relevance lie in the range of 0.1 to 10 sec. There is a serious concern with extrapolating the above results to shorter time scales. In bone, deviation from simple exponential relaxation has been observed; stress relaxation at short time scales has followed a Kohlrausch-Williams-Watts (KWW) functional form (Sasaki *et al.*, 1993). Much more research, particularly at short time scales, is warranted.

No one has measured the frequency dependence of the loss tangent (Eq. 13⊞) for dentin. In the absence of this information, it is instructive to consider bone, which is compositionally similar to dentin. In a series of classic articles, Lakes and Katz (1979) provided the loss tangent in wet cortical bone over eight decades in relaxation time. Of interest was the observation that the loss tangent was a minimum, and also relatively constant, at physiologically relevant frequencies. If similar behavior can be inferred for dentin, then it would be reasonable to treat the dental hard tissues as perfectly elastic in physical models of mechanical deformation at physiologic strain rates, using, of course, the reduced values of the storage and loss moduli. More study is needed.

SUMMARY OF ELASTIC PROPERTIES

The good agreement between indentation and sonic measurements of the Young's modulus of hydrated dentin allows us to assign its magnitude between 18 and 25 GPa. The bottom of this range (18-20 GPa) is probably more appropriate for strain rates encountered with physiologic loading. This is significantly greater than the previously accepted range (13-16 GPa). However, the larger Young's modulus is now more consistent with what has been observed in bone, a mineralized tissue of similar composition. Smaller

values of the Young's modulus that are frequently reported can most likely be attributed to a strain-rate-dependent viscoelastic response, non-uniform stress states in small specimens, improper storage conditions, or flaws introduced during specimen preparation.

Sonic methods provide the most direct and precise determination of the elastic constants. They are least affected by stress relaxation. Because of this, we propose that the data from the RUS (Kinney *et al.*, 2002) and sound speed measurements (Gilmore *et al.*, 1969) be used to define the most probable range for all of the elastic constants of dentin in the absence of viscoelastic effects (Table 1⊞). Because RUS is more likely to probe perfectly elastic behavior (the maximum strain in the specimen was 6×10^{-6}, and the Mach number was approximately 1.4×10^{-5}), and because RUS does not require assumptions as to the material's symmetry, we believe them to be the most accurate values of the elastic constants yet measured. However, because RUS has been applied only to coronal dentin from a single site, one should refrain from generalizing these results. It is probable that the elastic properties are site-dependent. Much more work remains to be done.

The intrinsic elastic constants provide only part of the story. The viscoelastic behavior of dentin must be explored in greater detail if a constitutive equation of state is to be developed for dentin. In the frequency range of physiological interest (0.1-10 Hz), the phase angle between stress and strain is most likely small, so that dentin can be modeled as a perfectly elastic solid. However, it is likely that the effective elastic moduli are reduced by about 10-20% from the values obtained with sonic measurements. This is consistent with the differences between the RUS measurements and those obtained by indentation and uni-axial testing. However, this observation is still speculative: The

mechanisms controlling viscoelastic behavior, and their possible dependence on the stress amplitude, remain unknown in dentin.

As our knowledge of the elastic properties of normal dentin improves, other questions are raised that have significant implications for dentin pathologies. Is there a functional relationship between the mineral density and the elastic moduli? Does age-related transparency alter the elastic properties of root dentin? Does reparative dentin that forms at the dentin/pulp interface have the same elastic properties as the secondary dentin it adjoins? Answers to these questions will be important in the continued development of minimally invasive approaches in restorative dentistry.

Hardness of Dentin

▲ Top
▲ Previous
▼ Next

Hardness tests measure the resistance of the dentin to deformation caused by penetration of an indenting stylus. Since its introduction, the Knoop (Knoop *et al.*, 1939) indenter has proved to be the workhorse in studies of dentin. The long aspect ratio (7.11 times longer in one dimension) allows for accurate measurements of area, even with shallow indentations. Knoop, therefore, is extremely useful for the small, thin specimens typical of studies of mineralized tissues.

Hardness is defined in units of pressure, or force *per* unit area of indentation. Unlike Vickers or Brinell methods, which use the contact area of the indenter stylus, the Knoop method uses the projected area, A_p, in the calculation of hardness (KNH):

$$KNH = \frac{P}{A_p} = 14.22 \frac{P}{l^2} \quad (21)$$

where P is the applied load (in kg) and l is the length (in mm) across the long axis of the remnant impression. In SI units, 1 kg/mm^2 ~ 9.8 MPa.

Many investigators have determined that dentin hardness depends on mineral concentration. Featherstone *et al.* (1983) developed an analytic expression relating Knoop hardness to the volume percent of mineral (V_m):

$$\sqrt{KNH} = 0.197 V_m - 0.24 \quad (22)$$

Though the validity of Eq. 22 obviously breaks down for low concentrations of mineral, the expression appears to fit the experimental data over a range of mineral concentrations associated with normal and carious dentin.

In addition to its association with the mineral concentration, hardness has been correlated with location in the tooth. The works of Ogawa (1983) and Wang and Weiner (1998b) show that the mantle dentin immediately subjacent to the enamel (KNH ~ 60 kg/mm^2) is softer than the underlying primary dentin (KNH ~ 70 kg/mm^2). Also, hardness gradually decreases with proximity to the pulp, falling precipitously in an inner layer of dentin of about 0.5 mm thickness that surrounds the pulp (KNH ~ 30 kg/mm^2).

Clearly, Eq. 22 mandates that V_m must be lower near the pulp than in the primary dentin. However, whether this is a result of increased porosity, or whether the intertubular dentin matrix is less mineralized, is an important question. In a careful and methodical study, Pashley and Parham (1985) determined that there was a significant correlation between decreased

hardness and increased density of tubule lumens. The authors concluded that the reduced hardness was an end result of the lower mineral concentration brought about by the increased tubule porosity. This conclusion, however, was seriously challenged in a later study by Kinney *et al.* (1996), who showed that most, if not all, of the decreased hardness near the pulp could be explained by a decrease in the hardness of the intertubular dentin matrix. Thus, it is likely that the intertubular dentin matrix near the pulp is less mineralized.

It is tempting to try to relate dentin hardness to other physical properties like yield stress, tensile strength, or Young's modulus. In ductile metals, for example, the yield stress and tensile strengths are often observed to scale with hardness. However enticing these scalings, we must remember that they were derived from plasticity theory for materials that display significant yielding. In contrast, mineralized tissues are more brittle, showing little if any yielding prior to failure.

Though we should not anticipate similar relationships with dentin hardness, there is a possibility that its hardness might scale with the Young's modulus. Eq. 22⊞ describes a relationship between hardness and mineral concentration, and there is strong evidence that the Young's modulus is also dependent on the amount of mineral. However, because hardness also depends on yielding, microstructural features in the dentin that do not influence the elastic properties might mask any such correlation. In many materials, for example, the grain size controls yield strength by the Hall-Petch relationship. Therefore, the ratio of hardness to modulus need not be constant. Nevertheless, a relationship between hardness and modulus in dentin is worth seeking. Although several papers have reported hardness and modulus values for enamel and dentin, a systematic analysis of their relationship has not been

undertaken.

Ultimate Strength of Dentin

▲ Top
▲ Previous
▼ Next

Failure data have largely been limited to measurements of shear strength or ultimate compressive or tensile strength. For dentin specimens failed in tension, reported magnitudes of the ultimate strength range from 52 MPa (Bowen and Rodriguez, 1962) to 105 MPa (Sano *et al.*, 1994). It is likely that the two-fold differences in the tensile strength were related to flaws in the specimens, since both a size effect and an improvement in strength with surface sanding of the specimens have been noted (Sano *et al.*, 1994). Moreover, measurements of compressive strength, which are less likely to be affected by flaws, were more consistent. Values of compressive strength range from 275 to 300 MPa (Craig and Peyton, 1958).

Shear strength, measured either by punching or lap-shear, also has been highly variable. Using a shear punch apparatus, Cooper and Smith (1968) obtained values for shear strength that ranged from 64 to 132 MPa, not too dissimilar from later measurements by Roydhouse (1970) (69-147 MPa). More recent measurements by single-plane lap shear produced shear strengths of 36 MPa; this low value may have been due to the specimens having been from dentin closer to the pulp, or to problems with the experimental design, or with bending of the specimen (Gwinnett, 1994).

Our group (Watanabe *et al.*, 1996) demonstrated that some of the disparity in reported values of the shear strength could be attributed to tubule orientation and location within the tooth. The lowest values of lap shear strength were obtained in less mature dentin nearer the pulp, with the tubules oriented

parallel to the shear plane (54 MPa). The highest values were obtained in mature cuspal dentin with the shear plane perpendicular to the tubules (92 MPa). Others also have observed a similar orientation dependence with the tensile strength (Lertchirakarn *et al.*, 2001).

The large standard deviations common to all measurements of dentin strength suggest that strength is controlled by the flaw distribution in a specimen. A flaw is similar to the weakest link in a chain: Variations in the flaw size lead to variations in the failure strength. Specimens with large flaws will fail at lower stresses than will specimens containing smaller flaws. For a random distribution of flaws, the tensile strength should obey a Weibull probability distribution function (pdf), where the probability, P_f, that a specimen fails at a stress level σ is given by the expression:

$$P_f = 1\ exp\ (-\ V(\frac{\sigma}{\sigma_o})^{m}) \tag{23}$$

In Eq. 23, V is the volume of the gauge region of the specimen, σ_o is the shape factor, and m is the dimensionless Weibull modulus. A specimen size effect follows naturally from the Weibull pdf. For two specimens with identical flaw distributions, the failure strengths will scale with the respective volumes (V_1 and V_2) of the gauge region as:

$$\frac{\sigma_1}{\sigma_2} = (\frac{V_2}{V_1})^{1/m} \tag{24}$$

The Weibull modulus, m, determines the size-sensitivity of the failure strength; smaller values of m lead to greater sensitivity to specimen size.

Most studies of tensile strength have recorded only the means and standard deviations of the experimental measurements. An exception was the early work of Lehman (1967), who tabulated the test results of all 100 of his tensile strength measurements of root dentin. These results are recast in a Weibull distribution in Fig. 9. Included for comparison are the tensile strength results from mid-coronal dentin reported by Staninec *et al.* (2002). Both data sets are well-described by the Weibull distribution function ($R^2 = 0.97$). However, the Weibull moduli are different for the two examples shown ($m \sim 6$ for Lehman's data; $m \sim 3$ for the displayed example from Staninec *et al.* [2002]). Staninec *et al.* observed that the Weibull modulus did not vary statistically with depth or location in the tooth; the average Weibull modulus was 4.5, with a range between 3 and 6. The large variations in the Weibull modulus may reflect differences in the flaw population between teeth, or may simply be the result of random defects introduced during specimen preparation. It has also been suggested that the Weibull modulus might decrease with age, reflecting an age-related change in either the distribution of flaws or their stress-sensitivity (Tonami and Takahashi, 1997). The flaws are cryptogenic; the precise nature of these flaws, whether they are intrinsic to dentin or created in specimen preparation, needs to be determined.

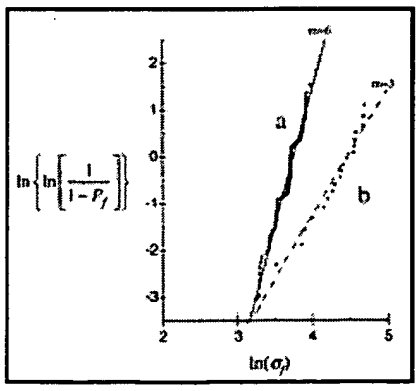

View larger version

Figure 9. Ultimate tensile strength data from Lehman (1967) (open circles) and Staninec *et al.*2002 (solid circles). The data have been graphed in the form of a Weibull probability distribution function, with the abscissa given by the natural log of the failure stress, and the failure probability, P_f, given by Eq. 23. Both sets of data fit the Weibull distribution

(12K):
[in this window]
[in a new window]

function ($R^2 = 0.97$), although the slopes, *m*, are different. The slope of the curve determines the sensitivity of the tensile strength to specimen size. Weibull behavior is an indication that a distribution of flaws determines the magnitude of the tensile strength of dentin.

Fracture Properties of Dentin

▲ Top
▲ Previous
▼ Next

The previous discussion of dentin strength suggests that a fracture mechanics approach would be more appropriate than a strength-of-materials approach for the study of tooth failure. Yet, surprisingly few studies have taken this approach. Important exceptions to an otherwise-absence of quantitative fracture data are the works by Rasmussen *et al.* (Rasmussen *et al.*, 1976; Rasmussen, 1984; Rasmussen and Patchin, 1984), El Mowafy and Watts (1986), and Imbeni *et al.* (2002). Rasmussen *et al.* determined the work-of-fracture of normal dentin in directions parallel and perpendicular to the tubule axis. This work was important in that it detected a small directional dependence in the work-of-fracture; it was energetically more favorable to fracture dentin perpendicular to the axis of the tubules than parallel to them. However, the relatively large works-of-fracture implied a toughening mechanism and the possibility of significant yielding ahead of the crack. Perhaps because of this, the authors stopped short of equating the work-of-fracture with any intrinsic material property such as fracture toughness.

The work by El Mowafy and Watts (1986) was of considerable importance. It was the first attempt to measure the intrinsic fracture toughness, K_c, of dentin with an ASTM standard specimen geometry: the compact tension specimen.

For normal coronal dentin, these investigators reported a value of 3.08 MPa $\sqrt{m}$ with a 10% standard deviation. Based upon an unpublished value of the yield stress, the authors assumed that the test resulted in a valid measure of K_c. They could therefore equate their fracture toughness measures with the energy release rate, *G*, and obtained good agreement with the earlier data of Rasmussen (Rasmussen *et al.*, 1976; Rasmussen, 1984; Rasmussen and Patchin, 1984).

Three valuable findings came from the work of El Mowafy and Watts (1986): (1) Compact tension specimens could be fabricated from coronal dentin; (2) fracture toughness was high for a brittle material, indicating that either the collagen fibrils or the tubule lumens provide a toughening mechanism; and (3) fracture toughness was independent of temperature through a range from 0 to 60°C. However, since the fracture plane was parallel to the tubules (*i.e.*, in the orientation associated with the highest work of fracture), it is possible that the fracture toughness could be considerably lower in the orthogonal plane. Furthermore, El Mowafy and Watts (1986) used a blunt notch instead of a fatigue precrack, so that notch toughening might have elevated their results. To explore these possibilities further, Imbeni *et al.* (2002) considered the effects of notch root radius on the measurement of fracture toughness in a direction perpendicular to the tubules.

Imbeni *et al.* (200) prepared 10-mm-long beam-shaped specimens from human molars. Tests were conducted in three-point bend, with a span between the loading points of approximately 5 mm. Two protocols were followed. For the first protocol, sharp notches were prepared in the specimens with the root radius ranging from 30 to 50 μm. For the second protocol, a fatigue precrack

was grown out of the notch by fatigue cycling at 2 Hz with a maximum stress intensity of about 1 MPa $\sqrt{m}$. The fracture toughness in the fatigue-precracked specimens was 1.8 MPa $\sqrt{m}$ (SD = 0.1), whereas, in the notched specimens, the fracture toughness was significantly higher (2.7 MPa $\sqrt{m}$; SD = 0.1). Upon further analysis, these authors found evidence of an apparent relationship between the fracture toughness and the square root of the notch radius.

Was the lower value of the fracture toughness measured in Imbeni's work entirely the consequence of their having used a fatigue precrack, or was it also affected by the orientation of the fracture plane? This is important, since the critical flaw size, a_c, is a strong function of the fracture toughness K_c:

$$a_c \propto \frac{K_c^2}{\pi \sigma_{app}^2} \tag{25}$$

If the difference in fracture toughness was an artifact of the notch radius, then for the same far-field applied stress, σ_{app}, the critical flaw size would be roughly three times smaller than that predicted from the earlier values of El Mowafy and Watts (1986). The critical size of an elliptical flaw is graphed as a function of the far-field stress in Fig. 10. Since the critical flaw size has a profound importance on lifetime modeling (see following section), answers to these questions are needed.

Figure 10. The critical flaw size in dentin as a function of far-field applied stress (MPa). The critical flaw size is calculated for an elliptical flaw according to Eq. 25. The dashed line corresponds to the fracture toughness established

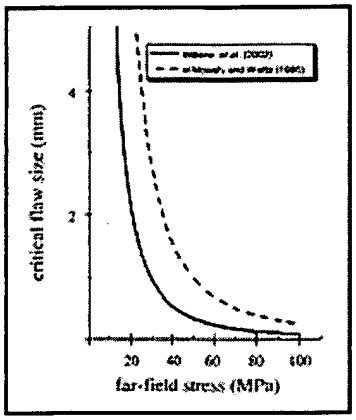

View larger version (18K):
[in this window]
[in a new window]

by El Mowafy and Watts (1986): K_c = 3.08 MPa $\sqrt{m}$. The solid line corresponds to the more conservative estimate of the fracture toughness determined by Imbeni *et al.* (2002): K_c = 1.8 MPa $\sqrt{m}$. Knowledge of the critical flaw size is of great importance in lifetime modeling.

Fatigue Properties of Dentin

▲ Top
▲ Previous
▼ Next

Teeth are subject to cyclic loads during mastication. The frequency of the loading is nominally 1 Hz, and stress amplitudes of 20 MPa can be estimated at the cervical margins (Anderson, 1956). Therefore, it is important to know the response of the tooth to cyclic loading: its fatigue behavior. Characterizing fatigue behavior involves determining the total life to failure in terms of a cyclic stress range. This method is often referred to as the "S/N" (stress/life) approach, and requires the measurement of the number of cycles required to induce failure in a flaw-free material at a given alternating stress. Some materials exhibit a fatigue limit: a stress below which failure does not occur. Many materials, however, do not have a fatigue limit. For those cases, it is convenient to define a material lifetime in terms of the endurance strength, which is the alternating stress below which the material will not fail before a predefined number of cycles.

Does dentin exhibit classic S/N behavior, and, if so, are the cyclic stresses of mastication below its endurance strength? A partial answer to this question was provided in a study of tensile fatigue behavior in bovine dentin (Tonami and Takahashi, 1997). In that study, tensile specimens with 1.5 x 1 x 1-mm-gauge sections were subjected to a sinusoidal cyclic unipolar load at 5 Hz. The load ratio, R, which is defined as the minimum load divided by the maximum load, was allowed to vary between 0.15 and 0.25. A staircase method was used to determine the stress at which the specimen failed at 10^5 cycles. For example, if a specimen did not fail at 10^5 cycles at a stress of 45 MPa, another specimen was tested at a stress level 5 MPa higher. With this procedure, Tonami and Takahashi (1997) established the endurance strength, for failure at 10^5 cycles, to lie between 45 and 50 MPa. This would suggest that fatigue is not a factor in tooth failure under conditions of normal masticatory loading.

The work of Tonami and Takahashi was important in establishing the existence of fatigue failure in dentin. However, there were several shortcomings that limit its usefulness. First, the endurance strength was established for failure at 10^5 cycles. This was short, especially considering that 10^6 cycles are expected in a year from mastication. Second, the load frequency used in the study (5 Hz) was five times greater than that observed in physiological loading (1 Hz); the investigators assumed that there would be no frequency dependence on the fatigue life. This was a questionable assumption, however, especially considering the pronounced frequency dependence of fatigue in bone (Zioupos *et al.* 2001). Finally, the work was performed on bovine dentin.

The recent work of Nalla *et al.* (2002) was designed to address many of these issues. In this study, specimens of human dentin were subjected to fatigue

loading at a constant load ratio, R = 0.10, and at two different cyclic frequencies: 2 and 20 Hz. The authors observed the existence of a classic S/N fatigue response to repetitive loading, and identified an apparent fatigue limit at 10^6-10^7 cycles, which was estimated to lie between 25 and 45 MPa at frequencies of 2 and 20 Hz, respectively. Failure appeared to be caused by the initiation and growth of a single, dominant crack.

In the absence of intrinsic flaws, it appears that fatigue failure will not occur in human teeth. However, the Weibull nature of tensile failure indicates that there is an inherent population of pre-existing flaws in normal dentin. Thus, the existence of a fatigue limit in a nominally flaw-free specimen of dentin cannot be generalized to the whole tooth. The classic S/N approach is not conservative enough; it does not address the question of whether a pre-existing flaw can grow to a critical size during normal loading conditions. This requires the measurement of fatigue growth crack rates, *da/dN*, for a fracture-mechanics-based approach to failure of human dentin.

Nalla *et al.* (2002) determined the fatigue crack growth rate by measuring stiffness loss in the specimen during cyclic loading. They observed a Paris power law relationship of the crack growth rate with the stress intensity, ΔK. The experimentally derived crack growth rate for human dentin was determined to be:

$$\frac{da}{dN} = C(\Delta K)^m = 6.24 \times 10^{-11} (\Delta K)^{8.76} \quad (26)$$

The Paris law exponent, $m = 8.76$, was smaller than that of carbonated apatite bone substitute ($m = 17$; Morgan *et al.* 1997), but larger than that frequently observed in ductile metals ($m \sim 2$-4; Ritchie, 1999). The Paris power law

relationship provides a method for estimating a threshold stress intensity, ΔK_{TH}, below which crack growth cannot occur. Extrapolation of Eq. 26 yielded a threshold stress intensity of 1.1 MPa $\sqrt{m}$. For stress intensities greater than ΔK_{TH}, subcritical crack growth will occur.

When a crack reaches a critical size, a_c, determined by equating the fracture toughness, K_c, with the stress intensity at the crack tip, the structure will fail. Nalla *et al.* (2002) used lifetime modeling to estimate the number of cycles, N_f, required for an incipient crack of length a_o to grow to the critical size under a far-field applied stress $\Delta\sigma_{app}$:

$$N_f \approx \frac{2(f(a/b)\Delta\sigma_{app})^{-m}\,\pi^{-m/2}[a_o^{1-m/2} - a_c^{1-m/2}]}{(m-2)C} \qquad (27)$$

In Eq. 27, m and C were determined from the experimental data (Eq. 26); the dimensionless function $f(a/b)$ was determined for a small, elliptical surface flaw; for this configuration, $f(a/b)$ was equal to 1.12.

Eq. 27 was an important result. Now it was possible to estimate the number of cycles (time) required for an incipient crack to reach catastrophic proportions. It also placed a limit on the necessary spatial resolution of a clinical imaging system to detect the smallest flaw size that could eventually grow large enough to cause failure. In a hypothetical example, consider the smallest crack that could grow to critical size in a year's time as a result of mastication forces of 20 MPa (~ 10^6 cycles). With a conservative estimate of K_c of 1.8 MPa $\sqrt{m}$, the critical flaw size is about 2 mm. Eq. 27 predicts that a

0.9-mm crack would grow to critical size in 10^6 cycles. If the mastication forces were even higher, say 30 MPa, a pre-existing crack of 0.3 mm would grow to critical size in the same number of cycles (see Fig. 11). Whereas the classic S/N approach predicts that fatigue failure cannot occur at stresses below 30 MPa, this more conservative damage-tolerant approach suggests that failure will occur at these stresses if there were a pre-existing flaw of sufficient size. The source of these flaws remains unknown; their existence can be inferred from the statistical nature of tensile failure.

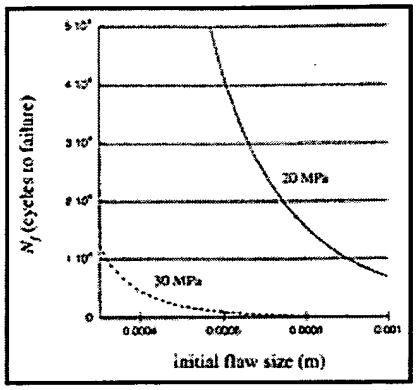

View larger version (19K):
[in this window]
[in a new window]

Figure 11. The number of required cycles for growing a flaw from an initial to critical size for two different far-field stresses (Eq. 27). The solid line is for a far-field stress of 20 MPa; it corresponds to the stresses of mastication. The dashed line corresponds to a slightly elevated stress level (30 MPa). An initial flaw 0.3 mm long will grow to catastrophic size in roughly 10^6 cycles at 30 MPa (approximately one year); at 20 MPa, a pre-existing flaw would have to be 0.9 mm long to grow to catastrophic size in the same number of cycles. Lifetime models such as Eq. 27 depend critically on the Paris law exponent, m (Eq. 26), the critical flaw size (Eq. 25), and the stress intensities at the head of the crack tip.

Two major assumptions have gone into the development of Eq. 27. First, the crack growth rate was inferred from stiffness loss in the specimens during cyclic loading. If there were a sizeable yield, or damage, zone ahead of the crack tip, its contribution to the stiffness loss would affect the estimate of the

crack length. Second, and perhaps more serious, is the fact that the crack growth rate measurements were performed in a controlled environment of Hanks' balanced salt solution. It is quite possible that the fluctuations of pH and mineral concentration in the mouth might have a pronounced effect on crack growth rate. Further study of environmental effects on fatigue crack growth is warranted.

Conclusions

▲ Top
▲ Previous
▼ Next

Many of our conceptions of basic biomechanical properties of dentin have changed since the last comprehensive review (Waters, 1980). The magnitudes of the elastic constants must be revised upward, and viscoelastic effects must be taken into account. Also, the concept of strength as an important engineering quantity must be replaced by a fracture mechanics approach to dentin failure, since pre-existing flaws can cause teeth to fail at stresses far less than their theoretical strength. In particular, a lifetime modeling, or damage-tolerant, approach appears promising for the development of a clinical predictor of tooth failure. These paradigm shifts have been facilitated by advances in measurement science combined with a better understanding of dentin microstructure.

It now appears that the elastic constants of dentin have hexagonal symmetry, with the stiffest direction oriented in the plane perpendicular to the tubules. This finding is consistent with a micromechanics model that suggests that the peritubular dentin has negligible influence on material symmetry. Furthermore, it is also consistent with the observations in other tissues that the stiffest orientation is in the direction of the mineralized collagen fibrils. We can conclude, then, that the elastic properties of dentin are explainable in

terms of the microstructure of the intertubular dentin matrix, and that any correlation of the elastic properties with the tubule direction is a necessary consequence of the orthogonal relationship between the tubules and collagen fibrils. Therefore, research must focus on the mineralized collagen scaffold, and explore the coupling between the mineral and collagen phases and its effects on biomechanical properties.

The Weibull behavior of tensile strength data suggests that failure initiates at flaws. These flaws may be intrinsic, perhaps regions of altered mineralization, or extrinsic, caused by cavity preparation, wear, or damage. Clearly, identifying the flaws responsible for failure is important, as is the understanding of how sub-critical flaws can grow and coalesce with cyclic loading. Though the cyclic forces of mastication are insufficient to cause failure in perfect dentin, it now appears that pre-existing flaws in normal dentin can grow to catastrophic size with application of small cyclic loads. Furthermore, understanding how shifts in the chemical environment affect the crack growth rate will be essential for developing lifetime models. At present, many of these data are lacking.

Finally, little is known about the biomechanical properties of altered forms of dentin. Studies seem to suggest that there are at least two forms of transparent dentin, a form associated with caries and a form associated with age-related changes in the root. Each type of transparency may exhibit unique biomechanical signatures. In addition, there are caries lesions and genetic disorders, such as dentinogenesis imperfecta, which appears to lack the phosphoproteins that promote binding between the mineral and the collagen. It is absolutely essential that the properties of these altered forms of dentin be obtained before an understanding of how dentin pathologies affect tooth

strength can be developed.

Current conservative dental practice is increasingly oriented toward efforts to arrest and remineralize caries lesions with either solution chemistry or more fundamental tissue engineering approaches. An accurate understanding of the properties of the dental hard tissues is a requirement for assessment of the effectiveness of these approaches. Without knowledge of mineral-collagen coupling and its biomechanical consequences, we may not truly be restoring the affected tissues. This shift in emphasis from traditional filling procedures to tissue restoration requires a firm understanding of the structure/properties relationships in dentin at many length scales. It is hoped that this review has clarified what is known, and has raised awareness of what remains to be learned about the mechanical properties of dentin.

Acknowledgments

This work was supported in part by the National Institutes of Health, National Institute of Dental and Craniofacial Research (grants PO1 DE09859, DE 11526, and DE13029). The authors thank many investigators for sharing their time, comments, and data prior to publication. In particular, we thank Prof. David Pashley, Prof. Lawrence Katz, Prof. Robert O. Ritchie, Dr. James S. Stolken, Dr. Stefan Habelitz, and R.K. Nalla for valuable discussions.

References

▲ Top

Alfrey T, Doty P (1945). The methods of specifying the properties of viscoelastic materials. *J Appl Physics* 16:700–713.

Anderson DJ (1956). Measurement of stress in mastication. *J Dent Res*

35:664–670.[Abstract/Free Full Text]

Balooch M, Wu-Magidi IC, Balazs A, Lundkvist AS, Marshall SJ, Marshall GW, *et al.* (1998). Viscoelastic properties of demineralized human dentin measured in water with atomic force microscope (AFM)-based indentation. *J Biomed Mater Res* 40:539–544.[Medline]

Bonar LC, Lees S, Mook HA (1985). Neutron diffraction studies of collagen in fully mineralized bone. *J Molec Biol* 181:265–270.[Medline]

Bowen RL, Rodriguez MM (1962). Tensile strength and modulus of elasticity of tooth structure and several restorative materials. *J Am Dent Assoc* 64:378–387.

Christensen RM (1990). A critical evaluation for a class of micromechanics models. *J Mechan Physics Solids* 38:379–404.

Cooper WE, Smith DC (1968). Determination of the shear strength of enamel and dentine (abstract). *J Dent Res* 47:997.

Craig RG, Peyton FA (1958). Elastic and mechanical properties of human dentin. *J Dent Res* 37:710–718.[Free Full Text]

Doerner MF, Nix WD (1986). A method for interpreting the data from depth-sensing indentation instruments. *J Mater Res* 1:601–609.

El Mowafy OM, Watts DC (1986). Fracture toughness of human dentin. *J Dent Res* 65:677–681.[Abstract/Free Full Text]

Featherstone JD, ten Cate JM, Shariati M, Arends J (1983). Comparison of artificial caries-like lesions by quantitative microradiography and microhardness profiles. *Caries Res* 17:385–391.[Medline]

Feng G, Ngan AHW (2002). Effects of creep and thermal drift on modulus measurement using depth-sensing indentation. *J Mater Res* 17:660–668.

Ferry JD (1970). Viscoelastic properties of polymers. New York: John Wiley & Sons, pp. 60-71.

Gilmore RS, Pollack RP, Katz JL (1969). Elastic properties of bovine dentine

and enamel. *Arch Oral Biol* 15:787–796.

Goodis HE, Marshall GW Jr, White JM, Gee L, Hornberger B, Marshall SJ (1993). Storage effects on dentin permeability and shear bond strengths. *Dent Mater* 9:79–84.[Medline]

Gustafson MB, Martin RB, Gibson V, Storms DH, Stover SM, Gibeling J, *et al.* (1996). Calcium buffering is required to maintain bone stiffness in saline solution. *J Biomechan* 29:1191–1194.[Medline]

Gwinnett AJ (1994). A new method to test the cohesive strength of dentin. *Quintessence Int* 25:215–218.[Medline]

Habelitz S, Marshall GW, Balooch M, Marshall SJ (2002a). Nanoindentation and the storage of teeth. *J Biomechan* 35:995–998.[Medline]

Habelitz S, Balooch M, Marshall SJ, Balooch G, Marshall GW (2002b). In-situ atomic force microscopy of partially demineralized human dentin collagen fibrils. *J Struct Biol* 138:227–236.[Medline]

Hashin Z (1983). Analysis of composite materials—a survey. *J Appl Mechan* 50:481–503.

Huo B, Zheng QS, Zhang Q, Wang JD (2000). Effect of dentin tubules to the mechanical properties of dentin. Part II: Experimental study. *Acta Mechan Sinica* 16:75–82.

Imbeni V, Nalla RK, Bosi C, Kinney JH, Ritchie RO (2002). On the in vitro fracture toughness of human dentin. *J Biomed Mater Res* (in press).

Jones RM (1975). Mechanics of composite materials. Washington, DC: Scripta Book Company.

Jones SJ, Boyde A (1984). Ultrastructure of dentin and dentinogenesis. In: Dentin and dentinogenesis. Linde J, editor. Boca Raton: CRC Press, pp. 81-134.

Jung HK, Cheong YM, Ryu HJ, Hong SH (1999). Analysis of anisotropy in elastic constants of SiCp/2124 Al metal matrix composites. *Scripta Materialia* 41:1261–1267.

Katz JL (1971). Hard tissue as a composite material—1. Bounds on elastic behavior. *J Biomechan* 4:455–473.[Medline]

Katz JL, Ukraincik K (1971). On the anisotropic elastic properties of hydroxyapatite. *J Biomechan* 4:221–227.

Kinney JH, Balooch M, Marshall GW, Marshall SJ (1993). Atomic-force microscopic study of dimensional changes in human dentine during drying. *Arch Oral Biol* 38:1003–1007.[Medline]

Kinney JH, Balooch M, Marshall SJ, Marshall GW Jr, Weihs TP (1996). Hardness and Young's modulus of human peritubular and intertubular dentine. *Arch Oral Biol* 41:9–13.[Medline]

Kinney JH, Balooch M, Marshall GW, Marshall SJ (1999). A micromechanics model of the elastic properties of human dentine. *Arch Oral Biol* 44:813–22. [Medline]

Kinney JH, Oliveira J, Haupt DL, Marshall GW, Marshall SJ (2001a). The spatial arangement of tubules in human dentin. *J Mater Sci: Mater Med* 12:743–751.[Medline]

Kinney JH, Pople JA, Marshall GW, Marshall SJ (2001b). Collagen orientation and crystallite size in human dentin: a small angle x-ray scattering study. *Calcif Tissue Int* 69:31–37.[Medline]

Kinney JH, Gladden J, Marshall GW, Marshall SJ, So JH, Maynard JD (2002). Resonant ultrasound spectroscopy measurements of the second order elastic constants in human dentin. *J Biomechan* (in press).

Kishen A, Ramamurty U, Asundi A (2000). Experimental studies on the nature of property gradients in the human dentine. *J Biomed Mater Res* 51:650–659.[Medline]

Knoop F, Peters G, Emerson WB (1939). A sensitive pyramidal-diamond tool for indentation measurements. *J Res Natl Bur Stds* 23:39–61.

Korostoff E, Pollack SR, Duncanson MG (1975). Viscoelastic properties of human dentin. *J Biomed Mater Res* 9:661–674.[Medline]

Lakes RS, Katz JL (1979). Viscoelastic properties of wet cortical bone: 1. Torsional and biaxial studies. *J Biomechan* 12:657–678.[Medline]

Lees S, Rollins FR (1972). Anisotropy in hard dental tissues. *J Biomechan* 5:557–566.[Medline]

Lehman ML (1967). Tensile strength of human dentin. *J Dent Res* 46:197–201.[Abstract/Free Full Text]

Lertchirakarn V, Palamara JEA, Messer HH (2001). Anisotropy of tensile strength of root dentin. *J Dent Res* 80:453–456.[Abstract/Free Full Text]

Love AEH (1960). Mathematical theory of elasticity. New York: Dover Press.

Marshall GW, Marshall SJ, Kinney JH, Balooch M (1997). The dentin substrate: structure and properties related to bonding. *J Dentist* 25:441–458.

Marshall GW, Yucel N, Balooch M, Kinney JH, Habelitz S, Marshall SJ (2001). Sodium hypochlorite alterations of dentin and dentin collagen. *Surface Sci* 491:444–455.

Maynard J (1996). Resonant ultrasound spectroscopy. *Physics Today* 49:26–31.

Migliori A, Sarrao JL, Visscher WM, Bell TM, Lei M, Fisk Z, *et al.* (1993). Resonant ultrasound spectroscopic techniques for measurement of the elastic moduli of solids. *Physica B* 183:1–24.

Morgan EF, Yetkinler DN, Constantz BR, Dauskardt RH (1997). Mechanical properties of carbonated apatite bone mineral substitute: strength, fracture and fatigue behaviour. *J Mater Sci: Mater Med* 8:559–570.

Nalla RK, Imbeni V, Kinney JH, Staninec M, Marshall SJ, Ritchie RO (2002). On the in vitro fatigue behavior of human dentin with implications for life prediction. *J Biomed Mater Res* (in press).

Nye JF (1972). Physical properties of crystals: their representation by tensors and matrices. Oxford: Oxford University Press.

Ogawa K, Yamashita Y, Ichijo T, Fusayama T (1983). The ultrastructure and

hardness of the transparent layer of human carious dentin. *J Dent Res* 62:7–10.[Abstract/Free Full Text]

Oliver WC, Pharr GM (1992). An improved technique for determining hardness and elastic modulus using load and displacement sensing indentation experiments. *J Mater Res* 7:1564–1583.

Palamara JE, Wilson PR, Thomas CD, Messer HH (2000). A new imaging technique for measuring the surface strains applied to dentine. *J Dentist* 28:141–146.

Pashley DA (1989). Dentin: a dynamic substrate—a review. *Scanning Microsc* 3:161–176.[Medline]

Pashley D (2001). Private communication.

Pashley DA, Parham P (1985). The relationship between dentin microhardness and tubule density. *Endod Dent Traumatol* 1:176–179. [Medline]

Peyton FA, Mahler DB, Hershenov B (1952). Physical properties of dentin. *J Dent Res* 31:336–370.

Pidaparti RM, Chandran A, Takano Y, Turner CH (1996). Bone mineral lies mainly outside collagen fibrils: predictions of a composite model for osteonal bone. *J Biomechan* 29:909–916.[Medline]

Rasmussen ST (1984). Fracture properties of human teeth in proximity to the dentinoenamel junction. *J Dent Res* 63:1279–1283.[Abstract/Free Full Text]

Rasmussen ST, Patchin RE (1984). Fracture properties of human enamel and dentin in an aqueous environment. *J Dent Res* 63:1362–1368. [Abstract/Free Full Text]

Rasmussen ST, Patchin RE, Scott DB, Heuer AH (1976). Fracture properties of human enamel and dentin. *J Dent Res* 55:154–164. [Abstract/Free Full Text]

Renson CE, Braden M (1975). Experimental determination of the rigidity modulus, Poisson's ratio and elastic limit in shear of human dentine. *Arch*

Oral Biol 20:43–47.[Medline]

Rho JY, Zioupos P, Currey JD, Pharr GM (1999). Variations in the individual thick lamellar properties within osteons by nanoindentation. *Bone* 25:295–300.[Medline]

Ritchie RO (1999). Mechanisms of fatigue-crack propagation in ductile and brittle solids. *Int J Fracture* 100:55–83.

Roydhouse RH (1970). Punch shear tests for dental purposes. *J Dent Res* 49:131–136.[Abstract/Free Full Text]

Sano H, Ciucchi B, Matthews WG, Pashley DH (1994). Tensile properties of mineralized and demineralized human and bovine dentin. *J Dent Res* 73:1205–1211.[Abstract/Free Full Text]

Sasaki N, Nakayama Y, Yoshikawa M, Enyo A (1993). Stress relaxation function of bone and bone collagen. *J Biomechan* 26:1369–1376.[Medline]

Stanford JW, Wiegel KV, Paffenbarger GC, Sweeney WT (1960). Compressive properties of hard tooth tissues and some restorative materials. *J Am Dent Assoc* 60:746–756.

Staninec M, Marshall GW, Hilton JF, Pashley D, Gansky SA, Marshall SJ, *et al.* (2002). Ultimate strength of dentin: evidence for a damage mechanics approach to dentin failure. *J Biomed Mater Res* 63:342–345.[Medline]

Tengrove HG, Carter GM, Hood JA (1995). Stress relaxation properties of human dentin. *Dent Mater* 11:305–310.[Medline]

Tonami K, Takahashi H (1997). Effects of aging on tensile fatigue strength of bovine dentin. *Dent Mater J* 16:156–169.[Medline]

van Meerbeek B, Willems G, Celis JP, Roos JR, Braem M, Lambrechts P, *et al.* (1993). Assessment by nano-indentation of the hardness and elasticity of the resin-dentin bonding area. *J Dent Res* 72:1434–1442. [Abstract/Free Full Text]

Vlassak JJ, Nix WD (1994). Measuring the elastic properties of anisotropic materials by means of indentation experiments. *J Mechan Phys Solids*

42:1223–1245.

Wang RZ, Weiner S (1998a). Human root dentin: structural anisotropy and Vickers microhardness isotropy. *Connect Tissue Res* 39:269–279.[Medline]

Wang RZ, Weiner S (1998b). Strain-structure relations in human teeth using Moiré fringes. *J Biomechan* 31:135–141.[Medline]

Watanabe LG, Marshall GW, Marshall SJ (1996). Dentin shear strength: effects of tubule orientation and intratooth location. *Dent Mater* 12:109–115. [Medline]

Waters NE (1980). Some mechanical and physical properties of teeth. *Symp Soc Exp Biol* 34:99–135.[Medline]

Zioupos P, Currey JD, Casinos A (2001). Tensile fatigue in bone: are cycles, or time to failure, or both important? *J Theoret Biol* 210:389–399.[Medline]

This article has been cited by other articles:

[Abstract] [Full Text] [PDF]

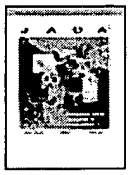

The Journal of the American Dental Association ▸HOME

C. S. Costa Pfeifer, R. R. Braga, and P. E. C. Cardoso

Influence of cavity dimensions, insertion technique and adhesive system on microleakage of Class V restorations

J Am Dent Assoc, February 1, 2006; 137(2): 197 - 202.

[Abstract] [Full Text] [PDF]

Journal of Dental Education ▸HOME

H. K. Fong, B. L. Foster, T. E. Popowics, and M. J. Somerman

The Crowning Achievement: Getting to the Root of the Problem

J Dent Educ., May 1, 2005; 69(5): 555 - 570.

[Abstract] [Full Text] [PDF]

JOURNAL OF DENTAL RESEARCH ▸HOME

R.K. Nalla, J.H. Kinney, S.J. Marshall, and R.O. Ritchie

On the in vitro Fatigue Behavior of Human Dentin: Effect of Mean Stress

J. Dent. Res., March 1, 2004; 83(3): 211 - 215.

[Abstract] [Full Text] [PDF]

This Article

- **Abstract** FREE
- **Figures Only**
- **Full Text (PDF)**

Services

- **Similar articles in this journal**
- **Similar articles in PubMed**

Available online at www.sciencedirect.com
ScienceDirect
Composites Science and Technology 67 (2007) 2795–2806
COMPOSITES SCIENCE AND TECHNOLOGY
www.elsevier.com/locate/compscitech

Mechanical behavior of unidirectional fiber-reinforced polymers under transverse compression: Microscopic mechanisms and modeling

Carlos González, Javier LLorca *

Departamento de Ciencia de Materiales, Universidad Politécnica de Madrid & Instituto Madrileño de Estudios Avanzados en Materiales (IMDEA-Materiales) E.T.S. de Ingenieros de Caminos, 28040 Madrid, Spain

Received 1 December 2006; received in revised form 2 February 2007; accepted 2 February 2007
Available online 15 February 2007

Abstract

The mechanical behavior of polymer–matrix composites unidirectionally reinforced with carbon or glass fibers subjected to compression perpendicular to the fibers was studied using computational micromechanics. The stress–strain curve was determined by the finite element analysis of a representative volume element of the microstructure idealized as a random dispersion of parallel fibers embedded in the polymeric matrix. The dominant damage mechanisms experimentally observed – interface decohesion and matrix plastic deformation – were included in the simulations, and a parametrical study was carried out to assess the influence of matrix and interface properties on the stress–strain curve, compressive strength, ductility and the corresponding failure modes. It was found that the composite properties under transverse compression were mainly controlled by interface strength and the matrix yield strength in uniaxial compression. Two different fracture modes were identified, depending on whether failure was controlled by the nucleation of interface cracks or by the formation of matrix shear bands. Other parameters, such as matrix friction angle, interface fracture energy or thermo-elastic residual stresses, played a secondary role in the composite mechanical behavior.

Keywords: Computational micromechanics; Interface fracture; Transverse compression; Fiber-reinforced polymers

1. Introduction

Unidirectional fiber-reinforced polymers show outstanding specific stiffness and strength along the fiber direction and this has led to a wide range of applications as structural materials. Moreover, the fiber and matrix behavior follows very closely the isostrain approximation until the onset of failure and it was possible to develop analytical models to accurately predict the tensile [1–3] and compressive [4,5] strength in the fiber direction. Conversely, the mechanical behavior under transverse loading cannot be represented by simplified isostrain or isostress approaches, and micromechanical models capable of predicting failure strength as a function of the constituent properties, volume fraction, shape and spatial distribution are not available. This is an important limitation because the experimental characterization of the lamina properties in the transverse direction is subjected to more uncertainties than in the longitudinal one and, in fact, experimental data are more scarce. In addition, the longitudinal compressive strength is severely affected by the transverse behavior [5,6], and the development of robust failure criteria for laminates which include the interaction between longitudinal and transverse stresses have to rely on a precise knowledge of the lamina behavior under transverse loading until failure.

Computational micromechanics is emerging as an accurate tool to study the mechanical behavior of composites due to the sophistication of the modeling tools and to the ever-increasing power of digital computers. Within this framework, the macroscopic properties of a composite lamina can be obtained by means of the numerical simula-

* Corresponding author. Tel.: +34 91 336 5375; fax: +34 91 543 7845.
E-mail address: jllorca@mater.upm.es (J. LLorca).

0266-3538/$ - see front matter © 2007 Elsevier Ltd. All rights reserved.
doi:10.1016/j.compscitech.2007.02.001

tion of the deformation and failure of a representative volume element of the microstructure [7–10]. As compared with the classic homogenization techniques, computational micromechanics presents two important advantages. Firstly, the influence of the geometry and spatial distribution of the phases (i.e. size, shape, clustering, connectivity, etc.) can be accurately taken into account. Secondly, the details of the stress and strain microfields throughout the microstructure are resolved, which leads to precise estimations of the onset and propagation of damage, and to accurate predictions of the failure strength. Recent advances in this area include the analysis of the effect of particle shape [11], particle clustering [12,13] and the influence of damage [14,15] on the mechanical behavior of particle-reinforced composites, the prediction of the mechanical behavior of foams and composites whose microstructure was obtained by means of X-ray computer-assisted tomography [16,17], or the computer simulation of "virtual fracture tests" in fiber-reinforced composites [18,19].

This strategy is applied in this investigation to analyze the mechanical behavior of a unidirectional fiber-reinforced polymer composite subjected to transverse compression. The composite microstructure was idealized by a random and homogeneous dispersion of parallel, circular elastic fibers embedded in the continuous polymeric matrix. The main deformation and failure mechanisms reported in the literature (namely matrix nonlinear behavior and interface failure) as well as the effect of thermal residual stresses were taken into account in the simulations and a parametrical study was carried out to assess the influence of these parameters on the stress–strain curve, failure strength, ductility and the corresponding failure modes.

2. Experimental background and simulation strategy

The experimental evidence shows that lamina of polymer–matrix composites unidirectionally reinforced with carbon or glass fibers fail under transverse compression along planes parallel to the fibers [20–22]. The angle α formed between the failure plane and the through-thickness (or perpendicular to the in-plane loading) direction is slightly above 45° and typical values reported are in the range 50–56° [23,21,24]. Significant non-linear deformation was often observed before the maximum load [25,26], and this behavior was associated to the plastic deformation of the polymeric matrix. This is supported by our observations on the lateral surfaces of a Hexcel 8552 epoxy matrix uniaxially reinforced with 57 vol.%

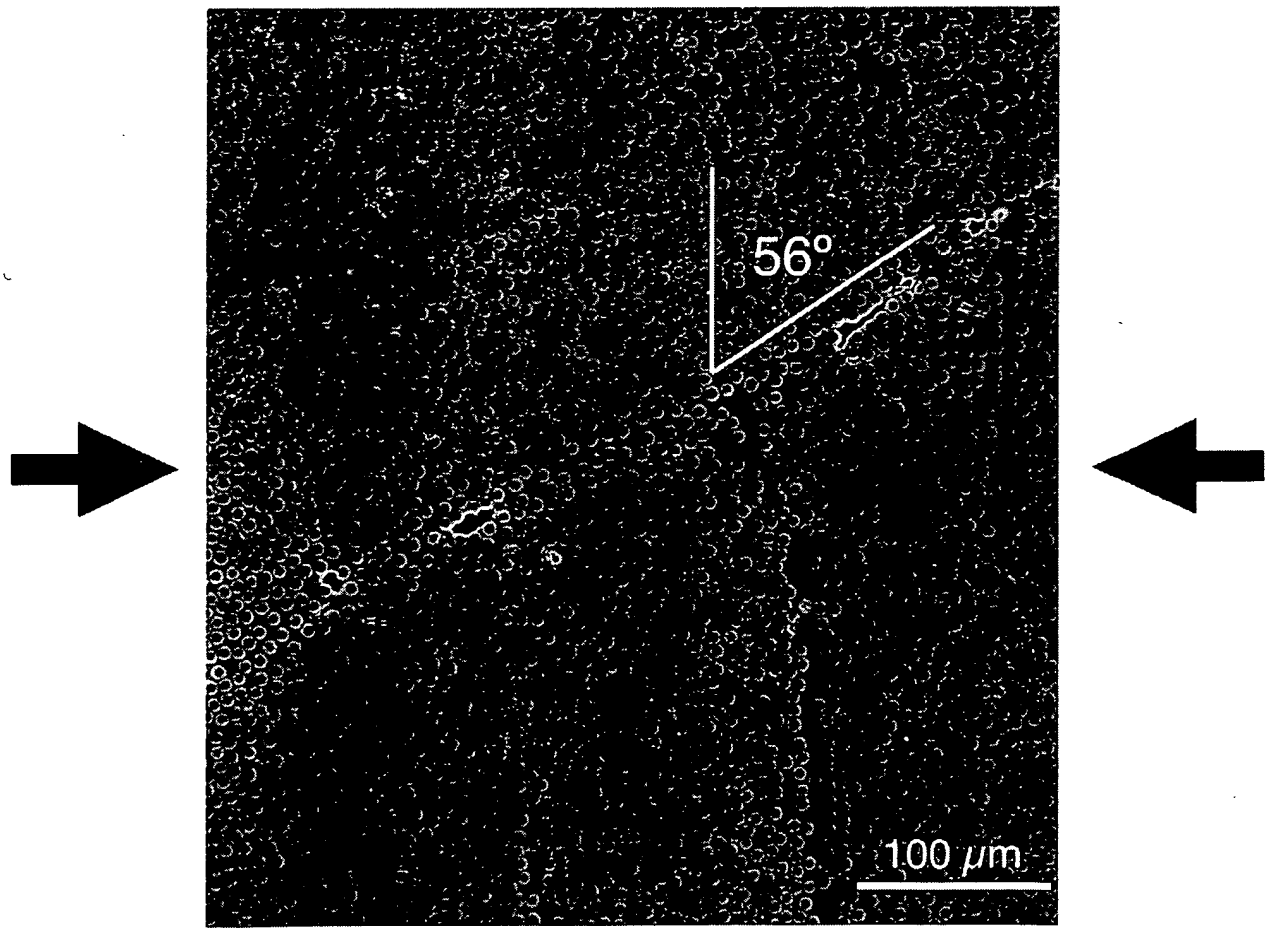

Fig. 1. Scanning electron micrograph of the lateral surface of an AS4/epoxy specimen loaded under transverse compression showing bands of intense plastic deformation in the matrix before the maximum load [24].

AS4 carbon fibers loaded under transverse compression. Bands of intense plastic deformation in the matrix, inclined at an angle of 56° with respect to the plane perpendicular to the loading axis, appeared before the maximum load was attained (Fig. 1). Damage by interface decohesion developed afterwards around these bands (Fig. 2a) and final fracture occurred by the failure of the matrix in shear, as evidenced by the numerous hackles in the matrix fracture surfaces (Fig. 2b).

These results show that the strength of fiber-reinforced polymers under transverse compression is controlled by two dominant mechanisms, namely the localization of the matrix plastic strain along shear bands and the development of damage by interface decohesion. Both processes (and their interaction) can be taken into account within the framework of computational micromechanics in which composite behavior is analyzed by means of the finite element simulation of a two-dimensional representative volume element (RVE) of the microstructure. The matrix was represented by an isotropic, elasto-plastic solid following the Mohr–Coulomb yield criterion, which assumes that yielding is induced by the shear stresses and that yield stress depends on the normal stress. This model has often been used to describe plastic deformation and failure of polymers [27] and of polymeric matrices in composites [28,23,21] as it explains the asymmetry between tensile and compressive yielding and failure in compression along planes forming an angle of ≈50–56° with respect to the plane perpendicular to the loading axis. Fiber/matrix decohesion was introduced by means of interface elements whose behavior is controlled by a cohesive crack model, a standard technique in the computational micromechanics of composites [29–32].

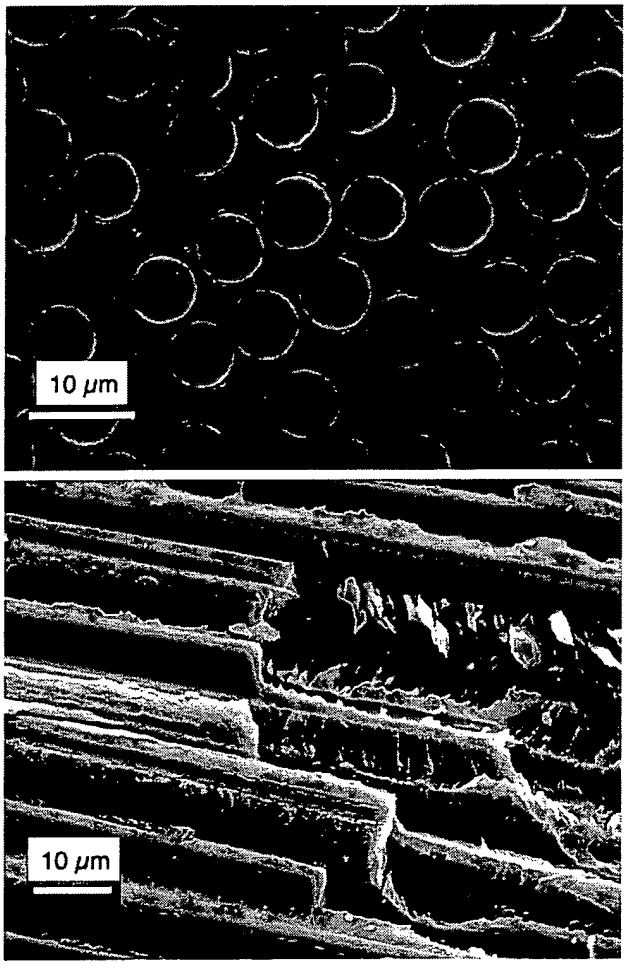

Fig. 2. Scanning electron micrographs of an AS4/epoxy composite loaded under transverse compression [24]. (a) Damage by interface decohesion around the matrix shear bands. The loading axis is horizontal. (b) Fracture surface. The presence of numerous hackles in the matrix is indicative of failure by shear.

3. Computational model

3.1. RVE generation and discretization

A square RVE, which contains a random and homogeneous dispersion of circular fibers embedded in the polymeric matrix, was selected to determine the behavior of the composite under transverse loading, following to Brockenbrough et al. [33]. An important issue in the simulations is the minimum size of the RVE, which should contain all the necessary information about the statistical description of the microstructure and its size should be large enough so that the average properties of this volume element are independent of its size and position within the material. Of course, the critical RVE size depends on the phase and interface properties and spatial distribution, and no estimates were available for our particular problem. It is also known that the accuracy provided by RVEs of a given size can be improved if the results of various realizations are averaged [34]. Thus, the compressive strength and ductility for each set of matrix and interface properties was given by the average value of the results obtained from six different fiber distributions in a RVE which included 30 fibers. They were compared in selected cases with those obtained with RVEs containing over 70 fibers to ensure that the size of the RVE did not influence significantly the model predictions.

Random and homogeneous dispersions of monosized fibers of radius $R = 5$ μm were generated in square RVEs of dimensions $L_0 \times L_0$ using the modified random sequential adsorption algorithm of Segurado and LLorca [9]. It was assumed that the microstructure of the composite was given by a indefinite translation of the RVE along the two coordinate axes and thus the fiber positions within the RVE should keep this periodicity condition. Fiber centers were generated randomly and sequentially, and each new fiber was accepted if the distance between neighboring fiber surfaces was $>0.07R$ to ensure an adequate discretization of this region. In addition, the distance between the fiber surface and the RVE edges should be $>0.1R$ to avoid distorted finite elements during meshing. Fibers intersecting the RVE edges were split into an appropriate number of parts and copied to the opposite sides of the square

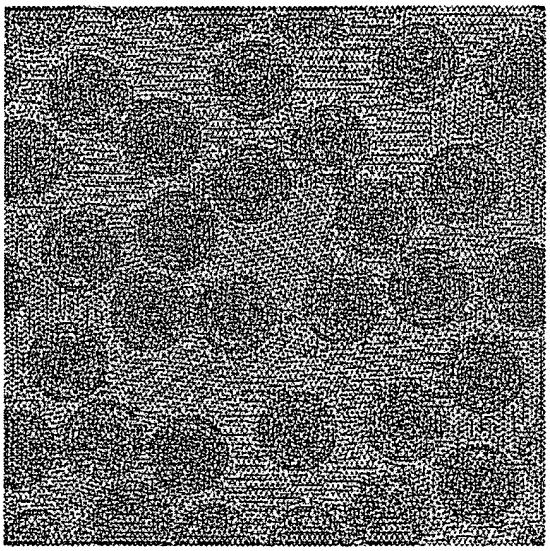

Fig. 3. Fiber distribution and finite element discretization of a representative volume element of the composite with 30 fibers.

RVE to create a periodic microstructure. New fibers were added until the desired volume fraction of 50% was reached. An example of the fiber distribution an RVE with 30 fibers is shown in Fig. 3. The RVE was automatically meshed using 6-node isoparametric modified triangles (CPE6M in Abaqus Standard [35]) with integration at three Gauss points and hourglass control. Special care was taken to obtain a very fine and homogeneous discretization throughout the RVE to resolve the plastic shear bands in the matrix during deformation (Fig. 3).

3.2. Finite element and material models

Periodic boundary conditions were applied to the edges of the RVE because the continuity between neighboring RVEs (which deform like jigsaw puzzles) is maintained and, in addition, because the effective behavior derived under these conditions is always bounded by those obtained under imposed forces or displacements [36,37]. Let X_1 and X_2 stand as the Cartesian coordinate axes parallel to the RVE edges and with origin at one corner of the RVE. The periodic boundary conditions can be expressed in terms of the displacement vectors $\vec{U}_1$ and $\vec{U}_2$ which relate the displacements between opposite edges according to

$$\vec{u}(0,X_2) - \vec{u}(L_0,X_2) = \vec{U}_1, \tag{1}$$

$$\vec{u}(X_1,0) - \vec{u}(X_1,L_0) = \vec{U}_2. \tag{2}$$

Uniaxial compression along the X_2 axis is imposed with $\vec{U}_2 = (0,-\delta)$ and $\vec{U}_1 = (u_1,0)$. δ stands for the imposed displacement in the loading direction and u_1 is computed from the condition that the average stresses on the edges perpendicular to the loading axis should be 0. Mathematically,

$$\int_0^L \vec{t}\,dX_2 = 0 \quad \text{on } X_1 = 0, \tag{3}$$

Table 1
Thermo-elastic constants of the fibers and the matrix [38]

E_f (GPa)	ν_f	α_f (10^{-6} K^{-1})	E_m (GPa)	ν_m	α_m (10^{-6} K^{-1})
40	0.25	10	4	0.35	50

where the integral stands for the resultant forces acting on the edge $X_1 = 0$ due to the traction vector $\vec{t}$. The logarithmic strain along the loading axis was given as $\epsilon = \ln(1 + \delta/L_0)$ and the corresponding true stress on the edge was computed as the resultant force divided by the actual cross-section.

Simulations were carried out with Abaqus/Standard [35] under plane strain conditions and within the framework of the finite deformations theory with the initial unstressed state as reference. Fibers were modeled as linear, thermo-elastic and isotropic solids. The thermo-elastic constants given in Table 1 are intermediate between those of glass and C fibers in the plane perpendicular to the fiber axis. The polymeric matrix was assumed to behave as an isotropic, thermo-elasto-plastic solid, and the thermo-elastic constants (typical of an epoxy matrix) are also given in Table 1. Plastic deformation was governed by the Mohr–Coulumb criterion and the total matrix strain was given by the addition of the thermo-elastic and plastic strain components. The Mohr–Coulomb criterion assumes that yielding takes place when the shear stress acting on a specific plane, τ, reaches a critical value, which depends on the normal stress σ acting on that plane. This can be expressed as

$$\tau = c - \sigma \tan\phi, \tag{4}$$

where c and ϕ stand, respectively, for the cohesion and the friction angle, two materials parameters which control the plastic behavior of the material. Physically, the cohesion c represents the yield stress under pure shear while the friction angle takes into account the effect of the hydrostatic stresses. $\phi = 0$ reduces the Mohr–Coulomb model to the pressure-independent Tresca model while $\phi = 90°$ leads to "tension cut-off" Rankine model. The value of both parameters for an epoxy can be assessed from its tensile and compressive strengths, σ_{mt} and σ_{mc}, according to

$$\sigma_{mt} = 2c\frac{\cos\phi}{1+\sin\phi} \quad \text{and} \quad \sigma_{mc} = 2c\frac{\cos\phi}{1-\sin\phi}. \tag{5}$$

The fracture surface of a solid which follows the Mohr–Coulomb criterion and it is subjected to uniaxial compression forms an angle α with plane perpendicular to the loading axis, which is related to the friction angle ϕ by

$$\alpha = 45° + \phi/2. \tag{6}$$

Typically $50° < \alpha < 60°$ in epoxy matrices [23,21,24], and thus ϕ is in the range 10–30°. Once ϕ was fixed for a given simulation, the corresponding cohesion c was computed from Eq. (5) assuming that the matrix tensile strength was 60 MPa [38]. If not indicated otherwise, the simulations presented in this paper used $\phi = 15°$ to represent the matrix behavior, which corresponds to a cohesion c of 39.1 MPa.

The corresponding values on the matrix tensile and compressive strength are, respectively, 60 MPa and 101.9 MPa.

The yield surface of the Mohr–Coulomb model, written in terms of the maximum and minimum principal stresses (σ_I and σ_{III}), is given by

$$F(\sigma_I, \sigma_{III}) = (\sigma_I - \sigma_{III}) + (\sigma_I + \sigma_{III})\sin\phi - 2c\cos\phi = 0 \tag{7}$$

and it was assumed that c and ϕ were constant and independent of the accumulated plastic strain. A non-associative flow rule was used to compute the directions of plastic flow in the stress space and the corresponding potential flow G was expressed as

$$G = \frac{4(1-e^2)\cos^2\Theta + (2e-1)^2}{2(1-e^2)\cos\Theta + (2e-1)\sqrt{4(1-e^2)\cos^2\Theta + 5e^2 - 4e}} \times \frac{3-\sin\phi}{6\cos\phi} \tag{8}$$

in which $e = (3 - \sin\phi)/(3 + \sin\phi)$ and Θ is obtained from

$$\Theta = \frac{1}{3}\arccos\left\{\frac{J_3}{J_2}\right\}^3, \tag{9}$$

where J_2 and J_3 are, respectively, the second and the third invariants of the deviatoric stress tensor. More details about the numerical implementation of the Mohr–Coulomb model can be found in [39,40].

The progressive interface decohesion upon loading was simulated by 4-node isoparametric linear interface elements (COH2D4 in [35]) inserted at the fiber/matrix interface. The mechanical behavior of these elements was expressed in terms of a traction-separation law which relates the displacement jump across the interface with the traction vector acting upon it. The initial response was linear in absence of damage and, therefore, the traction-separation law can be written as

$$t_n = K\delta_n \quad \text{and} \quad t_s = K\delta_s \tag{10}$$

where t_n, t_s, δ_n and δ_s stand for the normal and tangential tractions and displacement jumps across the interface respectively. An elastic stiffness of $K = 10^8$ GPa/m was selected for the interface, which was large enough to ensure the displacement continuity at the interface and to avoid any modification of the stress fields around the fibers in the absence of damage. The linear behavior ends at the onset of damage, which is dictated by a maximum stress criterion expressed mathematically as

$$\max\left\{\frac{\langle t_n\rangle}{N}, \frac{t_s}{S}\right\} = 1 \tag{11}$$

in which $\langle\rangle$ stand for the Macaulay brackets, which return the argument if positive and zero otherwise, to impede the development of damage when the interface is under compression, and N and S are the normal and tangential interfacial strengths which were assumed to be the equal for simplicity ($N = S$). Once the damage begins, the stress transferred through the crack is reduced depending on the interface damage parameter d, which evolves from 0 (in the absence of damage) to 1 (no stresses transmitted across the interface), as shown in Fig. 4. The corresponding traction-separation law is expressed by

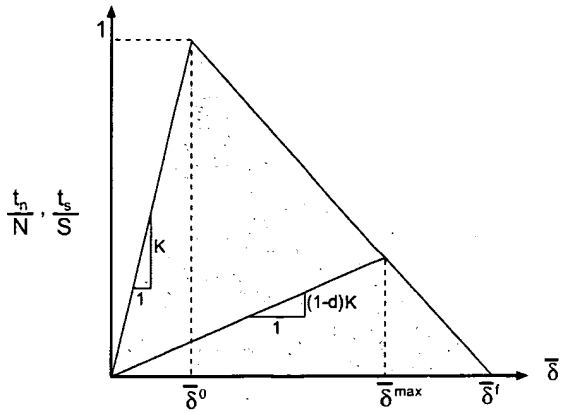

Fig. 4. Schematic of the traction-separation law which governs the behavior of the interface elements.

$$\begin{aligned} t_n &= (1-d)K\delta_n \quad \text{if } \delta_n > 0, \\ t_n &= K\delta_n \quad \text{if } \delta_n \leqslant 0, \\ t_s &= (1-d)K\delta_s \end{aligned} \tag{12}$$

The evolution of the damage parameter is controlled by an effective displacement, $\bar{\delta}$, defined as the norm of the displacement jump vector across the interface as

$$\bar{\delta} = \sqrt{\langle\delta_n\rangle^2 + \delta_s^2}, \tag{13}$$

and d depends on the maximum effective displacement at the interface attained during the loading history at each material integration point $\bar{\delta}^{max}$ according to

$$d = \frac{\bar{\delta}^f(\bar{\delta}^{max} - \bar{\delta}^0)}{\bar{\delta}^{max}(\bar{\delta}^f - \bar{\delta}^0)}, \tag{14}$$

where $\bar{\delta}^0$ and $\bar{\delta}^f$ stand for the effective displacement at the onset of damage ($d = 0$) and when the interface has failed completely ($d = 1$), respectively. In this cohesive model, the energy necessary to completely break the interface is always equal to Γ, the interface fracture energy, regardless of the loading path. If not indicated otherwise, the interface fracture energy in the simulations presented below was 100 J/m^2, a reasonable value for C and glass fibers embedded in a polymeric matrix [41].

4. Results

4.1. Validation of the RVE size

Most of the results presented in this paper were obtained by the numerical simulation of RVEs containing 30 fibers. The influence of the actual position of the fibers

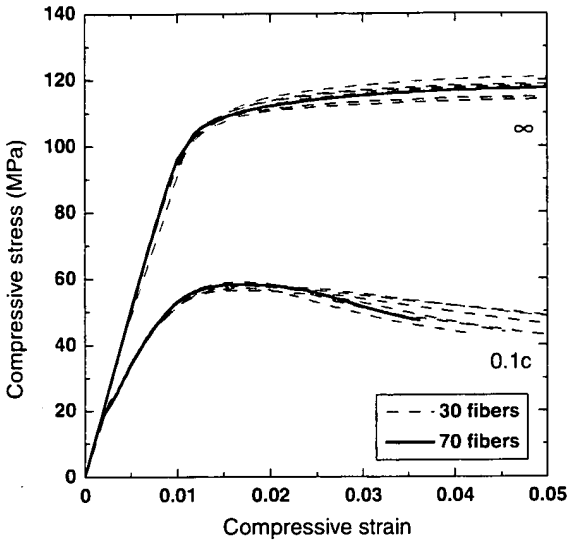

Fig. 5. Compressive stress–strain curves for six different fiber realizations in RVEs with 30 fibers (broken line) and one fiber realization in an RVE with 70 fibers (solid line). The two sets of curves are representative of materials with very strong (=∞) or very weak (=0.1c) fiber/matrix interfaces.

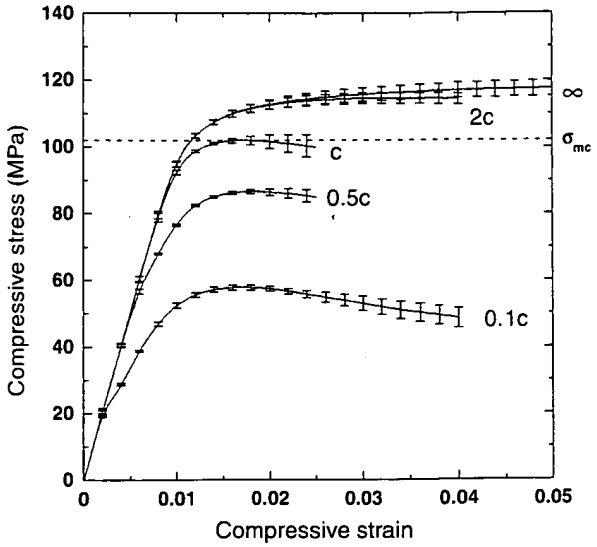

Fig. 6. Influence of the interface strength N on the mechanical response under transverse compression. The error bars stands for the standard deviation of six simulations. The figure next to each curve stands for the interface strength. The broken horizontal line represents the compressive strength of the epoxy matrix.

within the RVE on the mechanical response was analyzed by comparing the results obtained with six different fiber realizations for the typical values of the matrix and fiber properties given previously and two sets of interface properties corresponding to very weak ($N = 0.1c$) and perfect interfaces, respectively. The corresponding (compression) stress–strain curves are plotted in Fig. 5, together with those computed with an RVE which included 70 fibers. All the simulations were practically superposed in the elastic regime; divergences arose at the onset of matrix plastic deformation and increased in the composite with weak interfaces beyond the maximum load. These results are in agreement with previous numerical studies, which showed that the minimum size of the RVE increases with the mismatch between the phase properties (e.g. at the elasto-plastic transition) and especially with the localization of the deformation due to plastic flow and/or damage [42,10]. Nevertheless, the dispersion among the stress–strain curves was limited and the curve obtained by averaging the six simulations was very close to that computed with an RVE with 70 fibers for both sets of material properties.

4.2. Influence of the interface strength

The stress–strain curve under transverse compression is plotted in Fig. 6 for composite materials whose interface strength varied from $N = 0.1c$ to infinity. The matrix friction angle was 15° ($c = 39.1$ MPa) and the interfacial fracture energy was 100 J/m^2 in all cases. Each curve is the average of six different realizations with an RVE with 30 fibers and the error bars stand for the standard deviation of the simulations, which was negligible up to the maximum load and remained small afterwards. The initial composite stiffness was not affected by the interface strength but the composites with low interfacial strength ($N < c$) departed early from the linear behavior due to the nucleation of interface cracks. In isolated fibers, the cracks nucleated at the points equidistant from the poles and the equator (latitudes 45 °N and 45 °S), where the interfacial shear stress was maximum. They propagated towards the equator and merged. The stress concentrations at the tip of the interface cracks induced the formation of very short shear bands in the matrix linking up interface cracks in neighboring fibers, and the maximum strength was attained at this point (Fig. 7a). Further deformation led to formation of interfacial voids and to the localization of the strain in the matrix in shear bands whose path was dictated by the position of the voids which grew from the interface cracks (Fig. 7b).

On the contrary, composites without interface decohesion presented a linear behavior up to compressive stresses very close to the strength of the epoxy matrix in uniaxial compression, σ_{mc}. This linear regime was followed by a plastic response with very little hardening as the localization of the plastic strain in the matrix led to the formation of shear bands which percolated the entire RVE (Fig. 8). It is worth noting that the angle between the shear bands and the plane perpendicular to the loading axis was very close to $45° + \phi/2 = 52.5°$, the theoretical one for the matrix alone, regardless of the actual fiber distribution, and this indicates that the composite strength was determined by the propensity of the matrix to form shear bands.

The behavior of the composite with an intermediate interfacial strength ($N = c$) was initially similar to that of the materials with high interfacial strength, and the pattern

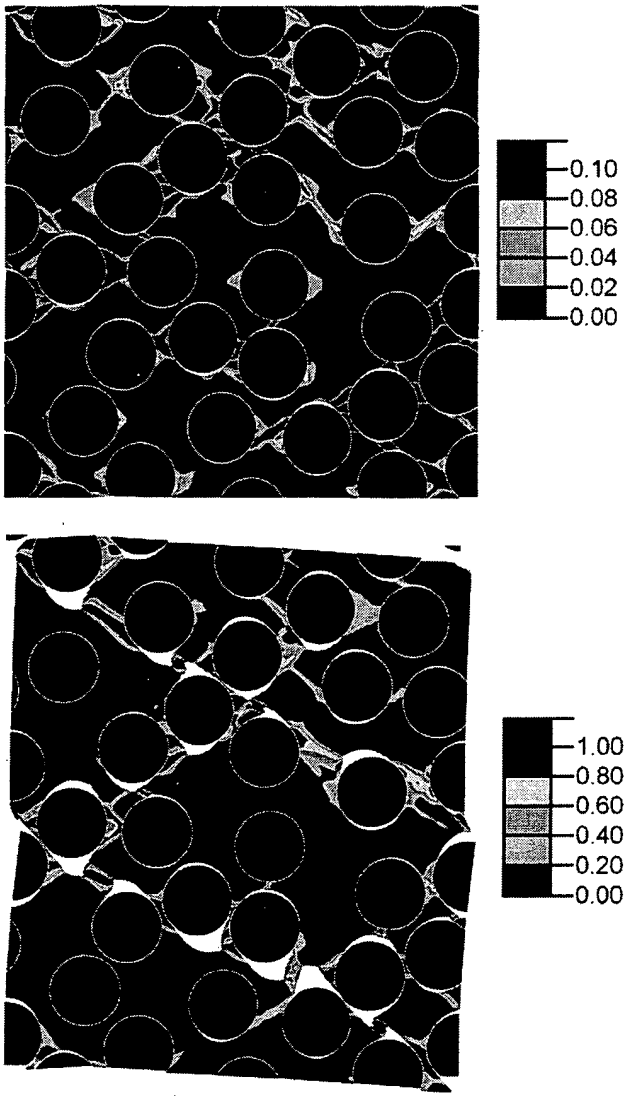

Fig. 7. Contour plot of the accumulated plastic strain in the matrix in the composite with low interfacial strength ($N = 0.1c$). (a) $\epsilon = -1.7\%$ corresponding to the maximum strength. (b) $\epsilon = -4\%$. The loading axis is horizontal. Notice that the strain values in legend (b) are 10 times higher than in (a).

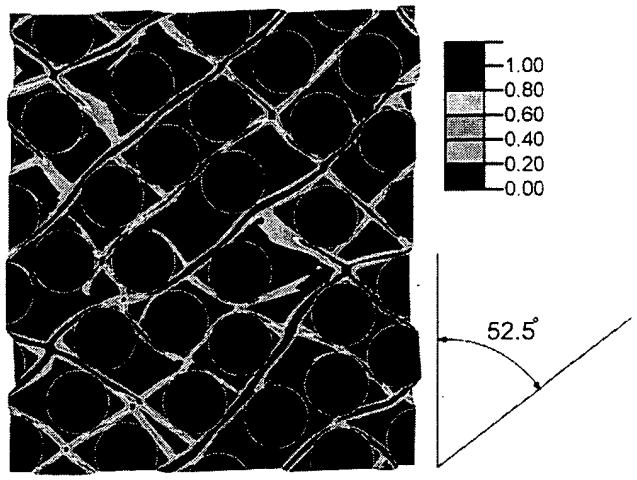

Fig. 8. Contour plot of the accumulated plastic strain in the matrix in the composite without interface decohesion ($N = \infty$) at $\epsilon = -7\%$. The loading axis is horizontal.

of plastic deformation in the matrix at the point of maximum stress showed the incipient development of shear bands oriented at 52.5° (Fig. 9a). However, final fracture occurred by the development of a single shear band, slightly misoriented with respect to the theoretical angle, whose orientation was dictated by the linking up of interface cracks in adjacent fibers (Fig. 9b). This fracture pattern is very similar to that observed in Fig. 2a, in which the matrix shear band is surrounded by interface cracks and points to a failure process in three steps: incipient development of shear bands in the matrix channels between the fibers, nucleation of interface cracks, and final localization of the deformation in the matrix in one dominant shear band.

The transverse compressive strength, Y_C, is given by the maximum of each curve in Fig. 6, and the overall effect of interface strength in the transverse compressive strength, Y_C, is plotted in Fig. 10. Failure is controlled by the matrix plastic deformation if $N/c \geqslant 2$ and the reinforcing effect of the stiff fibers increased the composite strength approximately 10% over the matrix flow stress in compression. The composite strength decreases rapidly with the interfacial strength as the stress concentrations associated with interface cracks favor the onset of plastic deformation in the matrix and the nucleation of shear bands at lower stresses. It is interesting to note that predictions of the micromechanics simulations are in good agreement with experimental results for epoxy–matrix composites reinforced with either glass or carbon fibers (Fig. 10). Experimental values of the matrix and composite properties under transverse compression were obtained from [38]; information of the interface strength for both composite systems was not available in this reference and the experimental data in [43] for C/epoxy and in [44] for glass/epoxy were used. Thus, although the actual interface strength is not known, it is evident that the model predictions for the transverse compressive strength and the failure micromechanisms (Figs. 1 and 2) support the validity of the current approach to simulate the mechanical behavior of unidirectional PMC.

The data in Fig. 10 also include the influence of the interface properties in the strain at Y_C, which stands for a rough approximation of the composite ductility under transverse compression. The ductility values presented more scatter (particularly for large interface strengths, in which the stress–strain curve is very flat near Y_C) but they clearly show the differences between interface- and matrix-dominated fracture. The former occurred when $N < c$ and it was characterized by a brittle behavior, while the latter was dominant if $N \geqslant 2c$ and led to much higher strain to failure (4–6%) controlled by the plastic deformation of the matrix.

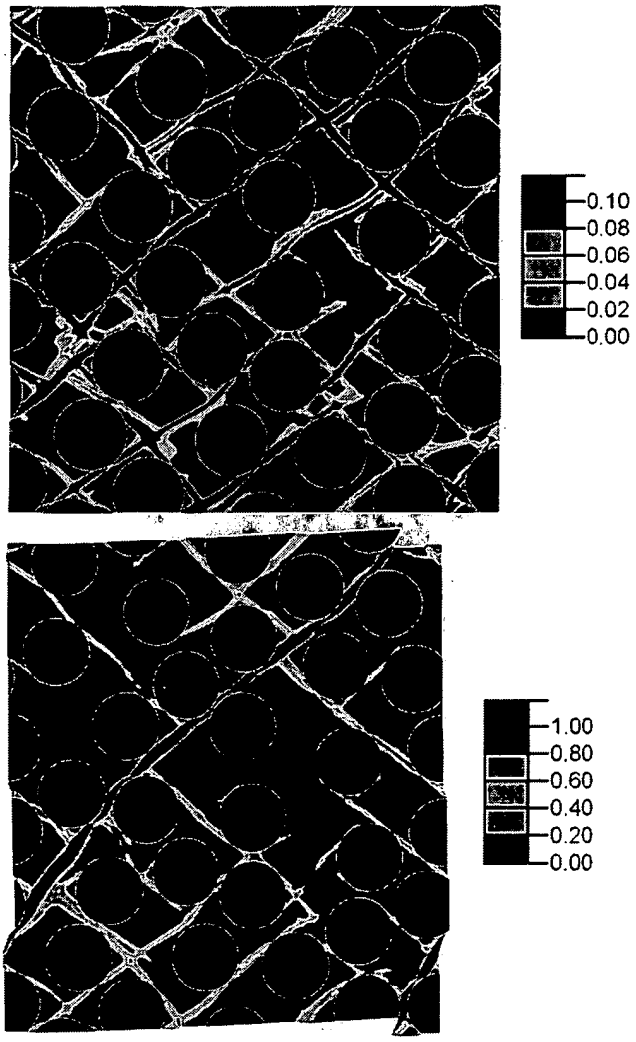

Fig. 9. Contour plot of the accumulated plastic strain in the matrix in the composite with intermediate interfacial strength ($N = c$). (a) $\epsilon = -1.7\%$ corresponding to the maximum strength. (b) $\epsilon = -2.5\%$. The loading axis is horizontal. Notice that the strain values in legend (b) are 10 times higher than in (a).

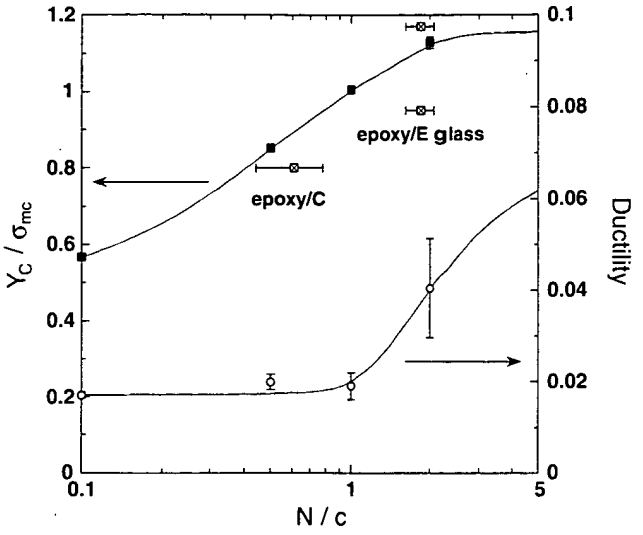

Fig. 10. Influence of the interface strength (normalized by the cohesion of the matrix c) in the transverse compressive strength, Y_C (normalized by the yield strength of the matrix in compression, σ_{mc}) and in the ductility, represented by the strain at Y_C. The error bars stand for the standard deviation of the six simulations with different RVEs.

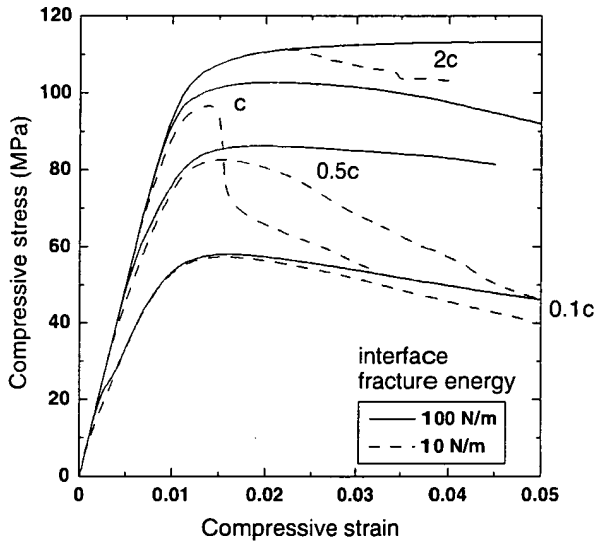

Fig. 11. Influence of the interface fracture energy on the stress–strain curve under transverse compression for different values of the interface strength.

4.3. Influence of the interface fracture energy

The influence of the interface fracture energy on the mechanical behavior in transverse compression is plotted in Fig. 11. Simulations were performed with the same RVE (whose behavior was very similar to the average of six simulations with different RVEs) and three interface fracture energies: 100 J/m^2 (the baseline value), 10 J/m^2 and 1000 J/m^2, while the interface strength was systematically varied from $0.1c$ up to $2c$. For a given value of the interface strength, the variations in the fracture energy modified the effective interface displacement at failure, δ^f (Fig. 4), leading to more brittle or more ductile behaviors. The rest of the fiber and matrix properties were those indicated in Section 3. The stress–strain curves of the materials with interface fracture energies of 10 and 100 J/m^2 are plotted in Fig. 11. The curves corresponding to the materials with interface fracture energies of 1000 J/m^2 were practically superposed to those with 100 J/m^2 up to the maximum stress in all cases, even though the fracture energies differed in one order of magnitude, and the differences beyond that point were minimum. They are not plotted in Fig. 10 for sake of clarity. Brittle fiber/matrix interfaces (which are represented by the curves obtained with $\Gamma = 10$ J/m^2 in Fig. 11) did not change significantly the compressive strength, although the reduction in load after the maximum was faster as a result of the easy propagation

of the cracks along particle/matrix interface. Thus, it can be concluded that the effect of the interface fracture energy on the transverse compressive strength of fiber-reinforced polymers is negligible, as compared with the influence of the interface strength.

4.4. Influence of the matrix friction angle

The stress–strain curves under transverse compression of one RVE are plotted in Fig. 12a–c for three composites with matrix friction angles of 0°, 15° and 30°, respectively. As the matrix tensile strength was assumed to be constant and equal to 60 MPa, changes in the friction angle modified the yield strength of the matrix in compression – as given in Eq. (5) – which increased from 60 MPa ($\phi = 0°$) up to 180 MPa ($\phi = 30°$). So the stresses in Fig. 12 were normalized by the corresponding yield strength of the matrix in compression to compare the composite behavior on the same basis. The curves in Fig. 12a ($\phi = 0°$) are representative of a metallic matrix, which follows the Tresca yield criterion, while those in Fig. 11b and c stand for the behavior of polymeric matrices which tend to form shear bands oriented at an angle of $45° + \phi/2$ with the plane perpendicular to the compression axis. In the absence of interface decohesion, the matrix with $\phi = 0°$ provided the highest compressive strength (relative to the σ_{mc}), and Y_C/σ_{mc} decreased progressively with the friction angle. This behavior is the result of the trend to localize the deformation in shear bands between the fibers, which increases with the friction angle. This effect was more marked in presence of interface decohesion, because matrix shear bands were triggered at lower strains by the stress concentrations around the interface cracks (Fig. 9a). Obviously, this mechanism is more efficient if the matrix friction angle

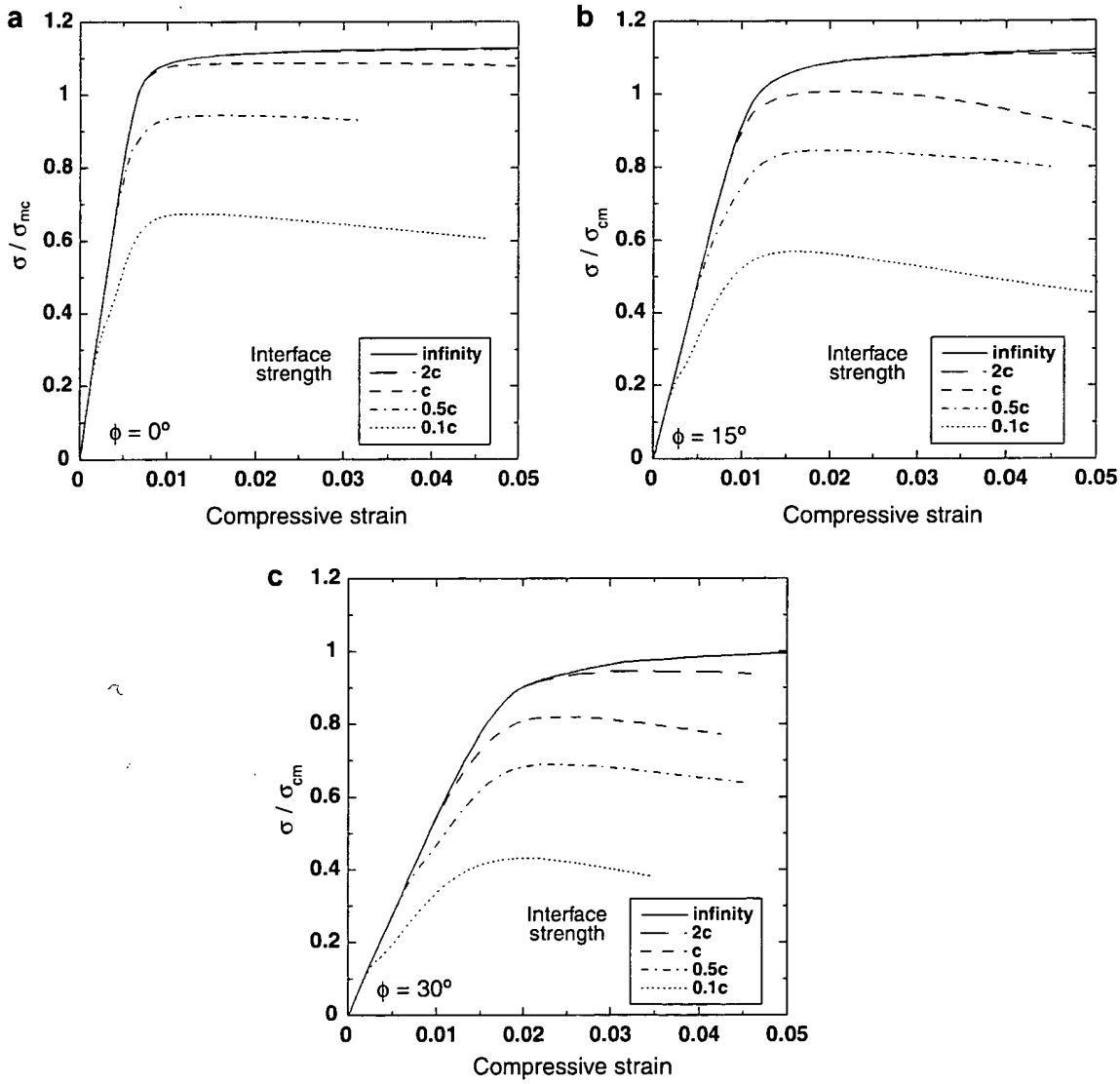

Fig. 12. Influence of the matrix friction angle on the stress–strain curve under transverse compression: (a) $\phi = 0°$; (b) $\phi = 15°$; (c) $\phi = 30°$. The stresses are normalized by the respective strength of the matrix in compression.

is high, and thus the degradation of the composite properties was faster as the interfacial strength decreased.

4.5. Influence of the thermal residual stresses

Residual stresses develop in PMC upon cooling at ambient temperature after curing as a result of the thermal expansion mismatch between the matrix and fibers. As the thermal expansion coefficient of the epoxy matrix is much higher than that of the fibers, tensile stress appears in the matrix and compressive in the fibers, and their influence on the behavior under transverse compression can be taken into account in the micromechanical model by simulating the composite behavior in two steps. In the first step, the RVE was subjected to a homogeneous temperature change of -100 °C from the stress-free temperature down to ambient temperature [38]. The computational model and the fiber and matrix properties were those given in Section 3 but the analyses were carried out under generalized plane strain conditions, instead of plane strain. The thickness of the model (perpendicular to the X_1–X_2) is constant in plane strain simulations, and this leads to unrealistic values of the thermal residual stresses along the X_3 axis. Conversely, the generalized plane strain theory assumes that the model lies between two parallel planes which can move with respect to each other and can accommodate the thermal strain induced by the temperature change. Once the residual stresses were generated, the thickness along the X_3 axis was held constant and the RVE was deformed under uniaxial compression. The stress–strain curves with and without residual stresses of one RVE are plotted in Fig. 13 for different values of the interface strength. The matrix and fiber properties correspond to those of the materials in Fig. 6. The non-linear deformation started at lower strains in the presence of residual stresses, but the compressive strength was not affected because the thermo-elastic residual stresses were rapidly smoothed out during deformation by the intense plastic deformation in the matrix and the interface cracks.

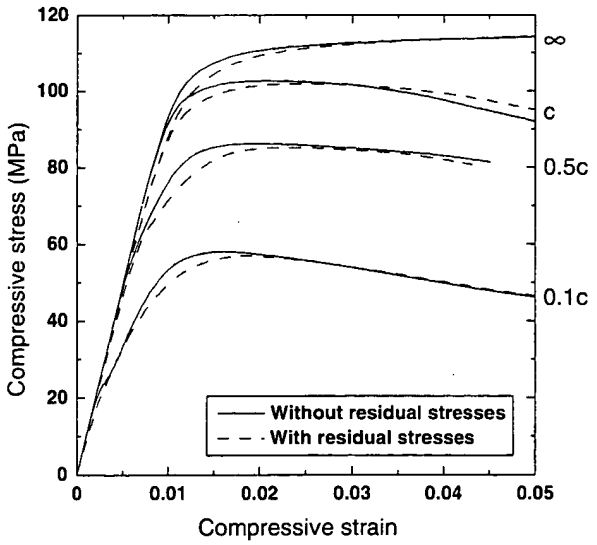

Fig. 13. Influence of the thermal residual stresses on the mechanical response under transverse compression for different values of the interface strength.

5. Conclusions

The compressive strength under transverse loading of fiber-reinforced polymers was studied by means of computational micromechanics. In this modeling strategy, the stress–strain curve was computed by means of the finite element analysis of an RVE of the composite microstructure. The simulations showed the role played by the two dominant damage mechanisms (decohesion at the interface and shear band formation in the matrix) in controlling the composite strength. On the one hand, if decohesion is inhibited, failure took place by the development of shear bands in the matrix, which propagated through the microstructure at an angle of $\pm(45° + \phi/2)$ with respect to the plane perpendicular to the compression axis. The compressive strength was slightly higher than the matrix strength under uniaxial compression due to the additional strengthening provided by the stiff fibers. On the other hand, interface cracks were nucleated at very low stresses in composites with weak interfaces, while the matrix was still in the elastic regime. The stress concentrations at the interface crack tips nucleated plastic shear bands between neighboring cracks, and led to the evolution of the cracks into large interfacial voids. Final fracture occurred by the development of bands of localized deformation formed by interfacial voids linked by matrix shear bands, the orientation of these bands being controlled by the particular distribution of the fibers in the RVE. When the interface strength was similar to the matrix flow stress in compression ($N \approx c$), the numerical simulation showed that the maximum strength was mainly controlled by the matrix, and coincided with the formation of an incipient pattern of shear bands in the matrix, inclined at $\pm(45° + \phi/2)$ with respect to the plane perpendicular to the compression axis. Final fracture took place thereafter by the propagation of a dominant shear band, slightly misoriented with respect to the theoretical angle, whose path was dictated by the linking up of interface cracks in adjacent fibers.

Parametrical studies showed that other factors (such as the matrix friction angle, the interface fracture energy and the thermo-elastic residual stresses) exerted a secondary influence on the compressive strength of PMC under transverse compression. The matrix was more susceptible to the formation of shear bands as the friction angle increased, and they developed earlier, but this effect was offset by the higher matrix flow stress in compression. Thermal residual stress reduced the stress for the onset of nonlinear deformation but they were rapidly smoothed out by the intense plastic deformation in the matrix and did not modify the compressive strength. Finally, changes in the interface fracture energy by two orders of magnitude

did not modify significantly the compressive strength either.

It is finally worth noting the potential of computational micromechanics to assess the mechanical behavior of engineering composites. By using the appropriate constitutive equations for the fiber, matrix and interfaces, this simulation tool can provide a detailed picture of deformation and fracture mechanisms at microscopic level, including the effect of all non-linear processes and of the interaction among them. This information can be used to develop more accurate and reliable failure criteria at the lamina level, which in turn can be used to predict the mechanical performance of laminates and composite structures.

Acknowledgments

This investigation was supported by the Spanish Ministry of Education and Science through the Grant MAT 2006-2602 and by the Comunidad de Madrid through the program ESTRUMAT-CM (reference MAT/0077).

References

[1] Aveston J, Cooper GA, Kelly A. Single and multiple fracture. In: The properties of fibre composites. IPC Science and Technology Press; 1971. p. 15–26.
[2] Curtin WA, Takeda N. Tensile strength of fiber-reinforced composites: II. Application to polymer matrix composites. J Compos Mater 1998;32:2060–81.
[3] González C, LLorca J. Micromechanical modelling of deformation and failure in Ti–6Al–4V/SiC composites. Acta Mater 2001;49:3505–19.
[4] Argon AS. Fracture of composites. In: Herman H, editor. Treatise on materials science and technology, vol. 1. Academic Press; 1972. p. 79–114.
[5] Budiansky B, Fleck NA. Compressive failure of fiber composites. J Mech Phys Solids 1993;41:183–211.
[6] Vogler TJ, Hsu S-Y, Kyriakides S. Composite failure under combined compression and shear. Int J Solids Struct 2000;37:1765–91.
[7] Michel JC, Moulinec H, Suquet P. Effective properties of composite materials with periodic microstructure: a computational approach. Comput Meth Appl Mech Eng 1999;172:109–43.
[8] Lusti HR, Hine PJ, Gusev AA. Direct numerical predictions for the elastic and thermoelastic properties of short fibre composites. Compos Sci Technol 2002;62:1927–34.
[9] Segurado J, LLorca J. A numerical approximation to the elastic properties of sphere-reinforced composites. J Mech Phys Solids 2002;50:2107–21.
[10] González C, Segurado J, LLorca J. Numerical simulation of elasto-plastic deformation of composites: evolution of stress microfields and implications for homogenization models. J Mech Phys Solids 2004;52:1573–93.
[11] Chawla N, Sidhu RS, Ganesh VV. Three-dimensional visualization and microstructure-based modeling of deformation in particle-reinforced composites. Acta Mater 2006;54:1541–8.
[12] Segurado J, González C, LLorca J. A numerical investigation of the effect of particle clustering on the mechanical properties of composites. Acta Mater 2003;51:2355–69.
[13] Segurado J, LLorca J. Computational micromechanics of composites: the effect of particle spatial distribution. Mech Mater 2006;38:873–83.
[14] Böhm HJ, Han W, Eckschlager A. Multi-inclusion unit cell studies of reinforcement stresses and particle failure in discontinuously reinforced ductile matrix composites. Comput Model Eng Sci 2004;5:5–20.
[15] LLorca J, Segurado J. Three-dimensional multiparticle cell simulations of deformation and damage in sphere-reinforced composites. Mater Sci Eng A 2004;365:267–74.
[16] Youssef S, Maire E, Gaertner R. Finite element modelling of the actual structure of cellular materials determined by X-ray tomography. Acta Mater 2005;53:719–30.
[17] Borbély A, Kenesei P, Biermann H. Estimation of the effective properties of particle-reinforced metalmatrix composites from microtomographic reconstructions. Acta Mater 2006;54:2735–44.
[18] González C, LLorca J. Multiscale modeling of fracture in fiber-reinforced composites. Acta Mater 2006;54:4171–81.
[19] González C, LLorca J. Virtual fracture testing of fiber-reinforced composites: a computational micromechanics approach. Eng Fract Mech 2007;74:1126–38.
[20] Collings TA. Transverse compressive behaviour of unidirectional carbon fibre reinforced plastics. Composites 1974;5:108–16.
[21] Pinho ST, Iannucci L, Robinson P. Physically-based failure models and criteria for laminated fibre-reinforced composites with emphasis on fibre-kinking. Part I: development. Compos: Part A 2006;37:63–73.
[22] Huang YK, Frings PH, Hennes E. Mechanical properties of Zylon/epoxy composite. Compos: Part B 2002;33:109–15.
[23] Puck A, Schürmann H. Failure analysis of frp laminates by means of physically based phenomenological models. Compos Sci Technol 2002;62:1633–62.
[24] Aragonés D. Fracture micromechanisms in C/epoxy composites under transverse compression, Master thesis, Universidad Politécnica de Madrid, 2007.
[25] Vogler TJ, Kyriakides S. Inelastic behavior of an AS4/PEEK composite under combined transverse compression and shear. Part I: Experiments. Int J Plast 1999;15:783–806.
[26] Hsiao HM, Daniel IM. Strain rate behavior of composite materials. Compos: Part B 1998;29:521–33.
[27] Kinloch AJ, Young RJ. Fracture behavior of polymers. Elsevier Applied Science; 1983.
[28] Hashin Z. Failure criteria for unidirectional fiber composites. J Appl Mech 1980;47:329–34.
[29] Segurado J, LLorca J. A new three-dimensional interface finite element to simulate fracture in composites. Int J Solids Struct 2004;41:2977–93.
[30] Segurado J, LLorca J. A computational micromechanics study of the effect of interface decohesion on the mechanical behavior of composites. Acta Mater 2005;53:4931–42.
[31] Hashagen F, de Borst R. Numerical assessment of delamination in fibre metal laminates. Comput Meth Appl Mech Eng 2000;185:141–59.
[32] Ghosh S, Ling Y, Majumdar B, Kim R. Interfacial debonding analysis in multiple fiber reinforced composites. Mech Mater 2000;32:561–91.
[33] Brockenbrough JR, Suresh S, Wienecke HA. Deformation of metal–matrix composites with continuous fibers: geometrical effects of fiber distribution and shape. Acta Metall Mater 1991;39:735–52.
[34] Hine PJ, Lusti HR, Gusev AA. Numerical simulation of the effects of volume fraction, aspect ratio and fibre length distribution on the elastic and thermoelastic properties of short fibre composites. Compos Sci Technol 2002;62:1445–53.
[35] Abaqus, Users' Manual, ABAQUS Inc; 2006.
[36] Suquet P. Effective properties of nonlinear composites. In: Continuum micromechanics. CISM Course and Lecture Notes; 1997, p. 197–264.
[37] Hazanov S, Huet C. Order relationships for boundary condition effects in heterogeneous bodies smaller than the representative volume. J Mech Phys Solids 1994;42:1995–2011.
[38] Soden PD, Hinton MJ, Kaddour AS. Lamina properties, lay-up configurations and loading conditions for a range of fibre-

reinforced composite laminates. Compos Sci Technol 1998;58: 1011–22.
[39] Abaqus, Theory manual, HKS Inc; 1998.
[40] Menetrey P, Willam KJ. Triaxial failure criterion for concrete and its generalization. ACI Struct J 1995;92:311–8.
[41] Zhou X-F, Wagner HD, Nutt SR. Interfacial properties of polymer composites measured by push-out and fragmentation tests. Compos: Part A 2001;32:1543–51.
[42] Khisaeva ZF, Ostoja-Starzewski M. On the size of RVE in finite elasticity of random composites. J Elast 2006;85: 153–73.
[43] Pitkethly MJ et al. A round robin programme on interfacial test methods. Compos Sci Technol 1993;48:205–14.
[44] Benzarti K, Cangemi L, Maso FD. Transverse properties of unidirectional glass/epoxy composites: influence of fibre surface treatments. Compos: Part A 2001;32:197–206.

Elastic Properties and Young Modulus for some Materials

The Young Modulus (Tensile Modulus) for common materials as steel, glass, wood and more

To describe elastic properties of linear objects like wires, rods, or columns which are stretched or compressed, a convenient parameter is the ratio of the stress to the strain, a parameter called the "*Young's modulus*" or "*Modulus of Elasticity*" of the material. Young's modulus can be used to predict the elongation or compression of an object as long as the stress is less than the yield strength of the material.

Material	Young's Modulus (Modulus of Elasticity) - E -	Ultimate Tensile Strength - S_u -	Yield Strength - S_y -
	10^9		10^6

	(10^6 psi)	(10^9 N/m^2)	(10^6 N/m^2)	(10^6 N/m^2)
ABS plastics		2.3	40	
Acrylic		3.2	70	
Aluminum	10.0	69	110	95
Antimony	11.3			
Beryllium	42			
Bismuth	4.6			
Bone		9	170 (compression)	
Boron				3100
Brasses		100 - 125	250	
Bronzes		100 - 125		
Cadmium	4.6			
Carbon Fiber Reinforced Plastic		150		
Cast Iron 4.5% C, ASTM A-48			170	

Chromium	36			
Cobalt	30			
Concrete,			40	
High Strength (compression)		30	(compression)	
Copper	17		220	70
Diamond		1,050 - 1,200		
Douglas fir Wood		13	50 (compression)	
Glass		50 - 90	50 (compression)	
Gold	10.8			
Iridium	75			
Iron	28.5			
Lead	2.0			
Magnesium	6.4	45		
Manganese	23			
Marble			15	
Mercury				
Molybdenum	40			
Nickel	31			

Niobium (Columbium)	15			
Nylon		2 - 4	75	45
Oak Wood (along grain)		11		
Osmium	80			
Pine Wood			40	
Platinum	21.3			
Plutonium	14			
Polycarbonate		2.6	70	
Polyethylene HDPE		0.8	15	
Polyethylene Terephthalate PET		2 - 2.7	55	
Polyimide		2.5	85	
Polypropylene		1.5 - 2	40	
Polystyrene		3 - 3.5	40	
Potassium				
Rhodium	42			
Rubber		0.01 - 0.1		

Selenium	8.4			
Silicon	16			
Silicon Carbide		450		3440
Silver	10.5			
Sodium				
Stainless Steel, AISI 302			860	502
Steel, Structural ASTM-A36		200	400	250
Steel, High Strength Alloy ASTM A-514			760	690
Tantalum	27			
Thorium	8.5			
Titanium	16			
Titanium Alloy		105 - 120	900	730
Tungsten		400 - 410		
Tungsten		450 -		

Tungsten Carbide		450 - 650		
Uranium	24			
Vanadium	19			
Wrought Iron		190 - 210		
Zinc	12			

- 1 N/m^2 = $1x10^{-6}$ N/mm^2 = 1 Pa = $1.4504x10^{-4}$ psi
- 1 psi (lb/in^2) = 144 psf (lb_f/ft^2) = 6,894.8 Pa (N/m^2) = $6.895x10^{-3}$ N/mm^2

Note! Use the pressure unit converter on this page to switch the values to other units.

Strain

Strain can be expressed as

strain = dL / L (1)

where

strain = (m/m) (in/in)

dL = elongation or compression (offset) of the object (m) (in)

L = length of the object (m) (in)

Stress

Stress can be expressed as

stress = F/A (2)

where

stress = (N/m^2) (lb/in^2, psi)

F = force (N) (lb)

A = area of object (m^2) (in^2)

Young's Modulus (Tensile Modulus)

Young's modulus or Tensile modulus can be expressed as

E = stress / strain = (F / A) / (dL / L) (3)

where

E = Young's modulus (N/m^2) (lb/in^2, psi)

Elasticity

Elasticity is a property of an object or material which will restore it to its original shape after distortion.

A spring is an example of an elastic object - when stretched, it exerts a restoring force which tends to bring it back to its original length. This restoring force is in general

back to its original length. This restoring force is in general proportional to the stretch described by Hooke's Law.

Hooke's Law

One of the properties of elasticity is that it takes about twice as much force to stretch a spring twice as far. That linear dependence of displacement upon stretching force is called Hooke's law which can be expressed as

$$F_s = -k\, dL \quad (4)$$

where

F_s = *force in the spring (N)*

k = *spring constant (N/m)*

dL = *elongation of the spring (m)*

Yield strength

Yield strength, or the yield point, is defined in engineering as the amount of strain that a material can undergo before moving from elastic deformation into plastic deformation.

Ultimate Tensile Strength

The Ultimate Tensile Strength (UTS) of a material is the limit stress at which the material actually breaks, with sudden release of the stored elastic energy.

Related Topics

- Material Properties Material properties - density, heat capacity, viscosity and more - for gases, fluids and solids
- Mechanics Kinematics, forces, vectors, motion, momentum, energy and the dynamics of objects

Related Documents

- Speed of Sound Formulas Calculation formulas for velocity of sound in gas, fluid or solid
- Young Modulus of Elasticity for Metals and Alloys Elastic properties and Youngs modulus for common metals and alloys as cast iron, carbon steel and more
- Thermoplastics - Physical Properties Physical properties of some common thermoplastics as ABS, PVC, CPVC, PE, PEX, PB and PVDF
- Stress in Bolts Calculating the stressed area in UN and UNR bolts
- Modulus of Rigidity Shear Modulus or Modulus of Rigidity is the coefficient of elasticity for a shearing or torsion force
- Stress in Thick-Walled Tubes or Cylinders Radial and

tangential stress in thick-walled tubes or cylinders with closed ends - internal and external pressure

- Stress, Strain and Youngs Modulus Stress is force per area - strain is deformation of a solid due to stress
- Bolt Stretching Bolt stretch according Hookes Law
- Poissons ratio When a material is stretched in one direction it tends to get thinner in the other two directions
- Engineering Materials Comparing some typical properties of common engineering materials like steel, plastics, ceramics and composites

ToolBox Short List

Difficult to find your favorite ToolBox page? **Add links** to your favorite pages in your own **personal Short List!**

• **Add** this Page! • **Delete** the ShortList!

SketchUp Engineering ToolBox - Online 3D modeling!

SketchUp Engineering ToolBox - enabled for use with the amazing, fun and free Google SketchUp.

Search the ToolBox

Google Search

Web The Engineering ToolBox

Translate the ToolBox

Arabic - Chinese (Simplified) - Chinese (Traditional) - French - German - Italian - Japanese - Korean - Portuguese - Russian - Spanish

About the ToolBox

We appreciate any comments and tips on how to make The Engineering ToolBox a better information source. Please contact us by email

- thorfot@yahoo.com

if You find any faults, inaccurate, or otherwise unacceptable information.

information should always be double checked with alternative sources. All applicable national and local regulations and practices concerning this aspects must be strictly followed and adhered to.

Home
- Acoustics
- Air Psychrometrics
- Basics
- Combustion
- Economics
- Electrical
- Environment
- Fluid Mechanics
- Gas and Compressed Air
- HVAC Systems
- Hydraulics and Pneumatics
- Insulation
- Material Properties
- Mathematics
- Mechanics
- Miscellaneous
- Physiology
- Piping Systems
- Process Control
- Pumps
- Standards Organizations
- Steam and

PrinterFriendly

ToolBox ShortList
• Add this Page!

Link to this Page!

BookMarkThe Engineering ToolBox!

BookMark this Page!

ADD THIS

- Steam and Condensate
- Thermodynamics
- Water Systems

ToolBox **ShortList**
• Add this Page!

Google
• Search this Site!
• Translate this Page!
• About Us!

Temperature
0
- ○ °C
- ○ °F

Convert !

Length
1
- ○ *m*
- ○ *km*
- ○ *in*
- ○ *ft*
- ○ *yards*
- ○ *miles*
- ○ *nautical miles*

Convert !

Volume

Volume

1

- ◉ m^3
- ○ liters
- ○ in^3
- ○ ft^3
- ○ us gal

Convert !

Velocity

1

- ◉ m/s
- ○ km/h
- ○ ft/min
- ○ ft/s
- ○ mph
- ○ knots

Convert !

Pressure

1

- ◉ Pa (N/m^2)
- ○ bar
- ○ mm H_2O
- ○ kg/cm^2
- ○ psi
- ○ inches H_2O

Convert !

Flow

1

- ◉ m^3/s
- ○ m^3/h
- ○ US gpm
- ○ cfm